Chapter 2
Erosion and Reservoir Sedimentation

Page

2.1 Introduction 2-1
2.2 Empirical Approach for Erosion Estimation 2-1
2.2.1 Universal Soil Loss Equation 2-2
2.2.2 Revised Universal Soil Loss Equation 2-8
2.2.3 Modified Universal Soil Loss Equation 2-16
2.2.4 Direct Measurement of Sediment Yield and Extension of Measured Data 2-17
2.2.5 Sediment Yield as a Function of Drainage Area 2-18
2.2.6 Sediment Yield Classification Procedure 2-19
2.3 Physically Based Approach for Erosion Estimates 2-19
2.4 Computer Model Simulation of Surface Erosion Process 2-29
2.4.1 Total Maximum Daily Load of Sediment 2-34
2.4.2 Generalized Sediment Transport Model for Alluvial River River Simulation (GSTARS) 2-36
2.4.3 Rainfall-Runoff Relationship 2-38
2.4.4 GSTAR-W Model 2-39
2.4.5 Erosion Index Map 2-41
2.5 Example Case Studies 2-41
2.5.1 Drainage Area Descriptions 2-41
2.5.2 Example Computations of Sediment Yield 2-42
2.5.3 Example Based on the RUSLE 2-42
2.5.4 Example Based on Drainage Area 2-44
2.5.5 Example Based on the Sediment Yield Classification Procedure 2-44
2.5.6 Example Based on Unit Stream Power 2-46
2.5.6.1 Flood Hydrology 2-46
2.5.6.2 Application of the Sheet Erosion Equation 2-48
2.5.6.3 Results 2-49
2.5.7 Comparison of Different Approaches 2-54
2.6 Reservoir Sedimentation 2-57
2.6.1 Reservoir Sediment Trap Efficiency 2-57
2.6.2 Density of Deposited Sediment 2-60
2.63 Sediment Distribution Within a Reservoir 2-64
2.6.4 Delta Deposits 2-73
2.6.5 Minimum Unit Stream Power and Minimum Stream Power Method 2-77
2.7 Summary 2-85
2.8 References 2-86

Chapter 2
Erosion and Reservoir Sedimentation

by
Timothy J. Randle, Chih Ted Yang, Joseph Daraio

2.1 Introduction

As a result of runoff from rainfall or snowmelt, soil particles on the surface of a watershed can be eroded and transported through the processes of sheet, rill, and gully erosion. Once eroded, sediment particles are transported through a river system and are eventually deposited in reservoirs, in lakes, or at sea. Engineering techniques used for the determination of erosion rate of a watershed rely mainly on empirical methods or field survey. This chapter reviews and summarizes these empirical methods.

During the 1997 19th Congress of the International Commission on Large Dams (ICOLD), the Sedimentation Committee (Basson, 2002) passed a resolution encouraging all member countries to (1) develop methods for the prediction of the surface erosion rate based on rainfall and soil properties, and (2) develop computer models for the simulation and prediction of reservoir sedimentation processes. Yang et al. (1998) outlined the methods that can be used to meet the goals of the ICOLD resolution. This chapter presents a physically based approach for erosion estimation based on unit stream power and minimum unit stream power theories. Details of the theories are given in Chapter 3 and in Yang's book, *Sediment Transport: Theory and Practice* (1996). This chapter also summarizes methods for the estimation of sediment inflow and distribution in a reservoir, based on empirical and computer model simulation.

2.2 Empirical Approach for Erosion Estimation

Sediment yield is the end product of erosion or wearing away of the land surface by the action of water, wind, ice, and gravity. The total amount of onsite sheet, rill, and gully erosion in a watershed is known as the gross erosion. However, not all of this eroded material enters the stream system. Some of the material is deposited as alluvial fans, along river channels, and across flood plains. The portion of the eroded material that is transported through the stream network to some point of interest is referred to as the sediment yield. Therefore, the amount of sediment inflow to a reservoir depends on the sediment yield produced by the upstream watershed. The factors that determine a watershed's sediment yield can be summarized as follows (Strand and Pemberton, 1982):

- Rainfall amount and intensity
- Soil type and geologic formation
- Ground cover
- Land use
- Topography
- Upland erosion rate, drainage network density, slope, shape, size, and alignment of channels

- Runoff
- Sediment characteristics—grain size, mineralogy, etc.
- Channel hydraulic characteristics

Most of the empirical approaches for the estimation of erosion rate are based on one of the following methods:

- Universal Soil Loss Equation (USLE) or its modified versions
- Sediment yield as a function of drainage area
- Sediment yield as a function of drainage characteristics

Empirical equations are developed using data collected from specific geographical areas; application of these equations should be limited to areas represented in the base data. Some investigators have attempted to revise or modify the USLE to apply it to areas other than the Central and Eastern United States.

2.2.1 Universal Soil Loss Equation

Soil erosion rates on cultivated land can be estimated by the use of the Universal Soil Loss Equation (Wischmeier and Smith, 1962, 1965, 1978). This method is based on statistical analyses of data from 47 locations in 24 states in the Central and Eastern United States. The Universal Soil Loss Equation is:

$$A = RKLSCP \tag{2.1}$$

where A = computed soil loss in tons/acre/year,
R = rainfall factor,
K = soil-erodibility factor,
L = slope-length factor,
S = slope-steepness factor,
C = cropping-management factor, and
P = erosion-control practice factor.

The rainfall factor R accounts for differences in rainfall intensity, duration, and frequency for different locations; that is, the average number of erosion-index units in a year of rain. Locational values of the R-factor can be obtained for the central and eastern parts of the United States from Figure 2.1. The R-factor thus obtained does not account for soil loss due to snowmelt and wind.

The soil-erodibility factor K is a measure of the intrinsic susceptibility of a given soil to soil erosion. It is the erosion rate per unit of erosion-index for a specific soil in cultivated, continuous fallow, on a 9-percent slope, 72.6 feet long. The K-factor values range from 0.7 for highly erodible loams and silt loams to less than 0.1 for sandy and gravelly soil with a high infiltration rate. Table 2.1 shows the K values for the Central and Eastern United States, recommended by Wischmeier and Smith (1965).

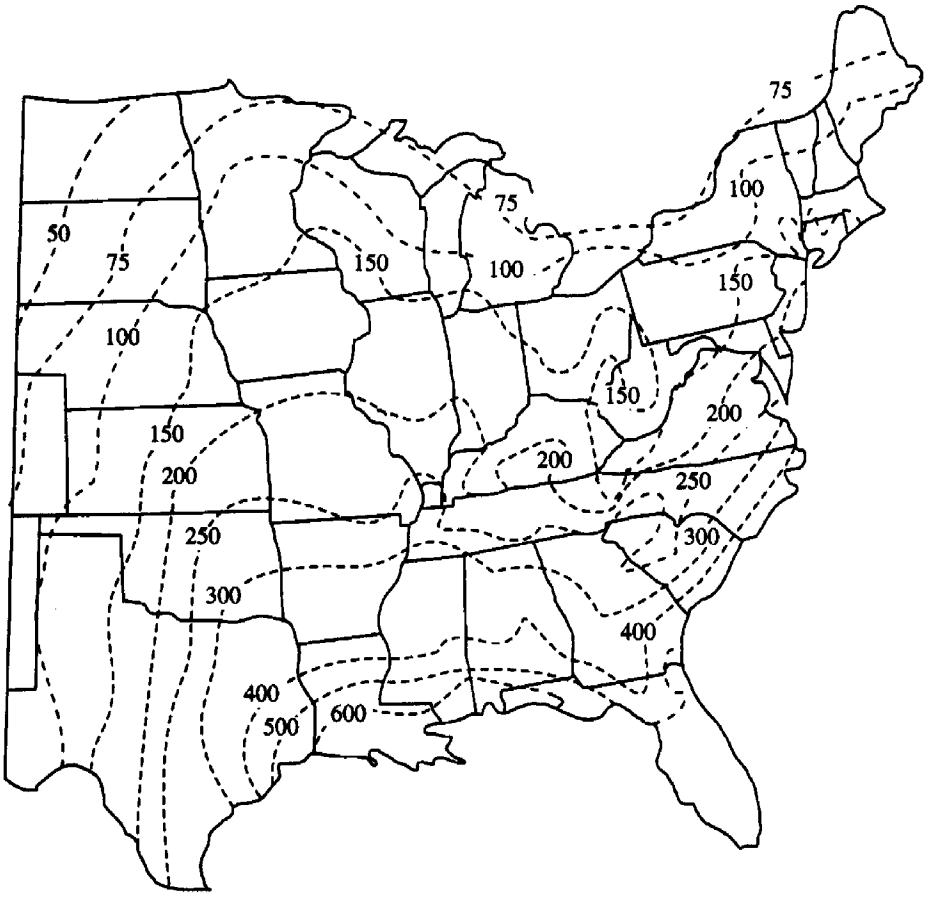

Figure 2.1. Isoerodent map of the *R*-factor values for the eastern portion of the United States (Wischmeier and Smith, 1965).

The slope-length factor L accounts for the increased quantity of runoff that occurs as distance from the top of the slope increases. It is the ratio of the soil loss from a given slope length to that from a 72.6-foot length, with all other conditions the same.

The slope-steepness factor S accounts for the increased velocity of runoff with slope steepness. It is the ratio of soil loss from a given slope steepness to that from a 9-percent slope. The effects of slope length and steepness are usually combined into one single factor; that is, the LS factor, which can be computed by:

$$LS = (\lambda / 72.6)^m (65.41 \sin^2 \theta + 4.56 \sin \theta + 0.065) \tag{2.2}$$

where λ = actual slope length in feet,
θ = angles of slope, and
m = an exponent with value ranging from 0.5 for slope equal to or greater than 5 percent to 0.2 for slope equal to or less than 1 percent.

Table 2.1. Relative erodibilities of key soils in the Central and Eastern United States (Wischmeier and Smith, 1965)

Soil	Location where evaluated	*K*-factor
Dunkirk silt loam	Geneva NY	0.69
Keene silt loam	Zanesville OH	0.48
Shelby loam	Bethany MO	0.41
Lodi loam	Blacksbury VA	0.39
Fayette silt loam	LaCrosse WI	0.38
Cecil sand clay loam	Watkinsville GA	0.36
Marshall silt loam	Clarinda IA	0.33
Ida silt loam	Castana IA	0.33
Mansic clay loam	Hays KS	0.32
Hagerstown silty clay loam	State College PA	0.31
Austin clay	Temple TX	0.29
Mexico silt loam	McCredie MO	0.28
Honeoye silt loam	Marcellus NY	0.28
Cecil sandy loam	Clemson SC	0.28
Ontario loam	Geneva NY	0.27
Cecil clay loam	Watkinsville GA	0.26
Boswell fine sandy loam	Tyler TX	0.25
Cecil sandy loam	Watkinsville GA	0.23
Zaneis fine sandy loam	Guthrie OK	0.22
Tifton loamy sand	Tifton GA	0.10
Freehold loamy sand	Marlboro NJ	0.08
Bath flaggy loam	Arnot NY	0.05
Albia gravelly loam	Beemerville NJ	0.03

Figure 2.2 expresses Equation (2.2) graphically. The results in Figure 2.2 were later extended to a slope length of 1,000 feet as shown in Table 2.2 (Wischmeier and Smith, 1978).

The cropping-management factor *C* accounts for the crop rotation used, tillage method, crop residue treatment, productivity level, and other agricultural practice variables. It is the ratio of soil loss from a field with given cropping and management practices to the loss from the fallow conditions used to evaluate the *K*-factor. The *C*-factor for an individual crop varies with the stage of crop growth, as shown in Table 2.3.

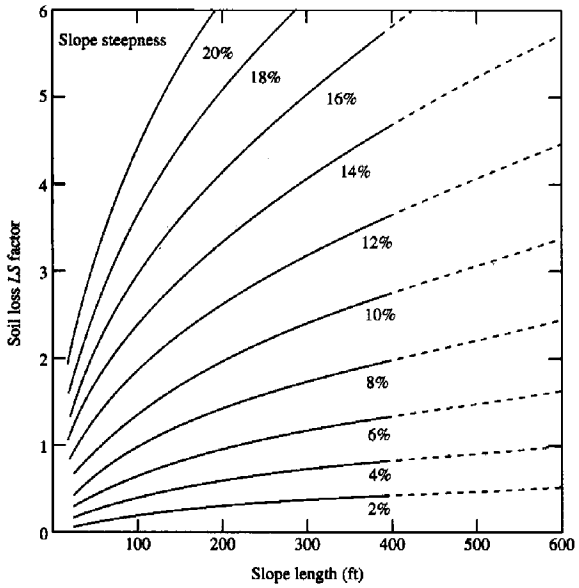

Figure 2.2. Topographic-effect graph used to determine *LS*-factor values for different slope-steepness—slope-length combinations (Wischmeier and Smith, 1965).

Table 2.2. Values of the topographic factor *LS* for specific combinations of slope length and steepness (Wischmeier and Smith, 1978)

Percent slope	Slope length (feet)											
	25	50	75	100	150	200	300	400	500	600	800	1,000
0.2	0.060	0.069	0.075	0.080	0.086	0.092	0.099	0.105	0.110	0.114	0.121	0.126
0.5	0.073	0.083	0.090	0.096	0.104	0.110	0.119	0.126	0.132	0.137	0.145	0.152
0.8	0.086	0.098	0.107	0.113	0.123	0.130	0.141	0.149	0.156	0.162	0.171	0.179
2	0.133	0.163	0.185	0.201	0.227	0.248	0.280	0.305	0.326	0.344	0.376	0.402
3	0.190	0.233	0.264	0.287	0.325	0.354	0.400	0.437	0.466	0.492	0.536	0.573
4	0.230	0.303	0.357	0.400	0.471	0.528	0.621	0.697	0.762	0.820	0.920	1.01
5	0.268	0.379	0.464	0.536	0.656	0.758	0.928	1.07	1.20	1.31	1.52	1.69
6	0.336	0.476	0.583	0.673	0.824	0.952	1.17	1.35	1.50	1.65	1.90	2.13
8	0.496	0.701	0.859	0.992	1.21	1.41	1.72	1.98	2.22	2.43	2.81	3.14
10	0.685	0.968	1.19	1.37	1.68	1.94	2.37	2.74	3.06	3.36	3.87	4.33
12	0.903	1.28	1.56	1.80	2.21	2.55	3.13	3.61	4.04	4.42	5.11	5.71
14	1.15	1.62	1.99	2.30	2.81	3.25	3.98	4.59	5.13	5.62	6.49	7.26
16	1.42	2.01	2.46	2.84	3.48	4.01	4.92	5.68	6.35	6.95	8.03	8.98
18	1.72	2.43	2.97	3.43	4.21	3.86	5.95	6.87	7.68	8.41	9.71	10.9
20	2.04	2.88	3.53	4.08	5.00	5.77	7.07	8.16	9.12	10.0	11.5	12.9

Table 2.3. Relative erodibilities of several crops for different crop sequences and yield levels at various stages of crop growth (Wischmeier and Smith, 1965)

Crop sequence	Crop yields		Soil-loss ratio for crop stage period[1]					
	Meadow	Corn	*F*	1	2	3	4*L*	4*R*
	(tons)	(bu)	(%)	(%)	(%)	(%)	(%)	(%)
Continuous fallow	-	-	100	100	100	100	-	100
1st-yr corn after meadow	1 to 2	40	15	32	30	19	30	50
1st-yr corn after meadow	2 to 3	70	10	28	19	12	18	40
1st-yr corn after meadow	3 to 5	100	8	25	17	10	15	35
2nd-yr corn after meadow, *RdR*[2]	2 to 3	70	60	65	51	24	-	65
2nd-yr corn after meadow, *RdL*	2 to 3	70	32	51	41	22	26	-
2nd-yr corn after meadow, *RdL+WC*	2 to 3	70	20	37	33	22	15	-
Corn, continuous, *RdR*	-	60	80	85	60	30	-	70
Corn, continuous, *RdL*	-	75	36	63	50	26	30	-
Corn, continuous, *RdL+WC*	-	75	22	46	41	26	15	-
Corn after oats with legume interseeding	-	60	25	40	38	24	30	-
Cotton, 1st-yr after meadow	2	-	15	34	40	30	30	-
Cotton, 2nd-yr after meadow	2	-	35	65	68	46	42	-
Cotton, continuous	-	-	45	80	80	52	48	-
Small grain with meadow interseeding, prior-crop residues on surface:								
After 1-yr corn after meadow	2	70	-	30	18	3	2	-
After 2-yr corn after meadow	2	70	-	40	24	5	3	-
After 2-yr cotton after meadow	2	-	-	50	35	5	3	-
Small grain after 1-yr corn after meadow, corn residues removed	2	-	-	50	40	15	3	-
Small grain on plowed seedbed, *RdR*	-	-	65	70	45	5	3	-
Established grass and legume meadow	3	-	0.4	0.4	0.4	0.4	0.4	0.4

[1] Crop stage periods: *F* = fallow; 1 = first month after seeding; 2 = second month after spring seeding; 3 = maturing crop to harvest; *4L* = residues; and *4R* = stubble.

[2] *RdR* = residues removed; *RdL* = residues left; *WC* = grass and legume winter-cover seeding.

The seasonal distribution of rainstorms in different locations influences the amount of erosion over the course of the year. The fraction of average annual erosion that occurs up to any point in the year varies according to geographical location. Figure 2.3 shows two sample erosion-index distribution curves for two parts of the United States.

The erosion-control practice factor *P* accounts for the effects of conservation practices, such as contouring, strip-cropping, and terracing, on erosion. It is the ratio of soil loss with a given practice to soil loss with straight-row farming parallel to the slope. For example, soil loss may be reduced by 50 percent on a 2- to 7-percent slope as a result of contouring. However, contouring

becomes less effective with increasing slope. For steep slopes, terracing is a more effective conservation practice. Table 2.4 provides some suggested values of *P* based on recommendations of the U.S. Environmental Protection Agency and the Natural Resources Conservation Service (formerly the Soil Conservation Service).

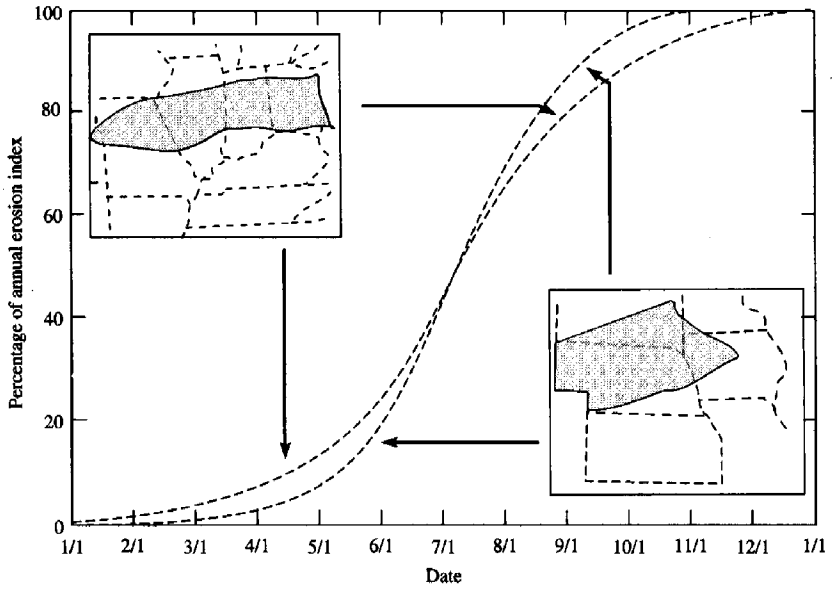

Figure 2.3. Erosion-index distribution curves for two sections of the United States (Wischmeier and Smith, 1965).

Table 2.4. Suggested *P* values for the erosion-control factor

Land slope (%)	Contouring[1]	Contour[2] furrows or pits	Contour ditches (wide spacing)
2.0 to 7	25.0 to 30	0.90	0.40
8.0 to 12	0.50	1.0	0.45
13.0 to 18	0.60	0.25	0.65
19.0 to 24	0.80	0.30	Factor values for this practice are not established.

[1] Topsoil spreading, tillage, and seeding on the contour. Contour limits–2%, 400 ft; 8%, 200 ft; 10%, 100 ft; 14 to 30%, 60 ft. The effectiveness of contouring beyond these limits is speculative.

2 Estimating values for surface manipulation of reclaimed land disturbed by surface mining. Furrows or pits installed on the contour. Spacing between furrows 40 to 60 inches with a minimum 6-inch depth. Pit spacing depends on pit size, but generally the pits should occupy 50% of the surface area.

The estimated soil loss from Equation (2.1) is the average value for a typical year, and the actual loss for any given year may be several times more or less than the average rate. It should also be

noted that the computed soil loss gives the estimated soil erosion rates, based upon plot-sized areas of upland. It does not account for sediment detention due to vegetation, flat areas, or low areas. In the estimation of sediment inflow to a reservoir, the effects of rill, gully, and riverbank erosion and other sources, or erosion and deposition between upland and the reservoir, should also be considered. Another limitation of the use of the Universal Soil Loss Equation is that the R values given in Figure 2.1 do not include the western portion of the United States and other countries. Because it is an empirical equation, and the fact that the factors are based on agriculture practices in the United States, the application of the USLE is mainly limited to the Central and Eastern United States, even though successful examples of application can be found in other countries. Consequently, Equation (2.1) cannot be used directly in the Western United States or other countries without further studies of all the factors used in that equation.

Example 2.1 Determine the annual amount of soil loss from a contouring upland farm in central Illinois in the United States. The farmland has a size of 800 acres, the soil is in a silt loam, and the slope length is 400 feet with a slope steepness of 4 percent. The soil is covered with matured grass (Yang, 1996).

Solution:

From Figure 2.1, $R = 200$
From Table 2.1, $K = 0.33$
From Figure 2.2 or Table 2.2, $LS = 0.697$
From Table 2.3, $C = 0.004$
From Table 2.4, $P = 0.5$
$A = RKLSCP = 200 \times 0.33 \times 0.697 \times 0.004 \times 0.5 = 0.092$ tons/acre/year
Total annual loss of soil = $0.092 \times 800 = 73$ tons

2.2.2 Revised Universal Soil Loss Equation

Continued research and a deeper understanding of the erosion process prompted some needed revisions to the USLE. The Revised Universal Soil Loss Equation (RUSLE) retains the basic structure of the USLE, Equation (2.1). However, significant changes to the algorithms used to calculate the factors have been made in the RUSLE (Renard et al., 1994). The R factor has been expanded to include the Western United States (Figure 2.4) and corrections made to account for rainfall on ponded water. The K factor has been made time varying, and corrections were made for rock fragments in the soil profile. Slope length and steepness factors LS have been revised to account for the relation between rill and interrill erosion. The C factor no longer represents seasonal soil-loss ratios; it now represents a continuous function of prior land use PLU, surface cover SC, crop canopy CC, surface roughness SR, and soil moisture SM. The factor P has been expanded to include conditions for rangelands, contouring, stripcropping, and terracing. Additionally, seasonal variations in K, C, and P are accounted for by the use of climatic data, including twice monthly distributions of EI_{30} (product of kinetic energy of rainfall and 30-minute precipitation intensity) (Renard et al., 1996). The RUSLE factors are distinguished from the USLE factors by the subscript R. The majority of the information in this section is from Renard et al. (1996).

Figure 2.4. R_R isoerodent map of the Western United States. Units are hundreds (ft tonf in)/(ac hr yr). (From Renard et al., 1996).

Determination of the rainfall-runoff erosivity R factor in the USLE and RUSLE is made by use of the EI_{30} parameter, where E is the total storm energy and I_{30} is the maximum 30-minute rainfall intensity for the storm. The average EI_{30} is used to establish the isoerodent maps for the R factor.

An empirical relationship for calculating the kinetic energy of rainfall, used in calculating E, is used in the RUSLE. Isoerodent maps of the U.S. were updated for the RUSLE using

$$ke = 916 + 331 \log_{10} i, \qquad i \leq 3 \text{ in h}^{-1} \tag{2.3}$$

$$ke = 1074, \qquad i > 3 \text{ in h}^{-1} \tag{2.4}$$

where ke = kinetic energy (ft ton acre^{-1} in^{-1}), and
i = rainfall intensity (in h^{-1}).

However, it is recommended by Renard et al. (1996) in the RUSLE handbook that the equation determined by Brown and Foster (1987)

$$ke_m = 0.29[1 - 0.72(e^{-0.05 i_m})] \tag{2.5}$$

where ke_m = kinetic energy of rainfall (MJ ha^{-1} mm^{-1} of rainfall), and
i_m = rainfall intensity (mm h^{-1}),

should be used for all calculations of the R factor. The kinetic energy of an entire storm is multiplied by the maximum 30-minute rainfall intensity I_{30} for that storm to get the EI_{30}.

An adjustment factor R_c is used to account for the protection from raindrops as a result of ponded water:

$$R_c = e^{(-0.49[y-1])} \tag{2.6}$$

where y = depth of flow or ponded water.

This adjustment in R is most important on land surfaces with little or no slope. Figure 2.5 shows the updated isoerodent map of the Eastern United States.

Corrections to the K factor have been made in the RUSLE to account for rock fragments in the soil matrix. Rock fragments present on the soil surface may act as an armoring layer causing a reduction in erosion and are accounted for by the C factor. Rock fragments present in the soil matrix have an effect on infiltration rates and hydraulic conductivity and, therefore, are accounted for with the K_R factor. The rate of reduction in saturated hydraulic conductivity resulting from the presence of rock fragments is given by:

$$K_b = K_f (1 - R_w) \tag{2.7}$$

where K_b = saturated hydraulic conductivity of the soil with rock fragments,
K_f = saturated hydraulic conductivity of the fine fraction of soil, and
R_w = percentage by weight of rock fragments > 2 mm.

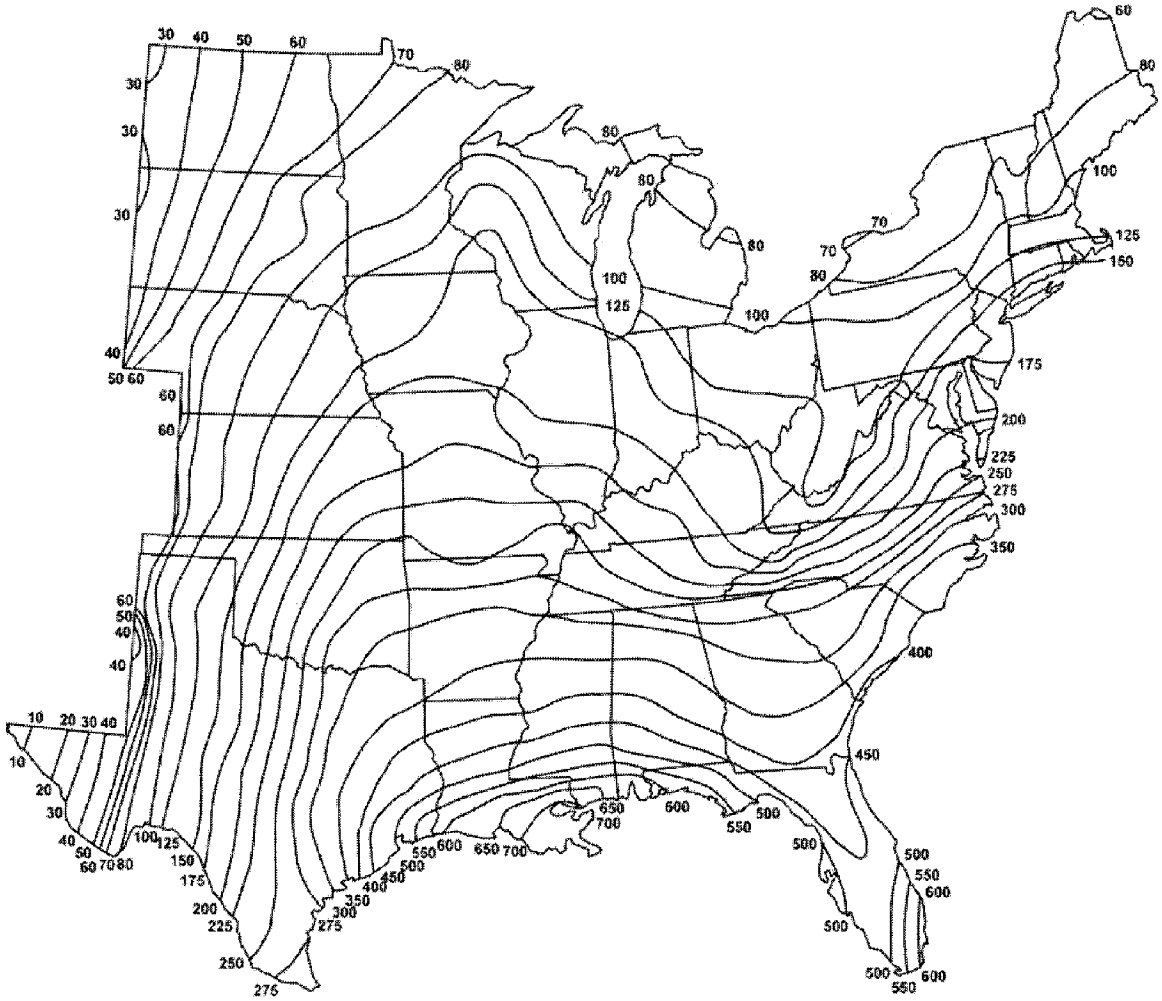

Figure 2.5. Adjusted R_R-factor isoerodent map of the Eastern United States. Units are hundreds (ft tonf in)/(ac hr yr). (From Renard et al., 1996).

An increase in rock fragments in the soil results in a corresponding decrease in the saturated hydraulic conductivity of the soil, thus leading to greater erosion potential and higher K_R factor values. Soil permeability classes that include the effects of rock fragments do not receive an adjustment of the K_R factor.

Additional changes to the K factor consist of the inclusion of seasonal effects as a result of soil freezing, soil texture, and soil water. Soil freezing and thawing cycles tend to increase the soil erodibility K factor by changing many soil properties, including soil structure, bulk density, hydraulic conductivity, soil strength, and aggregate stability. The occurrence of many freeze-thaw cycles will tend to increase the K factor, while the value of the soil erodibility factor will tend to decrease over the length of the growing season in areas that are not prone to freezing periods. An average annual value of K_R is estimated from:

$$K_{av} = \sum (EI_i)K_i / 100 \tag{2.8}$$

where EI_i = EI_{30} index at any time (calendar days),

$$K_i = K_{\max}(K_{\min} / K_{\max})^{(t_i - t_{\max})/\Delta t} \tag{2.9}$$

where K_i = soil erodibility factor at any time (t_i in calendar days),
K_{max} = maximum soil erodibility factor at time t_{max},
K_{min} = minimum soil erodibility factor at time t_{min}, and
Δt = length of the frost-free period or growing period.

Figure 2.6 gives two examples of the variation in K_i with time for two soil types in two different climates. Table 2.5 gives some initial estimates of K_R for further use in the RUSLE computer program. The new K_R factor is designed to provide a more accurate yearly average value for K_i; e.g., for similar soils in different climates. Additionally, it allows for the RUSLE to be applied at smaller time scales, though it still does not allow for single event erosion modeling.

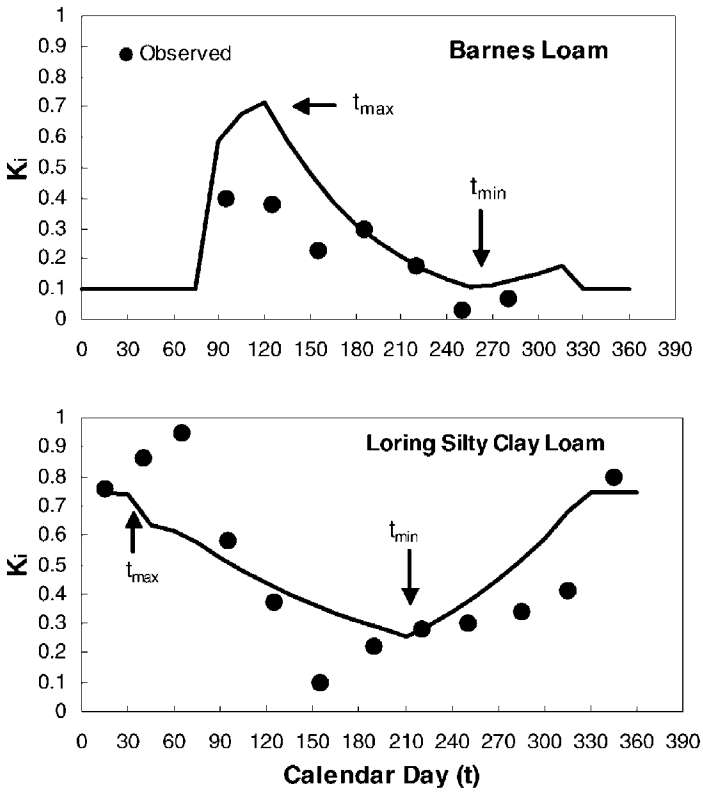

Figure 2.6 Relationship of K_i to calendar days for a Barnes loam soil near Morris, Minnesota, and a Loring silty clay loam soil near Holly Springs, Mississippi. K is given in U.S. customary units (from Renard et al., 1996).

Table 2.5. Initial K_R values for a variety of soil types in the Central and Eastern United States (Renard et al., 1996)

Soil type[1]	Location	Family	Period	Slope (%)	Length (ft)	K $\frac{ton}{acre\ eros.index}$
Bath sil.	Arnot, NY	Typic Fragiochrept	1938-45	19	72.6	0.05
Ontario l.	Geneva, NY	Glossoboric Hapludalf	1939-46	8	72.6	0.27
Cecil sl.	Clemson, SC	Typic Hapludalf	1940-42	7	180.7	0.28
Honeoye sil.	Marcellus, NY	Glossoboric Hapludalf	1939-41	18	72.6	0.28
Hagerstown sicl.	State College, PA	Typic Hapludalf	[2]NA	NA	NA	0.31
Fayette sil.	LaCrosse, WI	Typic Hapludalf	1933-46	16	72.6	0.38
Dunkirk sil.	Geneva, NY	Glossoboric Hapludalf	1939-46	5	72.6	0.69
Shelby l.	Bethany, MO	Typic Arguidoll	1931-40	8	72.6	0.53
Loring sicl.	Holly Springs, MS	Typic Fraguidalf	1963-68	5	72.6	0.49
Lexington sicl.	Holly Springs, MS	Typic Paleudalf	1963-68	5	72.6	0.44
Marshall sil.	Clarinda, IA	Typic Hapludoll	1933-39	9	72.6	0.43
Tifton ls.	Tifton, GA	Plinthic Paleudult	1962-66	3	83.1	[3]n.c.
Caribou grav. l.	Presque Isle, ME	Alfic Haplorthod	1962-69	8	72.6	n.c.
Barnes l.	Morris, MN	Udic Haploboroll	1962-70	6	72.6	0.23
Ida sil.	Castana, IA	Typic Udorthent	1960-70	14	72.6	0.27
Kenyon sil.	Independence, IA	Typic Hapludoll	1962-67	4.5	72.6	n.c.
Grundy sicl.	Beaconsfield, IA	Aquic Arguidoll	1960-69	4.5	72.6	n.c.

[1]si l. = silt loam, l. = loam, sl. = sandy loam, sicl. = silty clay loam, ls. = loamy sand, grav. l. = gravelly loam

[2]NA = Not available

[3]n.c. = Not calculated. However, soil-loss data for K-value computations are available from National Soil Erosion Laboratory, West Layfayette, Indiana

The slope length factor L is derived from plot data that indicate the following relation:

$$L = (\lambda / 72.6)^m \tag{2.10}$$

where λ = horizontal projection of the slope length, and
72.6 = RUSLE plot length in feet,

$$m = \beta / (1 + \beta) \tag{2.11}$$

where β = ratio of rill to interrill erosion.

The value of β when the soil is moderately susceptible to rill and interrill erosion is given by:

$$\beta = (\sin\theta / 0.0896) / [3.0(\sin\theta)^{0.8} + 0.56] \tag{2.12}$$

where θ = slope angle.

The parameter m in the RUSLE is a function of β (Equation 2.11). The newly defined L factor is combined with the original S factor to obtain a new LS_R factor. Values of m are in classes of low, moderate, and high, and tables are available in the RUSLE handbook for each of these classes to obtain values for LS_R. Table 2.6 gives an example of the new LS_R factor values for soils with low rill erosion rates. (Table 2.13 gives an example of LS_R values for soils with a high ratio of rill to interrill erosion.)

Table 2.6. Values of the topographic LS_R factor for slopes with a low ratio of rill to interrill erosion[1] (Renard et al., 1996)

	Horizontal slope length (ft)											
Slope (%)	25	50	75	100	150	200	250	300	400	600	800	1000
0.2	0.05	0.05	0.05	0.05	0.05	0.05	0.05	0.05	0.05	0.05	0.05	0.05
0.5	0.08	0.08	0.08	0.09	0.09	0.09	0.09	0.09	0.09	0.09	0.09	0.09
1.0	0.13	0.13	0.14	0.14	0.15	0.15	0.15	0.15	0.16	0.16	0.17	0.17
2.0	0.21	0.23	0.25	0.26	0.27	0.28	0.29	0.30	0.31	0.33	0.34	0.35
3.0	0.29	0.33	0.36	0.38	0.40	0.43	0.44	0.46	0.48	0.52	0.55	0.57
4.0	0.36	0.43	0.46	0.50	0.54	0.58	0.61	0.63	0.67	0.74	0.78	0.82
5.0	0.44	0.52	0.57	0.62	0.68	0.73	0.78	0.81	0.87	0.97	1.04	1.10
6.0	0.50	0.61	0.68	0.74	0.83	0.90	0.95	1.00	1.08	1.21	1.31	1.40
8.0	0.64	0.79	0.90	0.99	1.12	1.23	1.32	1.40	1.53	1.74	1.91	2.05
10.0	0.81	1.03	1.19	1.31	1.51	1.67	1.80	1.92	2.13	2.45	2.71	2.93
12.0	1.01	1.31	1.52	1.69	1.97	2.20	2.39	2.56	2.85	3.32	3.70	4.02
14.0	1.20	1.58	1.85	2.08	2.44	2.73	2.99	3.21	3.60	4.23	4.74	5.18
16.0	1.38	1.85	2.18	2.46	2.91	3.28	3.60	3.88	4.37	5.17	5.82	6.39
20.0	1.74	2.37	2.84	3.22	3.85	4.38	4.83	5.24	5.95	7.13	8.10	8.94
25.0	2.17	3.00	3.63	4.16	5.03	5.76	6.39	6.96	7.97	9.65	11.04	12.26
30.0	2.57	3.60	4.40	5.06	6.18	7.11	7.94	8.68	9.99	12.19	14.04	15.66
40.0	3.30	4.73	5.84	6.78	8.37	9.71	10.91	11.99	13.92	17.19	19.96	22.41
50.0	3.95	5.74	7.14	8.33	10.37	12.11	13.65	15.06	17.59	21.88	25.55	28.82
60.0	4.52	6.63	8.29	9.72	12.16	14.26	16.13	17.84	20.92	26.17	30.68	34.71

[1]Such as for rangeland and other consolidated soil conditions with cover (applicable to thawing soil where both rill and interrill erosion are significant).

The new cover-management factor C_R is based on a standard condition where a soil loss ratio SL_R is estimated relative to the reference condition (an area under clean-tilled continuous fallow). The SL_R is time variable, and values for SL_R are calculated every 15 days over the course of the year, based on the assumption that the important parameters remain constant over this time period. However, if, for example, a management operation changes in this time period, two values of SL_R are calculated for the 15-day time period. Soil Loss Ratio is calculated using the following relation:

$$SL_R = PLU \cdot CC \cdot SC \cdot SR \cdot SM \tag{2.13}$$

where PLU = prior-land-use subfactor,
CC = canopy-cover subfactor,
SC = surface-cover subfactor,
SR = surface-roughness subfactor, and
SM = soil-moisture subfactor.

(See Renard et al., 1996, for details on calculating SL_R.) Once the values of SL_R are calculated for each time period, they are multiplied by the percentage of annual EI_{30} that occurs in that same time period and summed over the entire time period of investigation. This provides a new C_R factor for the RUSLE.

The supporting practices factor P is refined in the RUSLE and includes the effects of contouring, including tillage and planting on or near contours, stripcropping, terracing, subsurface drainage, and also includes rangeland conditions. Values for the new P_R factor are the least reliable of all the factors in the RUSLE (Renard et al., 1994); therefore, the physically-based model CREAMS (Kinsel, 1980) is used to supplement empirical information used in the RUSLE. The effects of various practices were analyzed using the model and represented as P_R subfactors that are then used to calculate an overall P_R factor. If a variety of supporting practices are present on a particular plot of land, the P_R subfactors are used to calculate an overall P_R factor and then used in the RUSLE. Calculation of the revised P_R factor, along with the calculation of all other factors as revised in the RUSLE, is facilitated by the use of a computer program, which is available at http://www.sedlab.olemiss.edu/rusle/. Use of the RUSLE would not be possible without it.

Example 2.2 Using the information given in example 2.1, in addition to the following information, determine the amount of annual soil loss using the RUSLE. Soil is dominated by interrill erosion with little or no rill erosion, 2% rock cover, no residual vegetative cover, 4-inch contour ridges, mature Bahiagrass, mechanically disturbed at harvest time.

Solution: The K_R, C_R, and P_R factors must be calculated using the RUSLE 1.06b program (download from http://www.sedlab.olemiss.edu/rusle/download.html).

From Figure 2.5, $R_R = 175$.
From Table 2.5, initial K_R value is 0.43, and using the RUSLE program (use city code 13001), $K_R = 0.38$.
From Table 2.6, $LS_R = 0.67$.
In the RUSLE program, select time invariant average annual value for C_R, determine effective root mass from Table 2.7, $C_R = 0.007$.
In the RUSLE program, select the frequent-disturbance option $P_R = 0.295$.

$A = R_R K_R L S_R C_R P_R = 175 \times 0.385 \times 0.67 \times 0.011 \times 0.295 = 0.146$ tons/acre/year

Total annual soil loss = 0.146 x 800 = 117 tons/year, which is greater than the 73 tons/year computed by the original USLE.

Table 2.7. Typical values of parameters required to estimate the C_R factor with the RUSLE computer program (Renard et al., 1996)

Common Name	Root mass in top 4 in (lbs acre-1)	Canopy cover just prior to harvest (%)	Effective fall height (ft)	Average annual yield (tons acre-1)
Grasses:				
Bahiagrass	1,900	95	0.1	4
Bermudagrass, coastal	3,900	100	0.2	8
Bermudagrass, common	2,400	100	0.1	3
Bluegrass, Kentucky	4,800	100	0.1	3
Brome grass, smooth	4,500	100	0.1	5
Dallisgrass	2,500	100	0.1	3
Fescue, tall	7,000	100	0.1	5
Orchardgrass	5,900	100	0.1	5
Timothy	2,900	95	0.1	5
Legumes:				
Alfalfa	3,500	100	0.2	6
Clover, ladino	1,400	100	0.2	3
Clover, red	2,100	100	0.1	4
Clover, sweet	1,200	90	2.0	2
Clover, white	1,900	100	0.1	2
Lespedeza, sericea	1,900	100	0.5	3
Trefoil, birdsfoot	2,400	100	0.3	4

These values are for mature, full pure stands on well-drained nonirrigated soils with moderate-to-high available water-holding capacity. These values hold for species shown only within their range of adaptation. Except for biennials, most forages do not attain a fully-developed root system until end of second growing season. Root mass values listed can be reduced by as much as half on excessively drained or shallow soils and in areas where rainfall during growing season is less than 18 in.

2.2.3 Modified Universal Soil Loss Equation

Williams (1975) modified the USLE to estimate sediment yield for a single runoff event. On the basis that runoff is a superior indicator of sediment yield than rainfall—i.e., no runoff yields no sediment, and there can be rainfall with little or no runoff—Williams replaced the R (rainfall erosivity) factor with a runoff factor. His analysis revealed that using the product of volume of runoff and peak discharge for an event yielded more accurate sediment yield predictions, especially for large events, than the USLE with the R factor. The Modified USLE, or MUSLE, is given by the following (Williams, 1975):

$$S = 95(Qp_p)^{0.56} KLSCP \tag{2.14}$$

where S = sediment yield for a single event in tons,
Q = total event runoff volume (ft^3),
p_p = event peak discharge ($ft^3\ s^{-1}$), and
K, LS, C, and P = USLE parameters (Equation 2.1).

The comparison with the USLE was done by estimating the average annual soil loss with the USLE and comparing it to the annual soil loss calculated for each event over the course of the year using the MUSLE. The MUSLE has been tested (Williams, 1981; Smith et al., 1984) and found to perform satisfactorily on grassland and some mixed use watersheds. However, the utility of the MUSLE depends a great deal upon the accuracy of the hydrologic inputs.

Example 2.3 Using the same information from example 2.1, determine the sediment yield from a storm with a total runoff volume of 120 ft^3 and a peak discharge of 5 cfs.

Solution: From example 2.1, $K = 0.33$
$LS = 0.697$
$C = 0.004$
$P = 0.5$

$(Qp_p)^{0.56} = 120 \times 5 = 600^{0.56} = 36$

$S = 95(Qp_p)^{0.56}KLSCP = 95 \times 36 \times 0.33 \times 0.697 \times 0.004 \times 0.5 = 1.57$ tons

In order to obtain an estimate of the annual soil loss from the MUSLE, soil loss from each event throughout the year needs to be calculated.

While the USLE, RUSLE, and MUSLE have met with practical success as an aid for conservation management decisions and the reduction of soil erosion from agricultural lands, they are not capable of simulating soil erosion as a dynamic process distributed throughout a watershed and changing in time. Although the MUSLE can estimate soil loss from a single event, neither it nor the USLE and RUSLE can estimate detachment, entrainment, transport, deposition, and redistribution of sediment within the watershed and are of limited application.

2.2.4 Direct Measurement of Sediment Yield and Extension of Measured Data

The most accurate method for determining the long-term sediment yield from a watershed is by direct measurement of sediment deposition in a reservoir (Blanton, 1982) or by direct measurement of streamflow, suspended sediment concentration, and bedload. If long-term records are available, then daily and average annual sediment loads can be computed. The average annual sediment load can then be used to estimate the long-term sediment yield. However, long-term measurements of river discharge are not always available. Long-term measurements of suspended sediment concentration are not commonly available, and long-term measurements of bedload are rare.

In the absence of long-term streamflow measurements for the site of interest, it may be possible to extend short-term measurements by empirical correlation with records from another stream gauge in the watershed or from a nearby watershed with similar drainage characteristics.

A short-term record of suspended sediment concentrations can be extended by correlation with streamflow. A power equation of the form, $C = aQ^b$, is most commonly used for regression analysis, where C is the sediment concentration, Q is the rate of streamflow, and a and b are

regression coefficients. The relationship between streamflow and suspended sediment concentration can change with grain size, from low flows to high flows, from season to season, and from year to year. Therefore, enough measurements of suspended sediment concentration and streamflow are necessary to ensure that the regression equation is applicable over a wide range of streamflow conditions, seasons, and years.

A single regression equation may produce an acceptable correlation over a narrow range of conditions. However, separate regression equations may be necessary to achieve satisfactory correlations over a wide range of conditions. For example, the suspended sediment concentrations could be divided into wash load and bed-material load to develop separate regression equations for each. The data could also be sorted by streamflow to develop separate regression equations for low, medium, and high flows. The data may need to be sorted by season to develop separate regression equations for the winter and spring flood seasons. If enough data were available, a portion of the data could be used for the regression analysis, so that the remaining portion could be used for verification.

A short-term record of bedload measurements could be extended in the same manner as that described for the suspended sediment concentrations. If no bedload measurements were available, then bedload could be estimated as a percentage of the suspended sand load (typically 2 to 15%) or computed using one of many predictive equations (see Chapter 3, *Non-Cohesive Sediment Transport*). Strand and Pemberton (1982) presented a guide for estimating the ratio of bedload to suspended sediment load (Table 2.8). Table 2.8 presents five conditions that estimate the ratio of bedload to suspended sediment load as a function of the streambed material size, the fraction of the suspended load that is sand, and the suspended sediment concentration during floods. A bedload measurement program should be considered if the bedload could be more than 10 percent of the suspended sediment load.

Table 2.8. Bedload adjustment

Streambed material	Fraction of suspended sediment load that is sand (%)	Suspended sediment concentration (ppm)	Ratio of bedload to suspended sediment load
Sand	20–50	< 1,000	25–150
Sand	20–50	1,000–7,500	10–35
Sand	20–50	> 7,500	5
Compacted clay, gravels, cobbles, or boulders	< 25	Any	5–15
Clay and silt	Near 0	Any	< 2

2.2.5 Sediment Yield as a Function of Drainage Area

Empirical sediment yield equations can be developed strictly as a function of drainage area based on reservoir sediment survey data. For example, Strand (1975) developed the following empirical equation for Arizona, New Mexico, and California:

$$Q_s = 2.4\,A_d^{-0.229} \tag{2.15}$$

where Q_s = sediment yield in ac-ft/mi^2/yr, and
A_d = drainage area in mi^2.

Strand and Pemberton (1982) developed a similar empirical equation for the semiarid climate of the Southwestern United States:

$$Q_s = 1.84\,A_d^{-0.24} \tag{2.16}$$

This same approach can be used to develop equations for other regions.

2.2.6 Sediment Yield Classification Procedure

The Pacific Southwest Inter-Agency Committee (1968) developed a sediment yield classification procedure that predicts sediment yield as a function of nine individual drainage basin characteristics. These include surface geology, soils, climate, runoff, topography, ground cover, land use, upland erosion, and channel erosion. Each drainage basin characteristic is given a subjective numerical rating based on observation and experience. Table 2.9 presents the drainage basin characteristics considered by this method and their possible ratings. The sum of these ratings determines the drainage basin classification and the annual sediment yield per unit area (Table 2.10).

2.3 Physically Based Approach for Erosion Estimates

The minimum energy dissipation rate theory states that when a dynamic system reaches its equilibrium condition, its rate of energy dissipation is at a minimum (Yang and Song, 1986, and Yang, 1996). The minimum value depends on the constraints applied to the system. The rate of energy dissipation per unit weight of water is:

$$dY/dt = (dx/dt)\,(dY/dx) = VS = \text{unit stream power} \tag{2.17}$$

where Y = potential energy per unit weight of water,
t = time,
x = reach length,
dx/dt = velocity V, and
dY/dx = energy or water surface slope S.

For the equilibrium condition, the unit stream power VS will be at a minimum, subject to the constraints of carrying a given amount of water and sediment.

Table 2.9. List of drainage basin characteristics and possible range of numerical ratings (modified from Pacific Southwest Interagency Committee, Water Management Subcommittee, 1968)

Drainage basin characteristics	Sediment yield levels		
	High rating	Moderate rating	Low rating
Surface geology	10: marine shales and related mudstones and siltstones	5: rocks of medium hardness moderately weathered and fractured	0: massive hard formations
Soils	10: fine textured and easily dispersed or single grain salts and fine sands	5: medium textured, occasional rock fragments, or caliche crusted layers	0: frequent rock fragments, aggregated clays, or high organic content
Climate	10: frequent intense convective storms	5: infrequent convective storms, moderate intensity	0: humid climate with low intensity rainfall, arid climate with low intensity rainfall, or arid climate with rare convective storms
Runoff	10: high flows or volume per unit area	5: moderate flows or runoff volume per unit area	0: low flows or volume per unit area or rare runoff events
Topography	20: steep slopes (in excess of 30%), high relief, little or no flood plain development	10: moderate slopes (about 20%), moderate flood plain development	0: gentle slopes (less than 5%), extensive flood plain development
Ground cover	10: ground cover less than 20%, no rock or organic litter in surface soil	0: ground cover less than 40%, noticeable organic litter in surface soil	-10: area completely covered by vegetation, rock fragments, organic litter with little opportunity for rainfall to erode soil
Land use	10: more than 50% cultivated, sparse vegetation, and no rock in surface soil	0: less than 25% cultivated, less than 50% intensively grazed	-10: no cultivation, no recent logging, and only low intensity grazing, if any
Upland erosion	25: rill, gully, or landslide erosion over more than 50% of the area	10: rill, gully, or landslide erosion over about 25% of area	0: no apparent signs of erosion
Channel erosion	25: continuous or frequent bank erosion, or active headcuts and degradation in tributary channels	10: occasional channel erosion of bed or banks	0: wide shallow channels with mild gradients, channels in massive rock, large boulders, or dense vegetation or artificially protected channels

Table 2.10. Drainage basin sediment yield classification (Randle, 1996)

Drainage basin classification number	Total rating	Annual sediment yield (ac-ft/mi^2)
1	> 100	> 3
2	75 to 100	1.0 to 3.0
3	50 to 75	0.5 to 1.0
4	25 to 50	0.2 to 0.5
5	0 to 25	<0.2

Sediment transport rate is directly related to unit stream power (Yang, 1996). The basic form of Yang's (1973) unit stream power equation for sediment transport is:

$$\log C = I + J \log(VS/\omega - V_{cr}S/\omega) \tag{2.18}$$

where C = sediment concentration,
I, J = dimensionless parameters reflecting flow and sediment characteristics that are determined from regression analysis,
V = flow velocity,
S = energy or water surface slope of the flow,
ω = sediment particle fall velocity, and
V_{cr} = critical velocity required for incipient motion.

The unit stream power theory stems from a general concept in physics that the rate of energy dissipation used in transporting material should be related to the rate of material being transported. The original concept of unit stream power, or rate of potential energy dissipation per unit weight of water, was derived from a study of river morphology (Yang, 1971). The river systems observed today are the cumulative results of erosion and sediment transport. If unit stream power can be used to explain the results of erosion and sediment transport, it should be able to explain the process of erosion and sediment transport. The relationships between unit stream power and sediment transport in open channels and natural rivers have been addressed in many of Yang's publications. This section addresses the relationship between unit stream power and surface erosion.

For laminar flow over a smooth surface, the average flow velocity can be expressed by Horton et al. (1934):

$$V = (gSR^2)/(3v) \tag{2.19}$$

where V = average flow velocity,
S = slope,
g = gravitational acceleration,
R = hydraulic radius, which can be replaced by depth for sheet flow, and
v = kinematic viscosity.

The shear velocity is:

$$U_* = \sqrt{gRS} \tag{2.20}$$

From Equations (2.19) and (2.20)

$$\frac{VS}{U_*^4} = \frac{1}{3gv} \tag{2.21}$$

In other words, the ratio between the unit stream power and the fourth power of the shear velocity is a constant for a fluid of a given viscosity.

For laminar flow over a rough bed, the grain shear stress can be expressed by:

$$\tau' = \frac{1}{8}\rho F' V^2 \tag{2.22}$$

where ρ = density of fluid, and
F' = a parameter.

Savat (1980) found:

$$F' = \frac{K}{R_e} \tag{2.23}$$

where K = a constant with a theoretical value of 24, and
R_e = Reynolds number.

From Equations (2.22) and (2.23):

$$\tau' = \frac{K\mu V}{8R} \tag{2.24}$$

where μ = dynamic viscosity.

Govers and Rauws (1986) assumed that:

$$R = \sqrt{\frac{3\nu V}{gS}} \tag{2.25}$$

then

$$\frac{VS}{U_*'} = \frac{192}{K^2 g\nu} \tag{2.26}$$

where U_*' = grain shear velocity.

Equations (2.21) and (2.26) indicate that the relationship between unit stream power and shear velocity due to grain roughness for sheet flows is well defined, regardless of whether the surface is smooth or rough. Figure 2.7 shows the relationship between sheet sediment concentration and grain shear velocity by Govers and Rauws (1986), based on data collected by Kramer and Meyer (1969), Rauws (1984), and Govers (1985). When Govers and Rauws (1986) replotted the same data, as shown in Figure 2.8, they showed a much better-defined relationship between sediment concentration and unit stream power. Figure 2.9 shows an example of comparison between measured and predicted sediment concentration based on unit stream power.

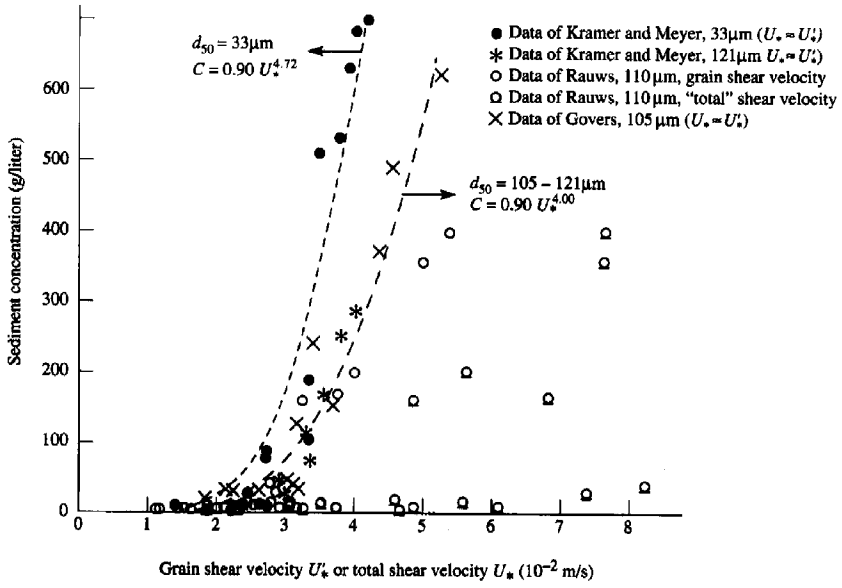

Figure 2.7. Relationship between sheet and rill flow sediment concentration and grain shear velocity (Govers and Rauws, 1986).

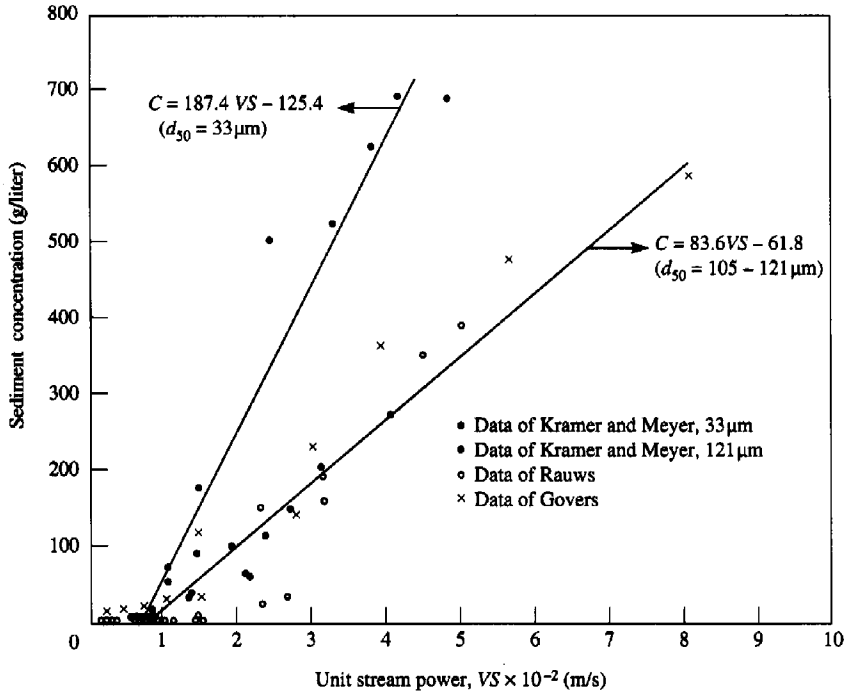

Figure 2.8. Relationship between sheet and rill flow sediment concentrations and unit stream power (Govers and Rauws, 1986).

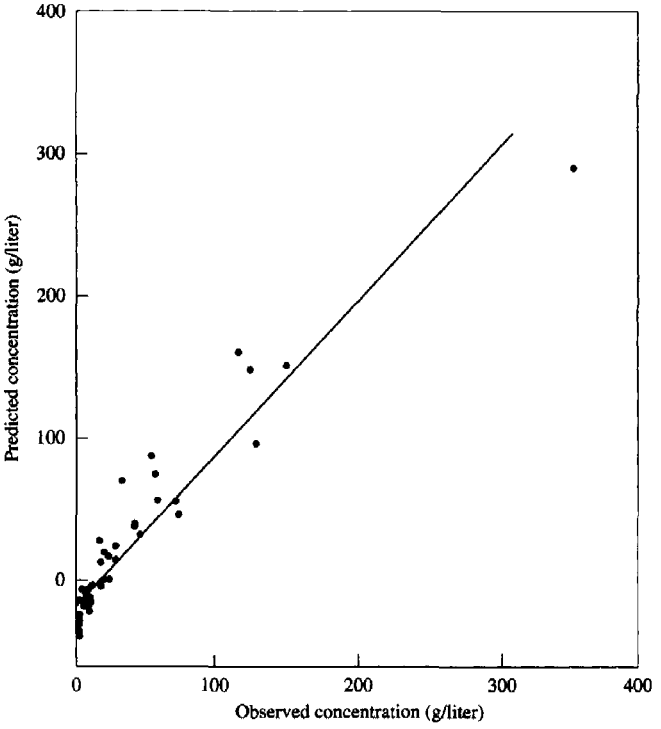

Figure 2.9. Comparison between measured and predicted sediment from surface erosion (Govers and Rauws, 1986).

Moore and Burch (1986) tested the direct application of Equation (2.18) to sheet and rill erosion. They reported from experimental results that:

$$I = 5.0105 \pm 0.0443 \tag{2.27}$$

$$J = 1.363 \pm 0.030 \tag{2.28}$$

Velocity was computed from Manning's equation, because it is difficult to measure for sheet flow, and they expressed unit stream power as:

$$VS = \left(\frac{Q}{B}\right)^{0.4} \frac{S^{1.3}}{n^{0.6}} \tag{2.29}$$

where Q = water discharge,
B = width of flow,
S = slope, and
n = Manning's roughness coefficient.

Similarly, the unit stream power for rill flow can be expressed by:

$$VS = \left(\frac{Q}{J}\right)^{0.25} \frac{S^{1.375}}{n^{0.75}} W \tag{2.30}$$

where J = number of rills crossing the contour element B, and
W = rill shape factor = (width/depth) $^{0.5}$.

It can be shown that for parabolic rills:

$$W = \sqrt{\frac{(1.5)^{0.5} a^{1.5}}{1.5a^2 + 4}} \tag{2.31}$$

for trapezoidal rills:

$$W = \left[\frac{(a+z)}{a + 2\sqrt{Z^2+1}}\right]^{0.5} \tag{2.32}$$

where a = rill width-depth ratio, and
Z = rill side slope.

Figure 2.10 shows the relationships among W, a, and Z for rills of different shapes. Figure 2.10 shows that when the width-depth ratio is greater than 2, the geometry has little impact on the value of the shape factor. Moore and Burch assumed that most natural rills can be approximated by a rectangular rill in the computation of W when a is greater than 2 or 3.

Yang's (1973) original unit stream power equation was intended for open channel flows. His dimensionless critical unit stream power required at incipient motion may not be directly applicable to sheet and rill flows. For sheet and rill flows with very shallow depth, Moore and Burch found that the critical unit stream power required at incipient motion can be approximated by a constant:

$$\frac{V_{cr} S}{\nu} = 4105 \text{ m}^{-1} \tag{2.33a}$$

or

$$V_{cr} S = 0.002 \text{ m/s} \tag{2.33b}$$

as shown in Figure 2.11. In Equation (2.33a), ν = kinematic viscosity of water.

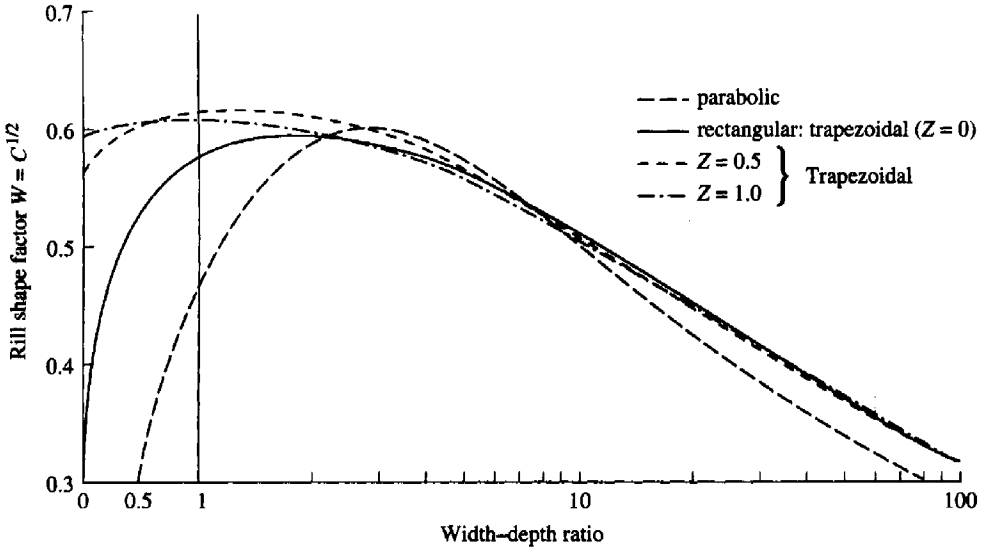

Figure 2.10. Relationship between rill shape factor and width-depth ratio for parabolic, rectangular, and trapezoidal rills (Moore and Burch, 1986).

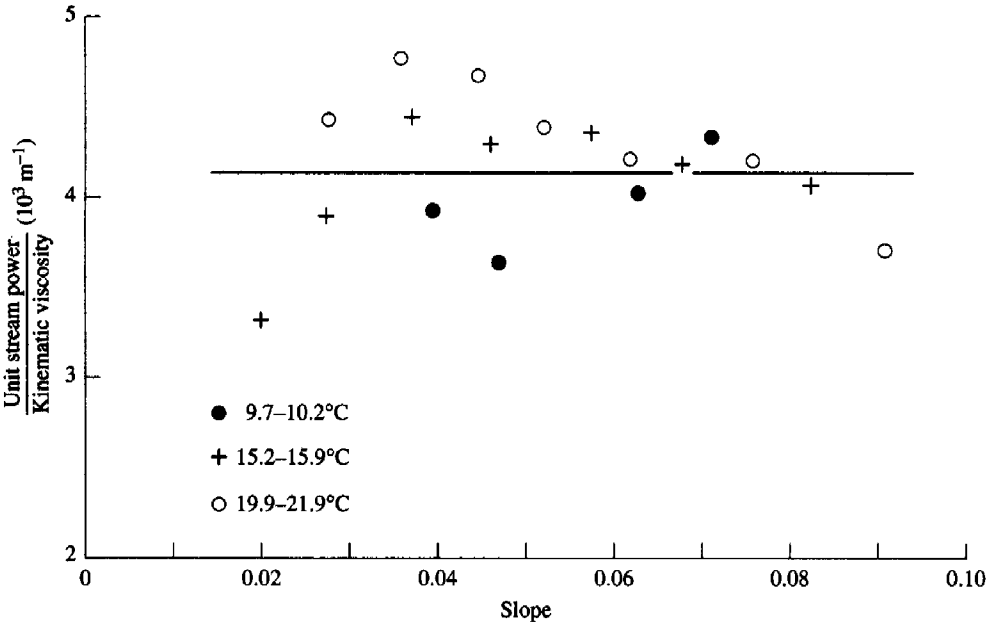

Figure 2.11. Relationship between the ratio of critical unit stream power and kinematic viscosity and the surface slope (Moore and Burch, 1986).

Moss et al. (1980) noted that sheet flow occurred initially, but as soon as general sediment motion ensued, the plane bed revealed its instability and rill cutting began. In accordance with the theory of minimum energy dissipation rate (Yang and Song, 1986, 1987; Yang et al., 1981) a rectangular channel with the least energy dissipation rate or maximum hydraulic efficiency should have a width-depth ratio of 2. For $a = 2$ and $Z = 0$, unit stream power for rill erosion can be computed by Equations (2.30) and (2.32). The number of rills generated by flow ranges from 1.5 at Q = 0.0015 m^3/s to 7 at Q = 0.0003 m^3/s. Substituting the unit stream power thus obtained and a constant critical unit stream power of 0.002 m/s required at incipient motion, the sediment concentration due to sheet and rill erosion in the sand size range can be computed directly from Yang's 1973 equation. Yang's 1973 equation was intended for the movement of sediment particles in the ballistic or colliding region instead of the individual jump or saltation region. The comparisons shown in Figure 2.12 by Moore and Burch indicate that the rate of surface erosion can be accurately predicted by the unit stream power equation when the movement of sediment particles is in the ballistic dispersion region. The numbers shown in Figure 2.12 are sediment concentrations in parts per million by weight.

Yang's 1973 equation should not be applied to soils in the clay or fine silt size range directly because the terminal fall velocities of individual small particles are close to zero. In this case, the effective size of the aggregates of the eroded and transported materials should be used. The effective size increases with increasing flow rate and unit stream power. The estimated terminal fall velocities of these fine particles in water should also be adjusted for differences in the measured aggregate densities. For example, after these adjustments, effective particle diameters of aggregate size of the Middle Ridge clay loam and Irving clay for inter-rill and rill flow were determined to be 0.125 mm and 0.3 mm, respectively. With these effective diameters and a constant critical unit stream power of 0.002 m/s at incipient motion, Yang's 1973 equation can also be used for the estimation of surface erosion rate in the clay size range. Figure 2.13 shows that observed clay concentrations and predicted clay concentrations by Yang's (1973) equation using effective diameter of the clay aggregate, are in close agreement.

Combining Equations (2.18), (2.27), (2.28), and (2.29) yields the following equation for sheet erosion:

$$\log C = 5.0105 + 1.363 \log [\{(Q/B)^{0.4} S^{1.3} / n^{0.6} - 0.002\}/\omega] \tag{2.34}$$

Similarly, the equation for rill erosion becomes:

$$\log C = 5.0105 + 1.363 \log [\{(Q/J)^{0.25} (S^{1.375} / n^{0.75}) W - 0.002\}/\omega] \tag{2.35}$$

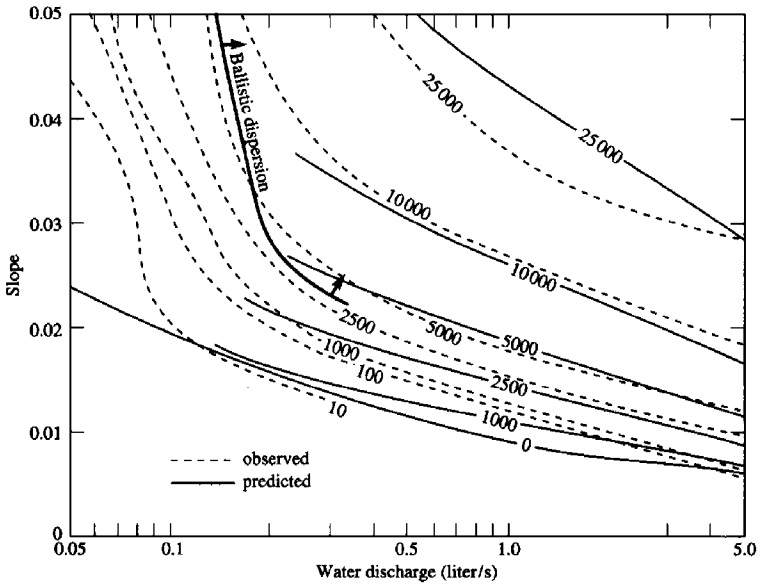

Figure 2.12. Comparison between observed and predicted sediment concentrations in ppm by weight from Yang's unit stream power equation with a plane bed composed of 0.43 mm sand (Moore and Burch, 1986).

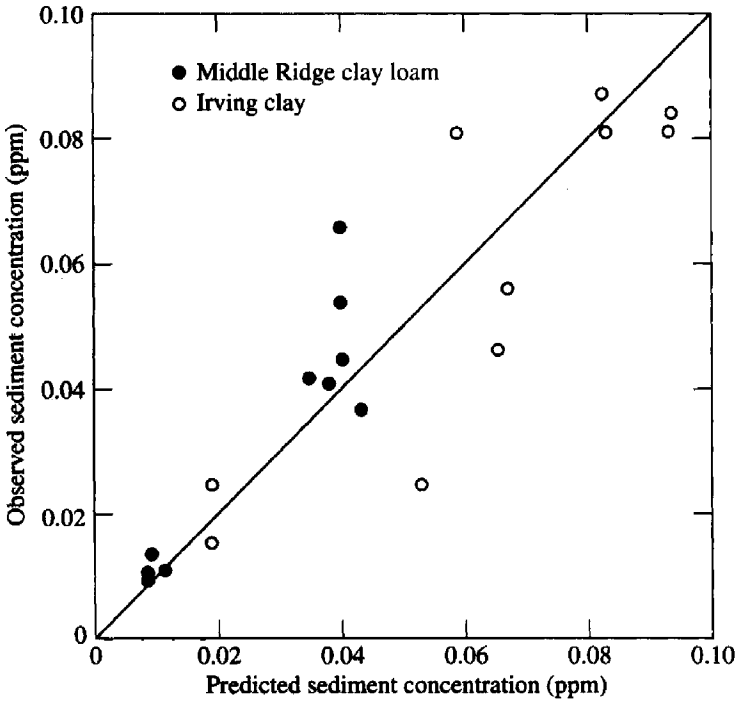

Figure 2.13. Comparison between observed and predicted clay concentrations from Yang's unit stream power equation (Moore and Burch, 1986).

The derivations and comparisons shown in this section confirm that with minor modifications, Yang's (1973) unit stream power equation can be used as a rational tool for the prediction of sheet and rill erosion rate, given the water discharge, surface roughness and slope, and median particle size or effective particle size and its associated fall velocity. This suggests that a rational method based on rainfall-runoff and the unit stream power relationship can be developed to replace the empirical Universal Soil Loss Equation for the prediction of soil loss due to sheet and rill erosion. It has been shown in the literature that Yang's unit stream power equations can be used to determine the rate of sediment transport in small and large rivers with accuracy. It is now possible to use the unit stream power theory to determine the total rate of sediment yield and transport from a watershed regardless of whether the sediment yield particles are transported by sheet, rill, or river flows. By doing so, the actual amount of sediment entering a reservoir can be determined by a consistent and rational method.

2.4 Computer Model Simulation of Surface Erosion Process

A multitude of computer models have been developed for various applications that utilize a wide array of techniques to simulate soil erosion within a watershed. Erosion models have been developed for different purposes including:

- Predictive tools for assessing soil loss for conservation planning, regulation, and soil erosion inventories.

- Predictive tools to assess where and when within a watershed soil erosion may be a problem.

- Research tools to better understand the erosion process (Nearing et al., 1994).

Watershed erosion models can be grouped into several categories:

- Empirically based, or derived, erosion models such as the USLE (Wischmeier and Smith, 1978) and the RUSLE (Renard et al., 1996).

- Physically based models, such as the Water Erosion Prediction Project (WEPP) (Nearing et al., 1989), Areal Non-point Source Watershed Environmental Response Simulation (ANSWERS) (Beasley et al., 1980), Chemicals, Runoff, and Erosion from Agricultural Management Systems (CREAMS) (Kinsel, 1980), Kinematic runoff and Erosion model (KINEROS) (Woolhiser et al., 1990), European Soil Erosion Model (EUROSEM) (Morgan et al., 1998), and Système Hydrologique Européen Sediment model (SHESED) (Wicks and Bathurst, 1996).

- Mixed empirical and physically based models, such as Cascade of Planes in Two Dimensions (CASC2D) (Johnson et al., 2000; Ogden and Julien, 2002), Agricultural Non- Point Source Pollution model (AGNPS) (Young et al., 1989), and Gridded Surface Subsurface Hydrological Analysis model (GSSHA) (Downer, 2002).

- GIS and Remote Sensing techniques that utilize one of the previously listed erosion models (Jürgens and Fander, 1993; Sharma and Singh, 1995; Mitasova et al., 2002).

Links to many other soil erosion models can be found on the World Wide Web at:

http://www3.bae.ncsu.edu/Regional-Bulletins/Modeling-Bulletin/
http://soilerosion.net/doc/models_menu.html

The performance of a given watershed-scale erosion model is best assessed within the context of its intended use. For instance, lumped empirical models of soil erosion, such as the USLE, are limited primarily to average sediment yield over a basin with the same characteristics as basins used in the model's development and cannot be used to assess spatial variability of erosion or to dynamically model the erosion process. Where applicable, USLE and RUSLE have been used with a good deal of success in assessing average yearly soil loss and in guiding land use and management decisions.

Distributed process-based models have been developed for a variety of different reasons (i.e., to assess and manage non-point source pollution; to explicitly model soil erosion; to model drainage basin evolution) and to be applied at a variety of different spatial and temporal scales with varying degrees of success. Synopsis of published reviews from applications of some of the available models are included below:

- An evaluation of WEPP in comparison to the USLE and the RUSLE indicates that WEPP predicts soil loss (kg/m^2) almost as well as the USLE and RUSLE at many sites, worse on others, and better on a few (Tiwari et al., 2000). Model efficiency, based on the Nash-Sutcliffe coefficient, ranged from -10.54 to 0.85 for the USLE and from -37.74 to 0.94 for WEPP. The Nash-Sutcliffe coefficient provides a measure of a model's performance over the course of an event as compared to the mean discharge for the event (Nash and Sutcliffe, 1970). A model efficiency of 1.0 represents a perfect fit of the model to observed values. Negative values indicate that use of the average (USLE in the evaluation of WEPP) is a better predictor than the model. The measured performance of WEPP compared to the USLE is considered a success given that the USLE performance at these sites is good and that the sites are where USLE parameters had been determined.

- A comparison by Bingner et al. (1989) of several erosion models applied to watersheds in Mississippi revealed that no model simulated sediment yield well on a consistent basis, though results are satisfactory to aid in management practice decisions. The models that were compared included CREAMS and the Simulator for Water Resources in Rural Basins (SWRRB) (Williams et al., 1985), the Erosion-Productivity Impact Calculator (EPIC) (Williams et al., 1984), ANSWERS, and AGNPS. For example, simulated results are within 50% of observed values for SWRRB (a modification of CREAMS) and AGNPS on one watershed and within 30% of observed values on another watershed. Error was as high as 500% for some models, and as low as 20% for others. The input

parameters varied for each of these models and each model was developed for different applications. For example, ANSWERS and AGNPS are designed as single-event models on large watersheds (up to 10,000 ha), EPIC is designed for small watersheds (~1 ha), and CREAMS is designed for field sized watersheds (Bingner et al., 1989). A model like ANSWERS that did not perform as well on watersheds in Mississippi may require more updates of parameters, in which case its performance would be improved.

- Wicks and Bathurst (1996) show that SHESED does well at predicting sediment volume over the course of a snowmelt season but simulations at smaller time and spatial scales are less successful.

- EUROSEM, a single event model, was tested by Parsons and Wainwright (2000) on a watershed in Arizona. The hydrologic component did very poorly with good results for only the last 10 minutes of the simulation. Though EUROSEM underestimated runoff, soil erosion was overestimated by an order of magnitude. In order to obtain reasonable results, changing a measured parameter well beyond its recommended value was required.

- Kothyari and Jain (1997) used GIS techniques in combination with the USLE to estimate watershed-scale sediment yield. Performance of this model was adequate to poor with error in the range of 0.65-6.60 (ratio of observed sediment yield to simulated), which is in the range seen with physically based models.

While erosion models have been widely tested and evaluated (Mitchell et al., 1993; Wu et al., 1993; Smith et al., 1995; Bingner, 1996; Bouraoui and Dillaha, 1996; Zhang et al., 1996; Folly et al., 1999; Schröder, 2000; Tiwari et al., 2000; Ogden and Heilig, 2001; Kirnak, 2002), it is difficult to objectively compare the performance of these models to each other. That is, determining "the best" model depends on the watershed characteristics and the purpose of the investigation. Additionally, physically based models vary in the degree to which they represent the physical processes of erosion (Wu et al., 1993). For instance, models such as CREAMS, WEPP, and EUROSEM explicitly and separately account for erosion in interrill areas and rills, whereas models such as ANSWERS, CASC2D, and GSSHA lump rill and interrill erosion into a single process. However, if success in watershed-scale erosion modeling is defined by accuracy in prediction of sediment discharge at a watershed outlet, the following general comments may be made.

Watershed-scale erosion models tend to be less accurate for event-scale prediction of sediment yield than for average soil loss per year, per month, or over a number of events. It is likely that spatial variability and the random nature of the erosion process are at least partially responsible for inaccuracies on small time scales. Over longer time scales, these effects tend to average out; hence, the increased accuracy in model prediction over longer time periods. There is a tendency for models to overpredict erosion for small runoff conditions and underpredict erosion for larger runoff conditions (Nearing, 1998). This is the case with the USLE, RUSLE, WEPP, and several other models. However, Ogden and Heilig (2001) report overprediction on large events for CASC2D.

Many models utilize a simple relation between soil particle detachment, interrill erosion, and rainfall intensity or kinetic energy of rainfall, $D_r = f(i)$, where D_r is the rate of soil detached by rainfall (kg/m^2/s) and i is rainfall intensity (mm/hr). Parsons and Gadian (2000) question the validity of such a simple relation and point out that lack of a clear-cut relation brings much uncertainty into modeling soil erosion. A great deal of error may be introduced into a model as a result. For instance, Daraio (2002) introduced a simple relation between kinetic energy of rainfall and soil particle detachment to GSSHA. Some improvement in model performance was seen on smaller scales in dynamic modeling of erosion, but the model performed better without the rainfall detachment term on larger spatial scales. There is a need to better understand the relationship between rainfall intensity, raindrop size distribution, kinetic energy of rainfall, and soil erosion and incorporate this understanding into erosion models.

Two-dimensional models provide a more accurate prediction of spatial distributions of sediment concentrations than one-dimensional models, but there is little difference between one- and two-dimensional models at predicting total sediment yield at a defined outlet (Hong and Mostaghimi, 1997). This is expected, given the success of lumped empirical models at sediment yield prediction. The complexity of flow on overland surfaces and the redistribution of sediment that occurs in such a flow regime can be more accurately modeled in two dimensions than in one dimension.

Understanding and predicting redistribution of sediment through detachment and deposition that results from variations in micro-topography on upland surfaces represents a major challenge in erosion modeling. There is also a need to better understand the relationship between interrill and rill flow; i.e., what is the relative contribution of sediment from interrill areas (raindrop impact) relative to rill areas. For instance, Ziegler et al. (2000) found that raindrop impact contributed from 38-45% of total sediment from erosion on unpaved roads. The application of this result to upland erosion is not clear, and there is a lack of information on this topic in the literature. These general deficiencies must be remedied in order to meet the need for more accurate erosion modeling.

Only a few erosion models have been developed for the purpose of dynamically simulating suspended sediment concentrations and to estimate Total Maximum Daily Load (TMDL) of sediment (see Section 2.4.1) in watersheds. One such model is CASC2D. The soil erosion component of CASC2D has been developed for the purpose of dynamically simulating suspended sediment concentrations with the aim of assessing the TMDL of sediment (Ogden and Heilig, 2001). It uses modifications to the semi-empirical Kilinc and Richardson (1973) equation that estimates sediment yield as a function of the unit discharge of water and the slope of the land surface. This function is further modified by three of the six parameters from the empirical USLE. The relation is given by the following equation (Johnson et al., 2000):

$$q_s = 25500 q^{2.035} S_f^{1.664} \left(\frac{KCP}{0.15} \right) \tag{2.36}$$

where q_s = sediment unit discharge (tons/m/s),
q = unit discharge of overland flow (m^2/s) (calculated within the overland flow component of CASC2D),
S_f = friction slope, and
K, C, and P = USLE parameters shown in Equation (2.1).

The factors K, C, and P are calibrated with constraints determined by values reported in the literature; e.g., as found in the RUSLE Handbook (Renard et al., 1996). These empirical factors have been derived as representing annual averages of soil loss, and use of them in an event-based dynamic model is problematic.

While the hydrologic component of CASC2D performs very well (Senarath et al., 2000), the overall performance of the erosion component of CASC2D is poor and there are several formulation areas in need of improvement (Ogden and Heilig, 2001). That is, major changes in the method of development are needed, such as using a purely process-based equation, rather than a semi-empirical equation, to simulate erosion. The sediment volume is underestimated by the model by up to 85%, and peak discharge is underestimated by an order of magnitude on internal sub-basins for the calibration event. Simulated sediment volume on a non-calibration event varied from 7 to 77% of observed volumes, and peak sediment discharge varied from 37 to 88% of observed values. The model grossly overestimated sediment yield on a heavy rainfall event, up to 360% error. The model does not reliably estimate sediment yield, nor does it dynamically model soil erosion accurately. GSSHA has been developed directly from CASC2D, and the erosion component in GSSHA is identical to the one in CASC2D. The preliminary indication, based upon an attempt to improve the erosion modeling capabilities of GSSHA (Daraio, 2002), is that Equation (2.36) is not a good predictor of erosion rates. It is likely that a new erosion algorithm and a new set of equations are needed to improve the model, including the addition of rill modeling capabilities. Currently, the erosion component of GSSHA and CASC2D is in its development phase and should not be used as a tool for determining the TMDL of sediment.

The GSTARS 2.1 and GSTARS3 models (Yang and Simões, 2000, 2002) were developed to simulate and predict river morphological changes as a result of human activities or natural events (see Section 2.4.2). The GSTARS models have broad capabilities and have had success in modeling sediment transport and deposition within rivers, lakes, and reservoirs. The inclusion of upland erosion capabilities has been proposed to be added to the GSTARS models. The addition of upland erosion capabilities to the GSTARS models would represent a comprehensive watershed model (GSTAR-W) that utilizes a systematic, consistent, and well-proven theoretical approach. The GSTARS models would apply the unit stream power theory (Yang, 1973, 1979) and the minimum energy dissipation rate theory (Yang and Song, 1987) towards modeling soil erosion resulting from rainfall and runoff on land surfaces.

Sediment yield from upland areas has been shown to be strongly related to unit stream power (Yang, 1996). Sediment concentrations in overland flow also show a good relationship with unit stream power (Nearing et al., 1997). Additionally, unit stream power has been shown to be superior to other relations at predicting erosion of loose sediment on soils over a wide variety of

conditions (Nearing et al., 1997; Yang, 1996; Hairsine and Rose, 1992; Govers and Rauws, 1986; Moore and Burch, 1986). The ICOLD Sedimentation Committee report also confirmed that unit stream power is a good parameter for sedimentation studies.

While the erosion component of GSTAR-W is in its early stages of development, the fact that the model was developed as a process-based model to simulate sediment transport and river morphology gives it a great advantage over empirical and semi-empirical soil erosion models. Additionally, the integrated approach being taken in developing the erosion modeling capabilities of GSTAR-W is much more promising than current process-based approaches that have met with limited success.

In addition to the need for continued model development, there are some inherent difficulties to erosion modeling. Physically based models tend to require a relatively large number of calibrated parameters. This creates the need for good quality data sets, and also sets further limits on the applicability of such models. That is, it is not advisable to use a model in a watershed that does not have the requisite data. The most important parameters for process-based models are rainfall parameters (e.g., duration, intensity) and infiltration parameters (e.g., hydraulic conductivity). Poor quality input data can lead to large errors in erosion modeling. Additionally, soil erosion models are built upon the framework of hydrologic models that simulate the rainfall-runoff process. Any error that exists in the hydrologic model will be propagated with the error from the soil erosion model. However the error introduced from the simulated runoff is generally much less than the error from the simulation of erosion (Wu et al., 1993).

Due to the complexity of the surface erosion process, computer models are needed for the simulation of the process and the estimation of the surface erosion rate. The need for the determination of TMDL of sediment in a watershed also requires a process-based comprehensive computer model. The following five sections will describe the approaches used for developing a comprehensive, systematic, dynamic, and process-based model (Yang, 2002).

2.4.1 Total Maximum Daily Load of Sediment

The 1977 Clean Water Act (CWA) passed by the United States Congress sets goals and water quality standards (WQS) to "restore and maintain the chemical, physical, and biological integrity of the Nation's waters." The CWA also requires states, territories, and authorized tribes to develop lists of impaired waters. These impaired waters do not meet the WQS that states have set for them, even after point sources of pollution have installed the required level of pollution control technology. The law requires that states establish priority rankings for waters on the list and develop TMDLs for these waters. A TMDL specifies the maximum amount of point and non-point pollutant that a water body can receive and still meet the water quality standard. By law, the Environmental Protection Agency (EPA) must approve or disapprove state lists and TMDLs. If a submission is inadequate, the EPA must establish the list or the TMDL (U.S. Environmental Protection Agency, 2001).

A TMDL consists of three elements—total point source waste loads, total non-point source loads, and a margin of safety to account for the uncertainty of the technology needed for the determination of allowable loads. TMDLs are a form of pollution budget for pollutant allocations in a watershed. In the determination of TMDLs, seasonal and spatial variations must be taken into consideration. The EPA is under court order or consent decrees in many states to ensure that TMDLs are established by either the state or the EPA.

Table 2.11 is a U.S. Environmental Protection Agency (2000) list of causes of impairments by pollutants. Sediment is clearly the number one pollutant that causes water to be impaired. It should be noted that sediment type impacts have been combined with siltation, turbidity, suspended solids, etc.

Table 2.11. Causes of impairments

Pollutant	Number of times named as cause
Sediments	6,502
Nutrients	5,730
Pathogens	4,884
Metals	4,022
Dissolved oxygen	3,889
Other habitat alterations	2,163
pH	1,774
Temperature	1,752
Biologic impairment	1,331
Fish consumption advisories	1,247
Flow alterations	1,240
Pesticides	1,097
Ammonia	781
Legacy	546
Unknown	527
Organic	464

Non-point source pollution is the largest source of water pollution problems. It is the main reason that 40 percent of the assessed water bodies in the United States are unsafe for basic uses such as fishing or swimming. Most sediment in rivers, lakes, reservoirs, wetlands, and estuaries come from surface erosion in watersheds and bank erosion along rivers as non-point source pollutants.

When a tributary with heavy sediment load meets the main stem of a river, the sediment load from the tributary can be treated as a point source of input to the main stem. Similarly, sediments caused by landslides or produced at a construction site can also be treated as a point source of input to a stream. A comprehensive approach for the determination of TMDL of sediment from point sources and non-point sources should be an integrated approach for the whole river basin or watershed under consideration.

Sediments can be divided into fine and coarse. Rivers transport fine sediments mainly as suspended load. Fine sediments often carry various forms of agrochemical and other pollutants. Consequently, fine sediments can have significant impacts on water quality. Rivers transport coarse sediments mainly as bedload. A good quality of coarse sediments or gravel is essential for fish spawning. A comprehensive model for sediment TMDL should have the capabilities of integrating watershed sheet, rill, and gully erosion; sediment transport, scour and deposition in tributaries and rivers; and, finally, sediment deposition in lakes, reservoirs, wetlands, or at sea. It should be a process-oriented model based on sound theories and engineering practice in hydrology, hydraulics, and sediment transport. The model should be applicable to a wide range of graded materials with hydraulic conditions ranging from subcritical to supercritical flows. A geographic information system (GIS) or other technology should be used to minimize the need of field data for model calibration and application.

Different authors have proposed different sediment transport formulas. Sediment transport concentrations or loads computed by different formulas for a given river may differ significantly from each other and from measurements. Chapters 3 and 4 address the subjects of sediment transport for non-cohesive and cohesive materials, respectively.

2.4.2 Generalized Sediment Transport Model for Alluvial River Simulation (GSTARS)

The sediment concentration or load computed by a formula is the equilibrium sediment transport rate without scour nor deposition. Natural rivers constantly adjust their channel geometry, slope, and pattern in response to changing hydrologic, hydraulic, and geologic conditions and human activities to maintain dynamic equilibrium. To simulate and predict this type of dynamic adjustment, a sediment routing model is needed. An example of this type of model is the Reclamation's GSTARS 2.1 model (Yang and Simões, 2000). GSTARS 2.1 uses the stream tube concept in conjunction with the theory of minimum energy dissipation rate, or its simplified theory of minimum stream power, to simulate and predict the dynamic adjustments of channel geometry and profile in a semi-three-dimensional manner.

Figure 2.14 demonstrates the capability of GSTARS 2.1 to simulate and predict the dynamic adjustments of channel width, depth, and shape downstream of the unlined emergency spillway of Lake Mescalero in New Mexico. Figure 2.14 shows that the predicted results with optimization based on the theory of minimum stream power can more accurately simulate and predict the dynamic adjustments of channel shape and geometry than the simulation without the optimization options. Figure 2.14 also shows that the process of channel bank erosion can be simulated and predicted fairly accurately.

GSTARS3 (Yang and Simões, 2002) is an enhanced version of GSTARS 2.1 to simulate and predict the sedimentation processes in lakes and reservoirs. It can simulate and predict the formation and development of deltas, sedimentation consolidation, and changes of reservoir bed profiles as a result of sediment inflow in conjunction with reservoir operation.

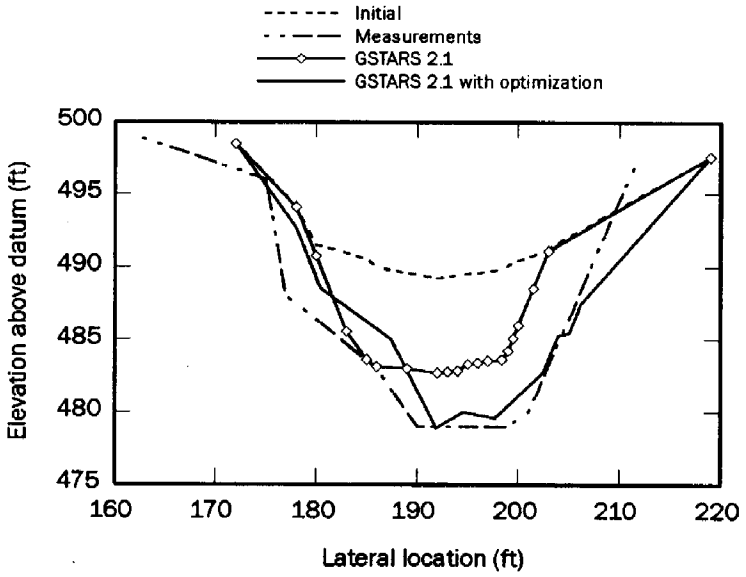

Figure 2.14. Comparison of results produced by GSTARS 2.1 and survey data for runs with and without width changes, due to stream power minimization (Yang and Simões, 2000).

Figure 2.15 shows an example of comparison between the predicted and observed delta formation (Swamee, 1974) in a laboratory flume. Figure 2.16 shows a comparison between the measured and simulated bed profiles using GSTARS3 for Tarbela Reservoir. GSTARS 2.1 and GSTARS3 enable us to simulate and predict the evolution of a river system with sediment from a tributary as a point source of sediment input and bank and bed erosion along a river reach as non-point source inputs to a river system. Reservoirs, lakes, and wetlands in a watershed can be considered as sinks for sediments.

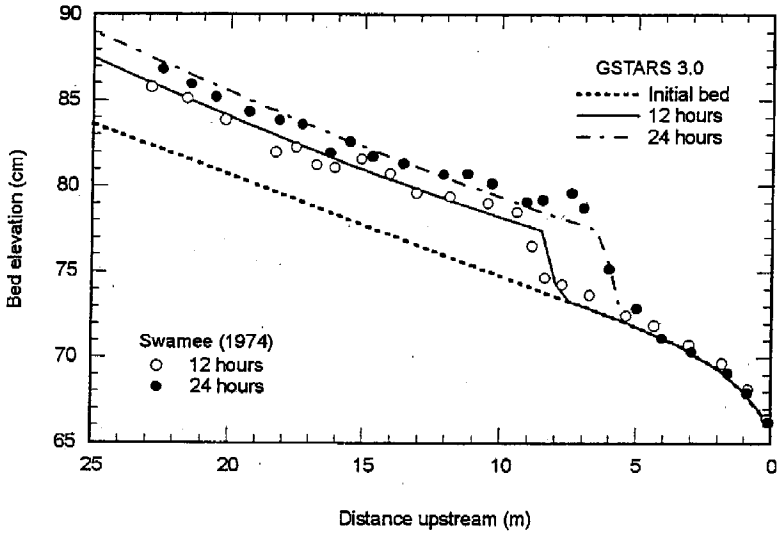

Figure 2.15. Comparison of experiments with simulations of reservoir delta development for two time instants (Yang and Simões, 2002).

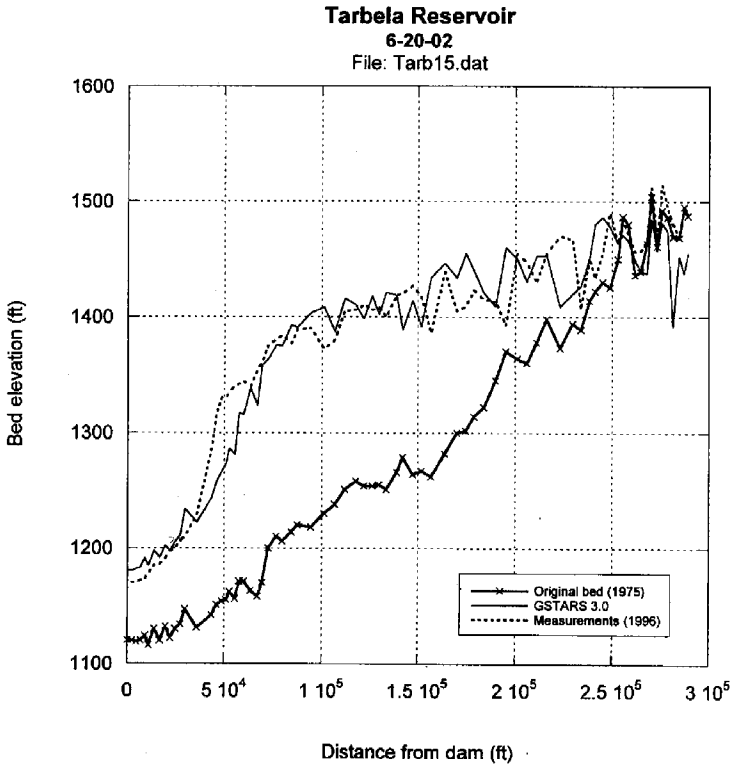

Figure 2.16. Comparison between measured and simulated bed profiles by GSTARS3 for the Tarbela Reservoir in Pakistan (Yang and Simões, 2001).

2.4.3 Rainfall-Runoff Relationship

Rainfall intensity, duration, and distribution in a watershed with given geologic and surface cover conditions will determine the surface runoff. Once the surface runoff is given, sheet, rill, and gully erosion rate of a watershed can be computed. *Computer Models of Watershed Hydrology* (Singh, 1995) summarizes some of the rainfall-runoff models. Some of these models also have certain abilities to simulate sheet erosion rates of a watershed. However, none of the existing models are based on a unified approach for the determination of erosion, sediment transport, and deposition in a watershed as described in this chapter. These models include, but are not limited to, the Precipitation-Runoff Modeling System (PRMS) by Leavesley et al. (1983) and the Hydrological Simulation Program—FORTRAN (HSPF) by Johanson et al. (1984). These models are modular, interactive programs. Input data include meteorologic, hydrologic, snow, and watershed descriptions. The outputs are runoff hydrographs, including maximum discharge, flow volume, and flow duration. Figure 2.17 is a schematic diagram of the PRMS model. The output information of these types of models can be used as part of the input information needed for a river sediment routing model such as Reclamation's GSTARS 2.1 and GSTARS3 computer models. Due to the complexity of sheet, rill, and gully erosion, a new model GSTAR-W needs to be developed and tested.

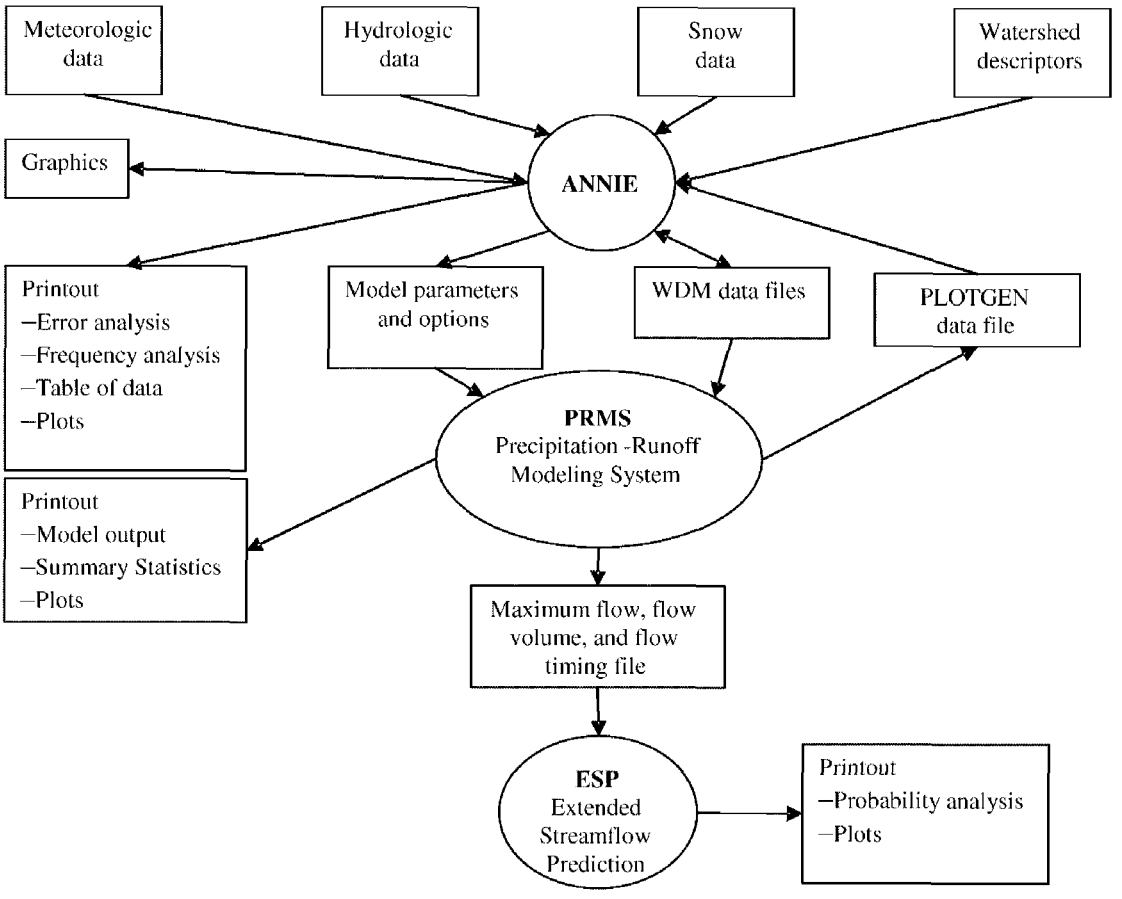

Figure 2.17. Flowchart of the PRMS model (Leavesley et al., 1993).

2.4.4 GSTAR-W Model

The loss of topsoil due to surface erosion not only can cause environmental problems, but it can also have adverse impacts on the agricultural productivity of a watershed. The United Nations Atomic Energy Agency has organized a 5-year international effort to determine surface erosion using radio isotopes as tracers. China has selected one watershed to test this fingerprinting technology. Reclamation will use the field data collected under different hydrologic, geologic, topographic, and sediment conditions for the calibration of GSTAR-W. Field data on rainfall-runoff relationships exist in the literature and will also be used for the calibration of GSTAR-W. GIS and other technology will be used to collect information on watershed topography, ground cover, and land use. With the calibrated and verified GSTAR-W and the already tested GSTARS 2.1 and GSTARS3 models, we can simulate and predict the sheet, rill, and gully erosion of a watershed as well as the river morphologic processes of bank and bed erosion, sediment transport, and depositions in rivers, lakes, reservoirs, and wetlands in a given watershed.

The EPA and other agencies can also use these integrated models to assess the impacts on TMDL of sediment due to a change of land use or other human activities. These models can become useful management tools for the selection of an optimum plan of action and the allocation of sediment TMDLs. Figure 2.18 is a decisionmaking flowchart of the integrated processes. It should be pointed out that computed hydraulic parameters from this integrated model can also be used for the determination of TMDLs of other pollutants in a watershed.

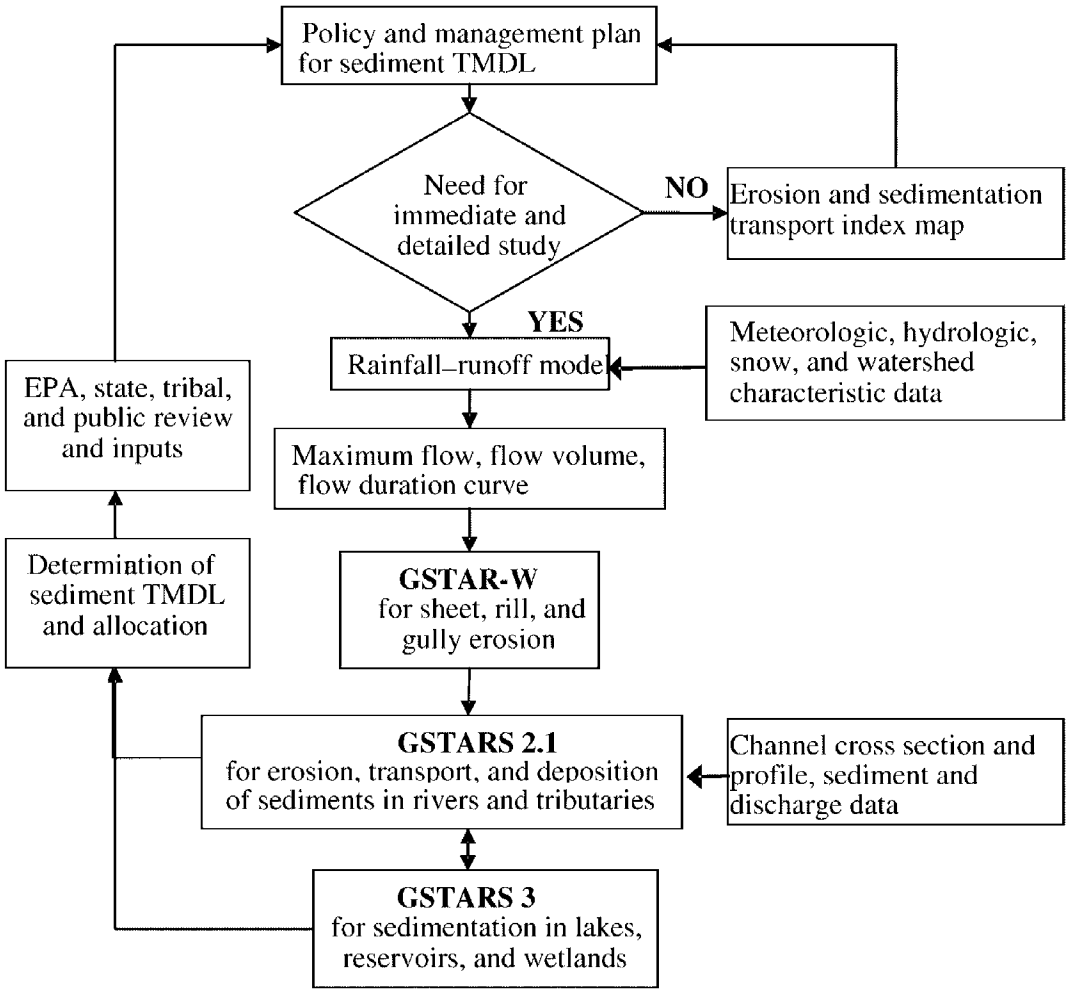

Figure 2.18. Sediment TMDL study and decision making flowchart.

2.4.5 Erosion Index Map

The amount of work and associated costs to determine TMDL of sediment are huge and will not be accomplished in a few years. A need exists to develop erosion index maps to identify areas that need immediate attention and possible remedial measures. It has been shown that the dimensionless unit stream power VS/ω is the most important parameter for the determination of erosion and sediment transport rates. GIS or topographic map information can be used for the estimation of slope S of a watershed. The average velocity V can be computed from Manning's formula for a given discharge Q, sediment size d, and surface roughness n. The fall velocity ω is proportional to the square root of particle diameter d. Thus, a preliminary estimation of VS/ω can be made, and erosion index maps can be developed based on the distribution of VS/ω. These maps may need to be modified with ground cover data which can also be obtained from GIS and other sources of information. Thus, a modified erosion index GVS/ω should be used. G is the ground cover factor with a value between 0 for paved surfaces and 1 for surfaces with no ground cover.

2.5 Example Case Studies

The methods described in this chapter are applied to an example case study in southwestern Arizona, where three small reservoirs have been proposed. The volume of sediment that would be expected to settle in these reservoirs over a 100-year period is computed for these examples. The study area is near the downstream end of the Colorado River basin in one of the driest desert regions of North America (Olmstead et al., 1973). The frequency of rainfall events that actually produce runoff is expected to be one to two times per year.

The first reservoir would have a storage capacity of 16,400 acre-feet and an average depth over 40 feet. The second reservoir would have a storage capacity of 8,700 acre-feet and an average depth of 21 feet. The third reservoir would have a storage capacity of 11,000 acre-feet and an average depth of 12 feet. Three separate drainage areas have been delineated for the first two reservoirs, and two separate drainage areas have been identified for the third reservoir.

2.5.1 Drainage Area Descriptions

The drainage areas for the proposed reservoir sites are desert foothills with steep to very steep terrain. The surface topography is composed of jagged rock, gravel, and sand. Little vegetation grows in these basins, except for sparsely spaced desert brush and clumps of grass. Stream bottoms are steep and sandy. The drainage areas are capable of producing flash flood conditions and large sediment volumes in the event of intense rainfall. Table 2.12 summarizes drainage basin characteristics for each of the proposed reservoir sites.

Since the reservoirs would normally be operated to completely contain runoff from local storms, they are expected to contain all of the sediment. Therefore, the trap efficiency for each reservoir is assumed to be 100 percent.

Table 2.12. Reservoir drainage basin characteristics

Proposed reservoir	Drainage basin	Drainage area (mi^2)	Drainage length (mi)	Average length (mi)	Drainage slope (%)
Reservoir 1	Unnamed Wash East	8.5	6.77	1.26	2.08
	Mission Wash	7.1	7.20	0.99	2.92
	Mission Wash East	2.2	1.50	1.47	6.00
Reservoir 2	Picacho Wash	43.7	16.20	2.70	0.90
	Unnamed Wash	30.2	12.60	2.40	1.39
	Picacho Wash East	2.0	3.44	0.58	1.43
Reservoir 3	Upper drainage area	9.72	2.86	3.40	2.67
	Lower drainage area	10.1	4.31	2.34	2.25

2.5.2 Example Computations of Sediment Yield

No stream gauges of flow or sediment load exist on any of the drainage areas, so the 100-year sediment yield cannot be based on direct measurements. The following four methods were used to estimate the amount of sediment inflow to the proposed reservoirs after 100 years (Randle, 1998):

- The Revised Universal Soil Loss Equation.
- Empirical equations that predict sediment yields as a function of drainage area.
- A sediment yield classification procedure that predicts sediment yields as a function of nine drainage basin characteristics.
- Unit stream power theory for sheet erosion that predicts sediment yields as a function of the runoff rate, velocity, drainage slope, and sediment particle characteristics.

2.5.3 Example Based on the RUSLE

Figure 2.4 gives a R_R value for southeastern Arizona that varies from 10 to 30. Some supplemental information is needed on the soil type and cover of the area, so a site assessment would be necessary before the RUSLE can be applied. The following is assumed to be the case for all sites. The soils are sandy with little or no structure, 80% silt and sand, no clay, and no organic matter. Assuming slow to moderate permeability with 20% coarse fragments > 3 inches and 80% less than 2 mm, calculation of K_R using the RUSLE program yields a value of 0.65. The area is a desert shrub habitat with approximately 10% canopy cover and 10% rock and residue

cover; calculation of C_R using the RUSLE program yields a value of 0.11 because the area is highly susceptible to rill erosion. Table 2.13 is used to estimate the LS_R factor. The LS_R values shown in Table 2.14 were obtained by assuming the maximum slope length. The P_R factor is equal to 1 because no management practices are used. The sediment yield results are shown in Table 2.14.

Table 2.13. Values of the topographic LS_R factor for slopes with a high ratio of rill to interrill erosion (Renard et al., 1996)

Slope (%)	Horizontal slope length (ft)											
	25	50	75	100	150	200	250	300	400	600	800	1000
0.2	0.05	0.05	0.05	0.05	0.05	0.06	0.06	0.06	0.06	0.06	0.06	0.06
0.5	0.07	0.08	0.08	0.09	0.09	0.10	0.10	0.10	0.11	0.12	0.12	0.13
1.0	0.10	0.13	0.14	0.15	0.17	0.18	0.19	0.20	0.22	0.24	0.26	0.27
2.0	0.16	0.21	0.25	0.28	0.33	0.37	0.40	0.43	0.48	0.56	0.63	0.69
3.0	0.21	0.30	0.36	0.41	0.50	0.57	0.64	0.69	0.80	0.96	1.10	1.23
4.0	0.26	0.38	0.47	0.55	0.68	0.79	0.89	0.98	1.14	1.42	1.65	1.86
5.0	0.31	0.46	0.58	0.68	0.86	1.02	1.16	1.28	1.51	1.91	2.25	2.55
6.0	0.36	0.54	0.69	0.82	1.05	1.25	1.43	1.60	1.90	2.43	2.89	2.30
8.0	0.45	0.70	0.91	1.10	1.43	1.72	1.99	2.24	2.70	3.52	4.24	4.91
10.0	0.57	0.91	1.20	1.46	1.92	2.34	2.72	3.09	3.75	4.95	6.03	7.02
12.0	0.71	1.15	1.54	1.88	2.51	3.07	3.60	4.09	5.01	6.67	8.17	9.57
14.0	0.85	1.40	1.87	2.31	3.09	3.81	4.48	5.11	6.30	8.45	10.40	12.23
16.0	0.98	1.64	2.21	2.73	3.68	4.56	5.37	6.15	7.60	10.26	12.69	14.96
20.0	1.24	2.10	2.86	3.57	4.85	6.04	7.16	8.23	10.24	13.94	17.35	20.57
25.0	1.56	2.67	3.67	4.59	6.30	7.88	9.38	10.81	13.53	18.57	23.24	27.66
30.0	1.86	3.22	4.44	5.58	7.70	9.67	11.55	13.35	16.77	23.14	29.07	34.71
40.0	2.41	4.24	5.89	7.44	10.35	13.07	15.67	18.17	22.95	31.89	40.29	48.29
50.0	2.91	5.16	7.20	9.13	12.75	16.16	19.42	22.57	28.60	39.95	50.63	60.84
60.0	3.36	5.97	8.37	10.63	14.89	18.92	22.78	26.51	33.67	47.18	59.93	72.15

Such as for freshly prepared construction and other highly disturbed soil condition with little or no cover (not applicable to thawing soil).

Table 2.14. Sediment yield estimates based on the empirical RUSLE

Proposed Reservoir	Drainage Basin	LS_R	Area (mi^2)	$R_R = 10$		$R_R = 30$	
				Average annual sediment yield (acre-ft/mi^2)	100-year sediment yield (acre-ft)	Average annual sediment yield (acre-ft/mi^2)	100-year sediment yield (acre-ft)
Reservoir 1	Unnamed Wash East	0.69	8.5	0.24	206	0.73	619
	Mission Wash	1.23	7.1	0.43	307	1.30	922
	Mission Wash East	3.3	2.2	1.16	256	3.48	767
	Total		17.8		769		2,308
Reservoir 2	Picacho Wash	0.24	43.7	0.08	369	0.25	1,108
	Unnamed Wash	0.43	30.2	0.15	457	0.45	1,371
	Picacho Wash East	0.44	2.0	0.15	31	0.46	93
	Total		75.9		857		2,572
Reservoir 3	Upper drainage area	1	9.72	0.35	342	1.06	1,026
	Lower drainage area	0.85	10.1	0.30	302	0.90	907
	Total		19.82		644		1,933

2.5.4 Example Based on Drainage Area

The empirical sediment yield equations for Arizona, New Mexico, and California (Equation 2.15) and for the semiarid climate of the southwestern United States (Equation 2.16) were applied to the drainage areas listed in Table 2.12. Table 2.15 presents the predicted sediment yields, using both of these equations, for each of the proposed reservoirs.

Table 2.15. Sediment-yield estimates based on empirical equations as a function of drainage area

Proposed reservoir	Drainage Basin	Area (mi^2)	Equation for New Mexico, Arizona, and California $Q_s = 2.4\,A^{-0.229}$		Equation for the southwestern United Sates $Q_s = 1.84\,A^{-0.24}$	
			Average annual sediment yield (acre-ft/mi^2)	100-year sediment yield (acre-ft)	Average annual sediment yield (acre-ft/mi^2)	100-year sediment yield (acre-ft)
Reservoir 1	Unnamed Wash East	8.5	1.47	1,250	1.10	936
	Mission Wash	7.1	1.53	1,090	1.15	816
	Mission Wash East	2.2	2.00	440	1.52	335
	Total	17.8		3,000		2,000
Reservoir 2	Picacho Wash	43.7	1.01	4,420	0.74	3,250
	Unnamed Wash	30.2	1.10	3,320	0.81	2,450
	Picacho Wash East	2.0	2.05	410	1.56	310
	Total	75.9		8,000		6,000
Reservoir 3	Upper drainage area	9.72	1.42	1,380	1.07	1,030
	Lower drainage area	10.1	1.41	1,430	1.06	1,070
	Total	19.8		3,000		2,000

These 100-year sediment volume estimates are computed only as a function of drainage area and do not consider site-specific characteristics of the drainage basin or individual runoff events. The sediment yields from the two equations are different but they are of the same order of magnitude. For the second reservoir, the sediment yield estimates are 70 to 90 percent of the proposed reservoir storage capacity. This would indicate that more detailed investigations are warranted.

2.5.5 Example Based on the Sediment Yield Classification Procedure

The sediment yield classification procedures presented in Tables 2.9 and 2.10 were applied to all of the proposed reservoir drainage basins as a whole. All ratings were based on field inspection. Table 2.16 presents the estimated ratings for each drainage basin characteristic. These drainage basins are a class 3 sediment yield based on the ratings for each of the nine drainage basin characteristics. Applying an annual sediment yield of 0.5 to 1.0 acre-ft/mi^2 to each of the separate drainage basins provides an estimate of the 100-year sediment volume (Table 2.17). The ranges of sediment yields computed using this method tend to be less than those computed as a function of drainage area, but they are of the same order of magnitude.

Table 2.16. Estimated numerical ratings for the proposed reservoir drainage basins

Drainage basin characteristics	Possible ratings		Estimated sediment yield rating	Estimate description
Surface geology	0 - 10	5	Moderate	Varies from hard, dense crystalline rocks to unconsolidated alluvium and windblown sand.
Soils	0 - 10	0	Low	Surface material is sand, rock fragments, and bedrock outcrops.
Climate	0 - 10	0	Low	Arid climate with rare convective storms.
Runoff	0 - 10	0	Low	On average, only 1 to 2 storms per year that produce runoff.
Topography	0 - 20	20	High	Desert foothill terrain that is steep to very steep and dissected Piedmont slopes.
Ground cover	-10 - 10	10	High	Little vegetation, except for sparsely spaced desert brush and grass.
Land use	-10 – 10	-10	Low	There is no cultivation or grazing.
Upland erosion	0 – 25	10	Moderate	Upland mountains and hills are composed of older, more consolidated rocks and are estimated to have moderate erosion rates.
Channel erosion	0 – 25	25	High	Erosion on the dissected Piedmont slopes is the dominant process today and has been for the past several thousand years. Desert pavement is generally conspicuous.
Total rating		60	Class 3	0.5 to 1.0 ac-ft/mi^2/yr.

Table 2.17. 100-year sediment yield estimates

Proposed reservoir	Drainage basin	Area (mi^2)	100-year sediment yield (ac-ft)	
			at 0.5 ac-ft/mi^2/yr	at 1.0 ac-ft/mi^2/yr
Reservoir 1	Unnamed Wash East	8.5	425	850
	Mission Wash	7.1	355	710
	Mission Wash East	2.2	110	220
	Total	17.8	900	2,000
Reservoir 2	Picacho Wash	43.7	2,185	4,370
	Unnamed Wash	30.2	1,510	3,020
	Picacho Wash East	2.0	100	200
	Total	75.9	4,000	8,000
Reservoir 3	Upper drainage area	9.7	485	970
	Lower drainage area	10.1	505	1,010
	Total	19.8	1,000	2,000

2.5.6 Example Based on Unit Stream Power

The physically based equation for sheet erosion (Yang, 1996; Moore and Burch, 1986) was combined with a flood hydrology analysis to compute the 100-year sedimentation volume for each reservoir drainage basin. Required input for this procedure includes the following data:

- Flood hydrology analysis, including magnitude, duration, and frequency.
- Manning's roughness coefficient.
- Drainage slope and average width.
- Sediment particle characteristics including size, fall velocity, and incipient motion velocity.

2.5.6.1 Flood Hydrology

Flood hydrographs were computed for return periods of 100, 50, 25, 10, and 5 years. These hydrographs were determined from regional rainfall data because no stream gauge measurements existed. The flood hydrographs were computed with a 5-minute time step with total durations ranging from 2.3 to 14.1 hours. Table 2.18 lists the peak discharge values for each of these rainfall-runoff floods. Table 2.19 is an annual flow-duration table for the flood return periods of 100, 50, 25, 10, 5, 2, and 1 years.

Table 2.18. Peak discharge values computed for each drainage basin

Reservoir	Drainage basin	Peak flood discharge (ft^3/s)				
		100-year flood	50-year flood	25-year flood	10-year flood	5-year flood
Reservoir 1	Unnamed Wash East	3,840	2,830	2,540	1,130	652
	Mission Wash	3,410	2,510	1,770	1,010	579
	Mission Wash East	1,930	1,420	996	569	324
Reservoir 2	Picacho Wash	7,740	5,690	4,010	2,280	1,310
	Unnamed Wash	6,620	4,870	3,430	1,950	1,130
	Picacho Wash East	1,840	1,350	948	540	315
Reservoir 3	Upper drainage area	8,310	NA	NA	NA	NA
	Lower drainage area	4,460	3,280	2,310	1,320	755

On average, one to two rainfall events that produce runoff are expected to occur each year over the drainage basins of the proposed reservoirs. Over a 100-year period, this would amount to between 100 and 200 runoff events. From Table 2.19, the total number of annual floods is assumed to be 100 over a 100-year period, because this procedure only accounts for the largest flood from each year. For example, a 5-year flood would not be counted if it occurred in a year in

which the peak discharge for that year was greater (i.e., had a return period of 10, 25, 50, or 100 years). Therefore, the annual series was transformed into a partial duration series using the method described by Linsley et al. (1975) and William Lane (Hydraulic Engineer, Reclamation, Denver, Colorado, personal communication). The partial series is made up of all floods above some selected base value. The base value is chosen so that not more than a certain number of floods N are included for each year. The partial series can then indicate the probability of floods being equaled or exceeded N times per year.

Table 2.19. Annual flow duration table

Flood return period	Number of times that the flood is equaled or exceeded during 100 years	Number of annual floods
100	1	1
50	2	1
25	4	2
10	10	6
5	20	10
2	50	30
1	100	50
Total		100

$$P_{annual} = 1/T_{partial} = 1 - (1 - P_{partial}/T_{annual})^{N} \tag{2.37}$$

where P_{annual} = the annual probability of floods being equaled or exceeded once per year,
T_{annual} = the annual return period, in years, associated with the annual probability,
$P_{partial}$ = the probability of floods being equaled or exceeded N times per year, and
N = the number of floods per year.

Solving for $P_{partial}$, Equation (2.37) can be expressed as:

$$P_{partial} = 1/T_{partial} = N\,[1 - (1 - 1/T_{annual})^{1/N}] \tag{2.38}$$

where $T_{partial}$ = the partial series return period, in years, associated with $P_{partial}$

The partial duration series was computed for a range of return periods, assuming no more than two floods per year for a total of 200 floods over a 100-year period (Table 2.20). The largest flood considered was that associated with the 200-year return period because, of all the floods exceeding the 100-year flood, half would be greater than the 200-year flood. From the partial duration series (last column of Table 2.20), the number of floods expected to occur during a 100-year period was used for the computation of the 100-year sediment volume.

Table 2.20. Transformation of annual flood series to a partial duration series, assuming no more than two floods per year

Annual peak flood series			Partial duration series			
Flood return period (yr)	Number of times exceeded in 100 yr	Number of floods in 100 yr	Flood return period (yr)	Flood return period (yr)	Number of times exceeded in 100 yr	Number of floods in 100 yr
>200.00	<0.500	1.000	200.00	99.505	<0.501	1.003
100.00	1.000	0.111	95.00	94.749	1.003	0.112
90.00	1.111	0.139	85.00	84.749	1.114	0.140
80.00	1.250	0.179	75.00	74.749	1.254	0.180
70.00	1.429	0.238	65.00	64.749	1.434	0.240
60.00	1.667	0.333	55.00	54.749	1.674	0.336
50.00	2.000	0.500	45.00	44.749	2.010	0.506
40.00	2.500	0.833	35.00	34.748	2.516	0.846
30.00	3.333	0.667	27.50	27.248	3.362	0.679
25.00	4.000	1.000	22.50	22.247	4.041	1.023
20.00	5.000	1.667	17.50	17.246	5.064	1.718
15.00	6.667	3.333	12.50	12.245	6.782	3.482
10.00	10.000	4.286	8.50	8.242	10.263	4.573
7.00	14.286	5.714	6.00	5.738	14.836	6.279
5.00	20.000	5.000	4.50	4.234	21.115	5.680
4.00	25.000	25.000	3.00	2.720	26.795	31.784
2.00	50.000	16.667	1.75	1.445	58.579	25.951
1.50	66.667	10.256	1.40	1.073	84.530	19.393
1.30	76.923	13.986	1.20	0.839	103.923	35.775
1.10	90.909	9.091	1.05	0.608	139.698	60.302
1.00	100.000	9.091	1.05	0.608	200.000	60.302
Total		100.00		Total		200.00

2.5.6.2 Application of the Sheet Erosion Equation

For each drainage basin, the sediment concentration was computed using Equation (2.18) for each 5-minute discharge of a given flood hydrograph. The sediment inflow volumes to each reservoir were computed for the 5-, 10-, 25-, 50-, and 100-year flood hydrographs. The sediment volumes corresponding to the return periods listed in Table 2.20 (5th column) were computed from a regression equation (specific to each drainage basin). The regression equations were computed from the logarithms of the sediment volumes (dependent variable) and the logarithms of the corresponding flood return periods (independent variable). The 100-year sediment volume was computed by accumulating the products of the sediment inflow volume, corresponding to a given range of floods, and the number of times floods in that range are expected to occur during a 100-year period (see Table 2.20, last column).

The Manning's n roughness coefficient in Equation (2.29) was assumed to be a constant of 0.030. Table 2.12 lists the drainage area and length, and slope S for each drainage basin. The drainage width was computed as the ratio of the drainage length to area. Sediment load was computed from each concentration, and a bulk density of 70 lbs/ft^3 was assumed to convert the sediment load to volume.

The soils of the drainage basins are primarily sand and coarser size material. The median sediment particle size was assumed to be within sand-size range (0.06 mm to 2.0 mm) but the size was not precisely known for any of the drainage basins. Therefore, 100-year sediment volumes were computed assuming a range of sand sizes. Table 2.21 lists the particle sizes and fall velocities used in the analysis.

Table 2.21. Sediment particle sizes and fall velocities (U.S. Committee on Water Resources, Subcommittee on Sedimentation, 1957)

Sediment particle size (mm)	Sediment particle fall velocity (cm/s)
0.06	0.25
0.1	0.60
0.2	1.81
0.5	5.72
1.0	11.4
2.0	19.0

2.5.6.3 Results

Tables 2.22 through 2.31 present summary results of the unit stream power procedure for each reservoir, drainage basin, flood, and assumed sediment particle size. Except for the 100-year flood, a flood- hydrology analysis was not completed for the upper drainage area.

The average 100-year sediment yield (per unit area) for the upper and lower drainage areas was assumed to be equal (Table 2.30). The 100-year sediment volume for the canal drainage area was computed by multiplying the average 100-year sediment yield per unit area by the canal drainage area of 9.72 mi^2 (see Table 2.31).

Sediment concentration was found to be sensitive to particle size. In some cases, the range of possible particle sizes could be reduced by examination of the computed peak sediment concentrations. A maximum concentration limit of 300,000 ppm was applied for the sand sizes of the study area. This is a reasonable limit, based on other streams, where long-term measurements exist. For example, the maximum mean daily concentration of record for the Rio Puerco near Bernardo, New Mexico (a major sediment-producing tributary of the Rio Grande) is 230,000 ppm.

Table 2.22. Reservoir 1, Unnamed Wash east drainage sediment yield estimates

Recurrence interval (yr)	Peak discharge (ft^3/s)	Sediment volume (ac-ft)					
		0.06 mm	0.1 mm	0.2 mm	0.5 mm	1 mm	2 mm
100	3,840	211.00	64.10	14.20	2.96	1.16	0.58
50	2,830	126.00	38.10	8.45	1.76	0.69	0.34
25	2,540	105.00	31.90	7.07	1.47	0.58	0.29
10	1,130	25.80	7.83	1.74	0.36	0.14	0.07
5	652	9.77	2.96	0.66	0.14	0.05	0.03
100-yr volume[1]			577.00	128.00	26.70	10.50	5.23

Recurrence interval (yr)	Peak discharge (ft^3/s)	Peak sediment concentration (ppm)					
		0.06 mm	0.1 mm	0.2 mm	0.5 mm	1 mm	2 mm
100	3,844	1,140,000	345,000	76,600	16,000	6,240	3,110
50	2,827	939,000	285,000	63,200	13,200	5,150	2,570
25	2,537	876,000	266,000	59,000	12,300	4,800	2,390
10	1,131	516,000	157,000	34,800	7,240	2,830	1,410
5	652	351,000	106,000	23,600	4,930	1,930	959

[1] See appendix for computation details.

Table 2.23. Reservoir 1, Mission Wash sediment yield estimates

Recurrence interval (yr)	Peak discharge (ft^3/s)	Sediment volume (ac-ft)					
		0.06 mm	0.1 mm	0.2 mm	0.5 mm	1 mm	2 mm
100	3,410	431.00	131.00	29.00	6.04	2.36	1.18
50	2,510	260.00	78.80	17.50	3.65	1.42	0.71
25	1,770	146.00	44.20	9.81	2.04	0.80	0.40
10	1,010	56.90	17.20	3.83	0.80	0.31	0.16
5	579	22.50	6.82	1.51	0.32	0.12	0.06
100-yr volume				256.00	53.30	20.80	10.40

Recurrence interval (yr)	Peak discharge (ft^3/s)	Peak sediment concentration (ppm)					
		0.06 mm	0.1 mm	0.2 mm	0.5 mm	1 mm	2 mm
100	3,410	2,350,000	713,000	158,000	33,000	12,900	6,420
50	2,510	1,960,000	595,000	132,000	27,500	10,800	5,360
25	1,770	1,590,000	482,000	107,000	22,300	8,720	4,340
10	1,010	1,130,000	341,000	75,800	15,800	6,170	3,080
5	579	795,000	241,000	53,500	11,200	4,360	2,170

Table 2.24. Reservoir 1, Mission Wash East sediment yield estimates

Recurrence interval (yr)	Peak discharge (ft^3/s)	Sediment volume (ac-ft)					
		0.06 mm	0.1 mm	0.2 mm	0.5 mm	1 mm	2 mm
100	1,930	249.00	75.60	16.80	3.50	1.37	0.68
50	1,420	150.00	45.40	10.10	2.10	0.82	0.41
25	996	81.90	24.80	5.51	1.15	0.45	0.22
10	569	31.80	9.65	2.14	0.45	0.17	0.09
5	324	12.30	3.74	0.83	0.17	0.07	0.03
100-yr volume				144.00	30.00	11.70	5.85

Recurrence interval (yr)	Peak discharge (ft^3/s)	Peak sediment concentration (ppm)					
		0.06 mm	0.1 mm	0.2 mm	0.5 mm	1 mm	2 mm
100	1,930	5,240,000	1,590,000	353,000	73,500	28,700	14,300
50	1,420	4,400,000	1,330,000	296,000	61,800	24,100	12,000
25	996	3,590,000	1,090,000	242,000	50,400	19,700	9,810
10	569	2,590,000	786,000	175,000	36,400	14,200	7,080
5	324	1,860,000	564,000	125,000	26,100	10,200	5,080

Table 2.25. Reservoir 1, total 100-year sediment volume

Total 100-year sediment volume (ac-ft)[1]					
0.06 mm	0.1 mm	0.2 mm	0.5 mm	1 mm	2 mm
1,000	1,000	500	100	40	20

[1] The total includes a sediment yield computed from a larger particle size. A larger particle size was used because the maximum probable concentration of 300,000 ppm was exceeded.

Table 2.26. Reservoir 2, Picacho Wash sediment yield estimates

Recurrence interval (yr)	Peak discharge (ft^3/s)	Sediment volume (ac-ft)					
		0.06 mm	0.1 mm	0.2 mm	0.5 mm	1 mm	2 mm
100	7,740	101.00	30.70	6.82	1.42	0.56	0.28
50	5,690	54.10	16.40	3.64	0.76	0.30	0.15
25	4,010	25.20	7.64	1.70	0.35	0.14	0.07
10	2,280	6.29	1.91	0.42	0.09	0.03	0.02
5	1,310	1.05	0.32	0.07	0.01	0.01	0.00
100-yr volume		664.00	201.00	44.70	9.31	3.62	1.81

Table 2.26. Reservoir 2, Picacho Wash sediment yield estimates (continued)

Recurrence interval (yr)	Peak discharge (ft^3/s)	Peak sediment concentration (ppm)					
		0.06 mm	0.1 mm	0.2 mm	0.5 mm	1 mm	2 mm
100	7,740	156,000	47,300	10,500	2,190	855	426
50	5,690	118,000	35,900	7,970	1,660	648	323
25	4,010	83,500	25,300	5,620	1,170	458	228
10	2,280	42,500	12,900	2,860	597	233	116
5	1,310	16,400	4,990	1,110	231	90	45

Table 2.27. Reservoir 2, Unnamed Wash sediment yield estimates

Recurrence interval (yr)	Peak discharge (ft^3/s)	Sediment volume (ac-ft)					
		0.06 mm	0.1 mm	0.2 mm	0.5 mm	1 mm	2 mm
100	6,620	215.00	65.10	14.50	3.01	1.18	0.78
50	4,870	124.00	37.70	8.38	1.75	0.68	0.48
25	3,430	65.70	19.90	4.42	0.92	0.36	0.27
10	1,950	22.52	6.83	1.52	0.32	0.12	0.11
5	1,130	7.39	2.24	0.50	0.10	0.04	0.59
100-yr volume			484.00	107.00	22.40	8.76	4.36

Recurrence interval (yr)	Peak discharge (ft^3/s)	Peak sediment concentration (ppm)					
		0.06 mm	0.1 mm	0.2 mm	0.5 mm	1 mm	2 mm
100	6,620	452,000	137,000	30,400	6,340	2,480	1,240
50	4,870	364,000	110,000	24,500	5,110	2,000	995
25	3,430	282,000	85,400	19,000	3,950	1,540	769
10	1,950	180,000	54,600	12,100	2,520	986	492
5	1,130	110,000	33,500	7,440	1,550	605	302

Table 2.28. Reservoir 2, Picacho Wash East sediment yield estimates

Recurrence interval (yr)	Peak discharge (ft^3/s)	Sediment volume (ac-ft)					
		0.06 mm	0.1 mm	0.2 mm	0.5 mm	1 mm	2 mm
100	1,840	36.30	11.00	2.45	0.51	0.20	0.10
50	1,350	20.60	6.25	1.39	0.29	0.11	0.06
25	948	10.80	3.27	0.73	0.15	0.06	0.03
10	540	3.77	1.14	0.25	0.05	0.02	0.01
5	315	1.30	0.39	0.09	0.02	0.01	0.00
100-yr volume			81.40	18.10	3.76	1.47	0.74

Recurrence interval (yr)	Peak discharge (ft^3/s)	Peak sediment concentration (ppm)					
		0.06 mm	0.1 mm	0.2 mm	0.5 mm	1 mm	2 mm
100	1,840	529,000	160,000	35,600	7,420	2,900	1,450
50	1,350	428,000	130,000	28,800	6,010	2,350	1,170
25	948	333,000	101,000	22,400	4,670	1,820	909
10	540	217,000	65,800	14,600	3,040	1,190	593
5	315	138,000	41,800	9,270	1,930	755	376

Table 2.29. Reservoir 2, total 100-year sediment volume

Total 100-year sediment volume (ac-ft)[1]					
0.06 mm	0.1 mm	0.2 mm	0.5 mm	1 mm	2 mm
11,000	800	200	40	10	7

[1] The total includes a sediment yield computed from a larger particle size. A larger particle size was used, because the maximum probable concentration of 300,000 ppm was exceeded.

Table 2.30. Reservoir 3, reservoir drainage area sediment yield estimates

Recurrence interval (yr)	Peak discharge (ft^3/s)	Sediment volume (ac-ft)					
		0.06 mm	0.1 mm	0.2 mm	0.5 mm	1 mm	2 mm
100	4,460	192.00	58.30	12.90	2.70	1.05	0.53
50	3,280	115.00	34.80	7.73	1.61	0.63	0.31
25	2,310	62.70	19.00	4.22	0.88	0.34	0.17
10	1,320	23.50	7.14	1.58	0.33	0.13	0.06
5	755	8.63	2.62	0.58	0.12	0.05	0.02
100-yr volume			481.00	107.00	22.20	8.67	4.34
Average 100-yr sediment yield (ac-ft/mi2)			47.60	10.60	2.20	0.86	0.43

Table 2.30. Reservoir 3, reservoir drainage area sediment yield estimates (continued)

Recurrence interval	Peak discharge	Peak sediment concentration (ppm)					
(yr)	(ft^3/s)	0.06 mm	0.1 mm	0.2 mm	0.5 mm	1 mm	2 mm
100	4,460	997,000	302,000	67,100	14,000	5,470	2,720
50	3,280	821,000	249,000	55,300	11,500	4,500	2,240
25	2,310	653,000	198,000	44,000	9,160	3,580	1,780
10	1,320	447,000	136,000	30,100	6,270	2,450	1,220
5	755	300,000	91,100	20,200	4,210	1,650	820

Table 2.31. Reservoir 3, total 100-year sediment volume

Drainage area	Total 100-year sediment volume[1] (ac-ft)					
	0.06 mm	0.1 mm	0.2 mm	0.5 mm	1 mm	2 mm
Upper drainage area		481	107	22.20	8.67	4.34
Lower drainage area		462	102	21.40	8.33	4.17
Total drainage area		900	200	40.00	20.00	9.00

[1] Computed by multiplying the average 100-year sediment yield per unit area (computed for the reservoir drainage area, see Table 2.24) by the canal drainage area of 9.72 mi^2.

2.5.7 Comparison of Different Approaches

Table 2.32 presents summary results from the three different methods. These results differ by two orders of magnitude for the low estimate and by up to one order of magnitude for the high estimate. Results from the RUSLE provided intermediate estimates as compared to the other empirical methods. The interpretation of the results from the RUSLE is complicated by the fact that the slope lengths in the basins are much greater than those used to determine the LS_R factor, and given the many assumptions made in determining the other factors.

Results from the empirical sediment yield equations consistently provide the largest estimates for the 100-year sediment volumes. These empirical equations are based on sedimentation measurements from reservoirs in Arizona, New Mexico, and California and from measurements of reservoirs throughout the southwestern United States. These reservoirs tend to be on drainage basins that have more annual rainfall than the proposed reservoirs in southwestern Arizona. Because the empirical equations are only a function of drainage area, they cannot take into account the drier and sandier conditions of the drainage areas. Therefore, the equations might be expected to overestimate the 100-year sediment yield.

Results from the sediment yield classification procedure provided the second highest sediment yield estimates. In a semi-quantitative fashion, this procedure takes into account many of the important variables affecting sediment yield from a drainage basin. The procedure is most

Table 2.32. Summary results of 100-year sediment volumes by four methods

Reservoir	Drainage area (mi^2)	Method	100-Year Sediment Volume (acre-ft) Low estimate	High estimate
Reservoir 1	17.8	Empirical RUSLE sediment estimate	800	2,300
		Empirical sediment yield equations	2,000	3,000
		Sediment yield classification procedure	900	2,000
		Unit stream power sheet erosion equation	20	1,000
Reservoir 2	75.9	Empirical RUSLE sediment estimate	900	2,600
		Empirical sediment yield equations	6,000	8,000
		Sediment yield classification procedure	4,000	8,000
		Unit stream power sheet erosion equation	7	1,000
Reservoir 3	19.8	Empirical RUSLE sediment estimate	600	1,900
		Empirical sediment yield equations	2,000	3,000
		Sediment yield classification procedure	1,000	2,000
		Unit stream power sheet erosion equation	9	900

sensitive to ratings for upland and channel erosion, topography, ground cover, and land use. In the case of the proposed reservoirs near Yuma, Arizona, the sediment yield ratings are high for the steep topography, sparse ground cover, and extensive erosion channel development. The ratings are low for the sandy soils and desert pavement, arid climate, and infrequent runoff. The procedure can be used to predict the relative difference in sediment yield between two or more drainage basins, but the procedure is still somewhat subjective when computing the actual sediment yield.

Results from the unit stream power sheet erosion equation provided the lowest sediment yield estimates. The sheet erosion equation accounts for the physical processes of erosion by taking into account the important variables of drainage slope, width, roughness, and sediment particle fall velocity and the runoff velocity, duration, and frequency. The drainage slope, S, runoff velocity, V, and sediment particle fall velocity, ω, are represented as dimensionless unit stream power (VS/ω), which Yang (1996) has shown to be applicable to a wide range of conditions. The sheet erosion equation is especially applicable to the drainage basins of the proposed reservoirs for the following reasons:

- The soils are mostly sand size, so particle cohesion can be ignored.
- Little or no vegetation exists to add cohesion to the sediment particles or complicate estimates of roughness.
- A reasonable estimate can be made for the total number of the runoff events over a 100-year period in this very arid climate.

- A maximum probable limit on sediment concentration can be applied to reduce the range of sediment particle sizes.

- The accuracy of the method could be improved if any of the following data were available:

  - A long-term record of rainfall, runoff, and sediment yield for each reservoir drainage basin.

  - A long-term record of rainfall, runoff, and sediment yield for a nearby and similar drainage basin for calibration purposes.

  - A sediment particle-size distribution of each drainage basin.

  - The areas of non-erodible and exposed bedrock of each drainage basin.

Results from the sheet erosion equation are believed to be the most accurate, because the most important variables are accounted for: dimensionless unit stream power and the magnitude, duration, and frequency of runoff events. Although results from this method are consistently lower than for the other two methods, 200 runoff events (over a 100-year period) are accounted for. Applying a maximum limit to the computed sediment concentration reduced the range of reasonable sediment particle sizes. The 100-year sediment volumes could only be greater if peak concentrations exceeded 300,000 ppm or if the runoff magnitudes or their frequency increased.

Sediment yield results for the assumed particle sizes of 1 and 2 mm were very low compared with smaller particle sizes and with the three other methods. The sediment particle size of 0.2 mm (fine sand) consistently provided the most reasonable high estimate in the sheet erosion equation for all drainage basins. Therefore, the results assuming a sediment particle size of 0.2 mm are used to represent the best estimate of the 100-year sediment volumes. Table 2.33 presents the 100-year sediment volume low estimates, high estimates, and best estimates for each proposed reservoir using the unit stream power sheet erosion equation.

Table 2.33. Low, high, and the best estimate of the 100-year sediment volume

Reservoir	Drainage area (mi^2)	Low estimate 100-year sedimentation volume (ac-ft)	High estimate 100-year sedimentation volume (ac-ft)	Best estimate 100-year sedimentation volume (ac-ft)
Reservoir 1	17.8	20	1,000	500
Reservoir 2	75.9	7	1,000	200
Reservoir 3	19.8	9	900	200

2.6 Reservoir Sedimentation

Rainfall, runoff, snowmelt, and river channel erosion provide a continuous supply of sediment that is hydraulically transported in rivers and streams. All reservoirs formed by dams on natural rivers are subject to some degree of sediment inflow and deposition. Because of the very low velocities in reservoirs, they tend to be very efficient sediment traps. Therefore, the amount of reservoir sedimentation over the life of the project needs to be predicted before the project is built. If the sediment inflow is large relative to the reservoir storage capacity, then the useful life of the reservoir may be very short. For example, a small reservoir on the Solomon River near Osborne, Kansas, filled with sediment during the first year of operation (Linsley and Franzini, 1979). If the inflowing sediments settle in the reservoir, then the clear water releases may degrade the downstream river channel (see Chapter 7, *River Processes and Restoration*).

There are several methods available for reducing reservoir sedimentation. These methods relate to the reservoir location and size, land use practices in the upstream watershed, and special considerations for the operation of the reservoir. In some cases, reservoirs can be operated for long-term sustainable use so that sedimentation eventually fills the reservoir (see Chapter 6, *Sustainable Development and Use of Reservoirs*).

Extensive literature exists on the subject of reservoir sedimentation. The book by Morris and Fan (1997), entitled *Reservoir Sedimentation Handbook* is an excellent reference and provides an extensive list of references.

2.6.1 Reservoir Sediment Trap Efficiency

The amount of sediment deposited within a reservoir depends on the trap efficiency. Reservoir trap efficiency is the ratio of the deposited sediment to the total sediment inflow and depends primarily upon the fall velocity of the various sediment particles, flow rate and velocity through the reservoir (Strand and Pemberton, 1982), as well as the size, depth, shape, and operation rules of the reservoir. The particle fall velocity is a function of particle size, shape, and density; water viscosity; and the chemical composition of the water and sediment. The rate of flow through the reservoir can be computed as the ratio of reservoir storage capacity to the rate of flow. The potential for reservoir sedimentation and associated problems can be estimated from the following six indicators:

- The reservoir storage capacity (at the normal pool elevation) relative to the mean annual volume of riverflow.

- The average and maximum width of the reservoir relative to the average and maximum width of the upstream river channel.

- The average and maximum depth of the reservoir relative to the average and maximum depth of the upstream river channel.

- The purposes for which the dam and reservoir are to be constructed and how the reservoir will be operated (e.g., normally full, frequently drawn down, or normally empty).

- The reservoir storage capacity relative to the mean annual sediment load of the inflowing rivers.

- The concentration of contaminants and heavy metals being supplied from the upstream watershed.

The ratio of the reservoir capacity to the mean annual streamflow volume can be used as an index to estimate the reservoir sediment trap efficiency. A greater relative reservoir size yields a greater potential sediment trap efficiency and reservoir sedimentation. Churchill (1948) developed a trap efficiency curve for settling basins, small reservoirs, flood retarding structures, semi-dry reservoirs, and reservoirs that are frequently sluiced.

Using data from Tennessee Valley Authority reservoirs, Churchill (1948) developed a relationship between the percent of incoming sediment passing through a reservoir and the sedimentation index of the reservoir (Figure 2.19). The sedimentation index is defined as the ratio of the period of retention to the mean velocity through the reservoir. The Churchill curve has been converted to a dimensionless expression by multiplying the sedimentation index by g, acceleration due to gravity.

The following description of terms will be helpful in using the Churchill curve:

Capacity—Capacity of the reservoir in the mean operating pool for the period to be analyzed in cubic feet.

Inflow—Average daily inflow rate during the study period in cubic feet per second.

Period of retention—Capacity divided by inflow rate.

Length—Reservoir length in feet at mean operating pool level.

Velocity—Mean velocity in feet per second, which is arrived at by dividing the inflow by the average cross-sectional area in square feet. The average cross-sectional area can be determined from the capacity divided by the length.

Sedimentation index—Period of retention divided by velocity.

Brune (1953) developed an empirical relationship for estimating the long-term reservoir trap efficiency for large storage or normal pond reservoir based on the correlation between the relative reservoir size and the trap efficiency observed in Tennessee Valley Authority reservoirs in the southeastern United States (see Figure 2.19). Using this relationship, reservoirs with the capacity to store more than 10 percent of the average annual inflow would be expected to trap between 75

and 100 percent of the inflowing sediment. Reservoirs with the capacity to store 1 percent of the average annual inflow would be expected to trap between 30 and 55 percent of the inflowing sediment. When the reservoir storage capacity is less than 0.1 percent of the average annual inflow, then the sediment trap efficiency would be near zero.

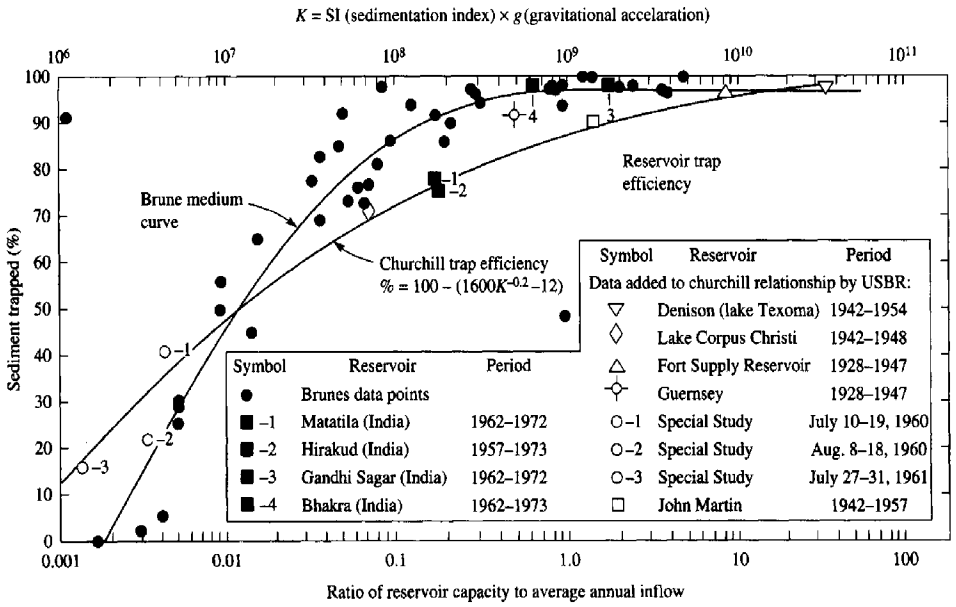

Figure 2.19. Trap efficiency curves (Churchill, 1948; Brune, 1953).

Figure 2.19 provides a good comparison of the Brune and Churchill methods for computing trap efficiencies using techniques developed by Murthy (1980). A general guideline is to use the Brune method for large storage or normal ponded reservoirs and the Churchill curve for settling basins, small reservoirs, flood retarding structures, semi-dry reservoirs, or reservoirs that are continuously sluiced. When the anticipated sediment accumulation is larger than 10 percent of the reservoir capacity, it is necessary that the trap efficiency be analyzed for incremental periods of the reservoir life.

The width and depth of the reservoir, relative to the width and depth of the upstream river channel, can also serve as indicators of reservoir sedimentation. Even if the reservoir capacity is small, relative to the mean annual inflow, a deep or wide reservoir may still trap some sediment.

The purposes for which a dam is constructed, along with legal constraints and hydrology, determine how the reservoir pool will be operated. The operation of the reservoir pool will influence the sediment trap efficiency and the spatial distribution and unit weight of sediments that settle within the reservoir. The reservoir trap efficiency of a given reservoir will be greatest if substantial portions of the inflows are stored during floods when the sediment concentrations are highest. If the reservoir is normally kept full (run of the river operation), floodflows pass through the reservoir and sediment trap efficiency is reduced. Coarse sediments would deposit as a delta at the far upstream end of the reservoir. When reservoirs are frequently drawn down, a

portion of the reservoir sediments will be eroded and transported father downstream. Any clay-sized sediments that are exposed above the reservoir level will compact as they dry out (Strand and Pemberton, 1982).

Once sediment capacity is reached, the entire sediment load supplied by the upstream river channel is passed through the remaining reservoir. For example, the pool behind a diversion dam is typically filled with sediment within the first year or two of operation. For a large reservoir like Lake Powell, the average annual sediment inflow is 0.1 percent of the reservoir storage capacity.

If contaminants and heavy metals are transported into a reservoir, they will likely settle with the sediments in the reservoir. This may improve the water quality of the downstream river, but the water quality in the reservoir may degrade over time as the concentrations of contaminants and metals accumulate.

Once the estimated sediment inflow to a reservoir has been established, attention must be given to the effect the deposition of this sediment will have upon the life and daily operation of the reservoir (Strand and Pemberton, 1982). The mean annual sediment inflow, the trap efficiency of the reservoir, the ultimate density of the deposited sediment, and the distribution of the sediment within the reservoir all must be considered in the design of the dam.

Usually, to prevent premature loss of usable storage capacity, an additional volume of storage equal to the anticipated sediment deposition during the life of the reservoir is included in the original design. Reclamation has designed reservoirs to include sediment storage space whenever the anticipated sediment accumulation during the period of project economic analysis exceeds 5 percent of the total reservoir capacity (Strand and Pemberton, 1982). A 100-year period of economic analysis and sediment accumulation was used for those reservoirs. The allocated sediment space is provided to prevent encroachment on the required conservation storage space for the useful life of the project.

A schematic diagram of anticipated sediment deposition (Figure 2.20) shows the effect of sediment on storage. A distribution study with 100-year area and capacity curves similar to those shown on the left side of Figure 2.20 is needed whenever the 100-year sediment accumulation is more than 5 percent of the total reservoir capacity. In operational studies of a reservoir for determining the available water supply to satisfy projected water demands over the project life, an average can be used for the sediment accumulation during the economic life period. However, the total sediment deposition is used for design purposes to set the sediment elevation at the dam, to determine loss of storage due to sediment in any assigned storage space, and to help determine total storage requirements.

2.6.2 Density of Deposited Sediment

Samples of deposited sediments in reservoirs have provided useful information on the density of deposits. The density of deposited material in terms of dry mass per unit volume is used to

convert total sediment inflow to a reservoir from a mass to a volume. The conversion is necessary when total sediment inflow is computed from a measured suspended and bed material sediment sampling program. Basic factors influencing density of sediment deposits in a reservoir are: (1) the manner in which the reservoir is operated; (2) the size of deposited sediment particles; and (3) the compaction or consolidation rate of deposited sediments.

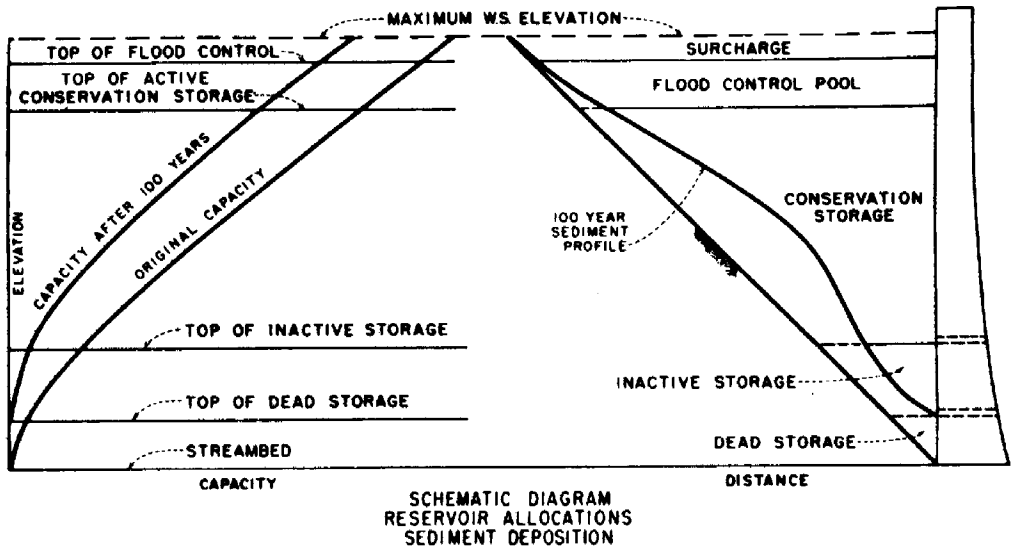

Figure 2.20. Schematic diagram of anticipated sediment deposition (Bureau of Reclamation, 1987).

The reservoir operation is probably the most influential of these factors. Sediments that have settled in reservoirs subjected to considerable drawdown are exposed to air for long periods and undergo a greater amount of consolidation. Reservoirs operating with a fairly stable pool do not allow the sediment deposits to dry out and consolidate to the same degree.

The size of the incoming sediment particles has a significant effect upon density. Sediment deposits composed of silt and sand will have higher densities than those in which clay predominates. The classification of sediment according to size as proposed by the American Geophysical Union (Vanoni, 1975) is as follows:

Sediment type	Size range in millimeters
Clay	Less than 0.004
Silt	0.004 to 0.062
Sand	0.062 to 2.0

The accumulation of new sediment deposits, on top of previously deposited sediments, changes the density of earlier deposits. This consolidation affects the average density over the estimated life of the reservoir, such as 100 years. Figure 2.21 shows a good example of consolidation of deposited sediments, taken from the report by Lara and Sanders (1970) for unit weights (densities) in Lake Mead at a sampling location with all clay-size material.

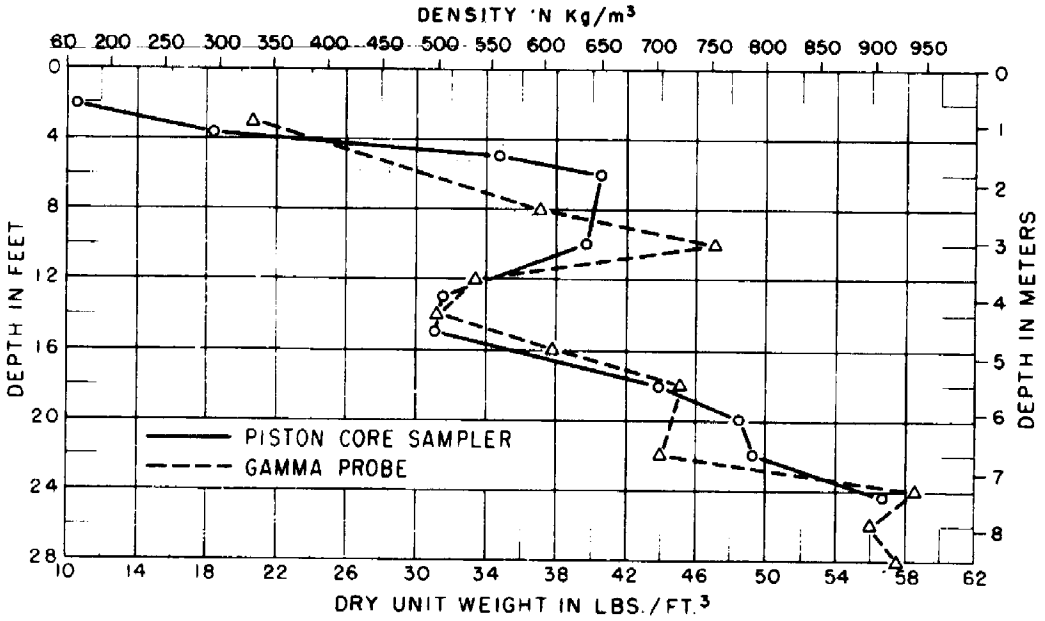

Figure 2.21. Comparison of densities on Lake Mead at location 5 (Bureau of Reclamation, 1987).

Three factors that should be taken into account in determining the density of deposited sediment are presented below. The influence of reservoir operation is the most significant because of the amount of consolidation or drying out that can occur in the clay fraction of the deposited material when a reservoir is subjected to considerable drawdown. The size of sediment particles entering the reservoir will also affect density, as shown by the variation in initial masses. Lara and Pemberton (1965) statistically analyzed some 1,300 samples for determining mathematical equations of variation of the unit weight of the deposits with the type of reservoir operation. Additional data on unit weight of deposited material from reservoir resurveys have supported the Lara and Pemberton (1965) equations (see Equation 2.39). The third factor is the years of operation of the reservoir.

Reservoir operations were classified according to operation as follows:

Operation	Reservoir operation
1	Sediment always submerged or nearly submerged
2	Normally moderate to considerable reservoir drawdown
3	Reservoir normally empty
4	Riverbed sediments upstream of reservoir

Selection of the proper reservoir operation number usually can be made from the operation study prepared for the reservoir.

Once the reservoir operation number has been selected, the density of the sediment deposits can be estimated using the following equation:

$$W = W_c p_c + W_m p_m + W_s p_s \tag{2.39}$$

where W = unit weight (lb/ft^3 or μg/m^3),
p_c, p_m, p_s = percentages of clay, silt, and sand, respectively, of the incoming sediment, and
W_c, W_m, W_s = unit weight of clay, silt, and sand, respectively, which can be obtained from the following tabulation:

Operation	Initial unit weight in lb/ft^3 (kg/m^3)		
	W_c	W_m	W_s
1	26 (416)	70 (1,20)	97 (1,50)
2	35 (561)	71 (1,40)	97 (1,50)
3	40 (641)	72 (1,50)	97 (1,50)
4	60 (961)	73 (1,70)	97 (1,50)

In determining the density of sediment deposits in reservoirs after a period of reservoir operation, it is recognized that part of the sediment will deposit in the reservoir in each of the T years of operation, and each year's deposits will have a different compaction time. Miller (1953) developed an approximation of the integral for determining the average density of all sediment deposited in T years of operation as follows:

$$W_T = W_o + 0.4343K \frac{T}{T-1}\left(\log_e T\right) - 1 \tag{2.40}$$

where W_T = average density after T years of reservoir operation,
W_o = initial unit weight (density) as derived from Equation (2.39), and
K = constant based on type of reservoir operation and sediment size analysis as obtained from the following table:

Reservoir operation	K for English units (metric units)		
	Sand	Silt	Clay
1	0	5.7	16
2	0	1.8	8.4
3	0	0	0

The K-factor of Equation (2.40) can be computed using Equation (2.41).

$$K = K_c p_c + K_m p_m + K_s p_s \tag{2.41}$$

where K_c, K_m, and K_s = the unit weight of clay, silt, and sand, respectively

As an example, the following data are known for a proposed reservoir with an operation number of 1 and a sized distribution of 23 percent clay, 40 percent silt, and 37 percent sand.

Then:

$$W = 26\ (0.23) + 70\ (0.40) + 97\ (0.37) = 6.0 + 28.0 + 35.9 = 70\ \text{lb/ft}^3\ (1120\ \text{kg/m}^3)$$

The 100-year average values to include compaction are computed as follows:

$$K = 16\ (0.23) + 5.7\ (0.40) + 0\ (0.37) = 3.68 + 2.28 + 0 = 5.96$$

$$W_{100} = 70 + 0.04343\,(5.96)\left[\frac{100}{99}(4.61) - 1\right] = 70 + 2.59\,(3.66) = 79\ \text{lb/ft}^3$$

This value may then be used to convert the initial weights (initial masses) of incoming sediment to the volume it will occupy in the reservoir after 100 years.

2.6.3 Sediment Distribution Within a Reservoir

The data obtained from surveys of existing reservoirs (U.S. Department of Agriculture, 1978) have been extensively used to develop empirical relationships for predicting sediment distribution patterns in reservoirs (Strand and Pemberton, 1982). Figures 2.22 and 2.23 illustrate the two most common techniques of showing sediment distribution, where sediment is distributed by depth and by longitudinal profile distance, respectively. Both methods clearly show that sediment deposition is not necessarily confined to the lower storage increments of the reservoir.

Sediment accumulation in a reservoir is usually distributed below the top of the conservation pool or normal water surface. However, if the reservoir has a flood control pool, and it is anticipated that the water surface will be held within this pool for significant periods of time, a portion of the sediment accumulation may be deposited within this pool. Figure 2.24 is a plot of data from 11 Great Plains reservoirs in the United States that may be used as a guide in estimating the portion of the total sediment accumulation that will deposit above the normal water surface. This plot should be regarded as a rough guide only, and the estimate obtained from it should be tempered with some judgment based upon the proposed reservoir operation and the nature of the incoming sediment. This curve is based on a limited amount of data and may be revised as more information becomes available.

The term "flood pool index" refers to the computed ratio of the flood control pool depth to the depth below the pool, multiplied by the percent of time the reservoir water surface will be within the flood control pool. This information for a proposed reservoir must be obtained from the reservoir operation study.

Once the quantity of sediment that will settle below the normal water surface has been established, the Empirical Area-Reduction Method may be used to estimate the distribution. This

method was first developed from data gathered in the resurvey of 30 reservoirs and is described by Borland and Miller (1960) with revisions by Lara (1962). The method recognizes that distribution of sediment depends upon: (1) the manner in which the reservoir is to be operated; (2) the size of deposited sediment particle; (3) the shape of the reservoir; and (4) the volume of sediment deposited in the reservoir. The shape of the reservoir was adopted as the major criterion for development of empirically derived design curves for use in distributing sediment.

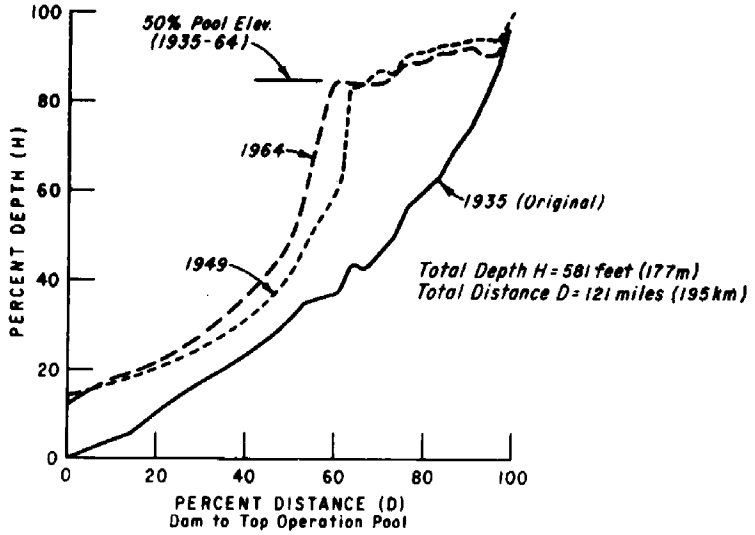

Figure 2.22. Sediment distribution from reservoir surveys of Lake Mead (Bureau of Reclamation, 1987).

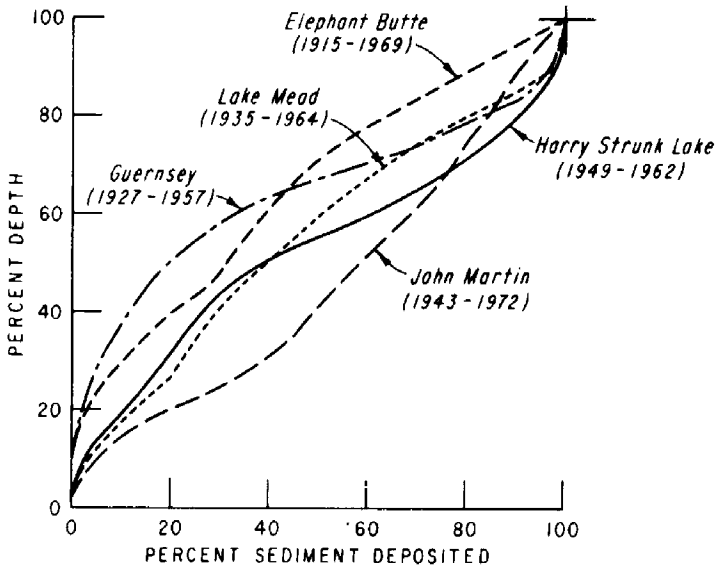

Figure 2.23. Sediment deposition profiles of several reservoirs (Bureau of Reclamation, 1987).

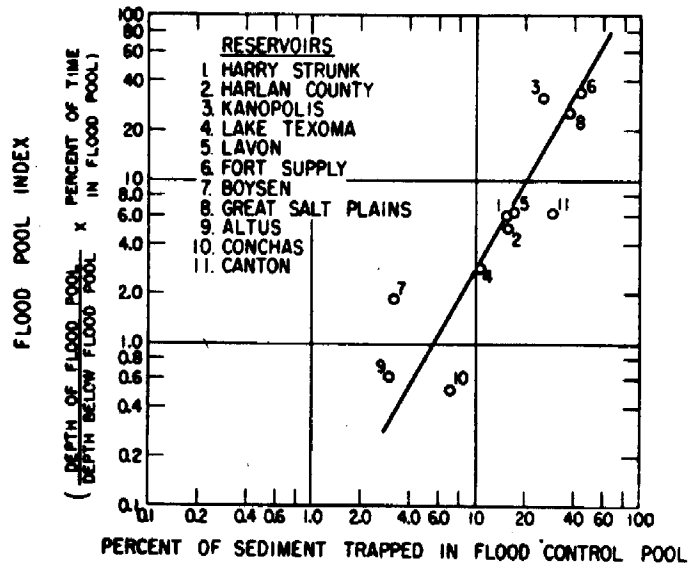

Figure 2.24. Sediment deposited in flood control pool (Bureau of Reclamation, 1987).

The design curve shown in Figure 2.25 can be used to predict reservoir sediment distribution as a function of depth. With equal weight applied to reservoir operation and shape, a weighted type distribution is selected from Table 2.34. In those cases where a choice of two weighted types are given, then a judicious decision can be made on whether the reservoir operation or shape of reservoir is more influential. The predominant size of reservoir sediment could be considered in this judgment of reservoir type from the following guidelines (see Figure 2.25):

Predominant size	Type
Sand or coarser	I
Silt	II
Clay	III

Table 2.34. Design type curve selection

Reservoir operation		Shape		
Class	Type	Class	Type	Weighted type
Sediment submerged	I	Lake	I	I
		Flood plain - foothill	II	I or II
		Hill and gorge	III	II
Moderate drawdown	II	Lake	I	I or II
		Flood plain - foothill	II	II
		Hill and gorge	III	II or III
Considerable drawdown	III	Lake	I	II
		Flood plain - foothill	II	II or III
		Hill and gorge	III	III
Normally empty	IV	All shapes		IV

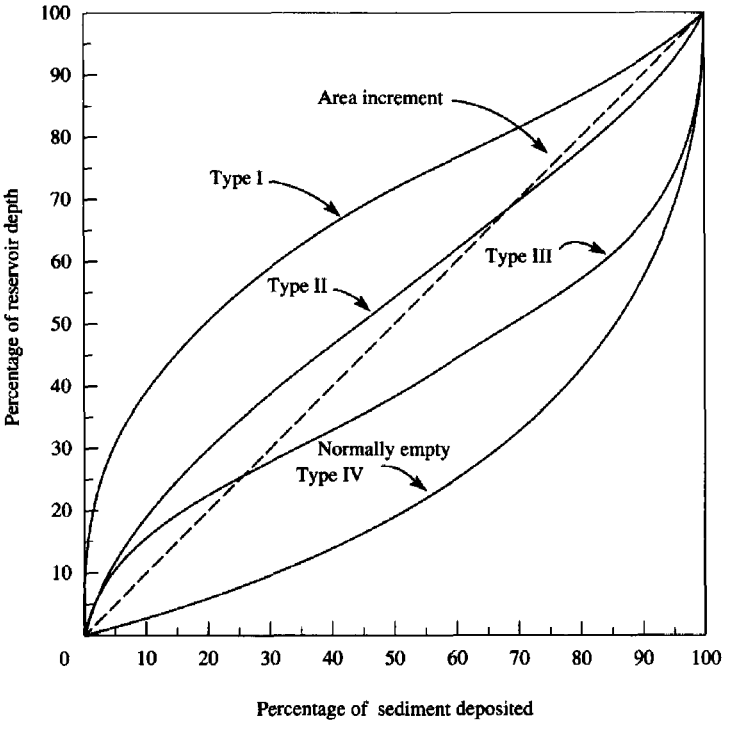

Figure 2.25. Sediment distribution design curves (Bureau of Reclamation, 1987).

Only for those cases with two possible type distributions should size of sediment be considered in selecting the design type curve. The size of sediments in most river systems is a mixture of clay, silt, and sand and has been found to be least important in selecting the design type curve from Figure 2.25.

Lara (1962) provides the detail on distributing sediment in a reservoir by the Empirical-Area Reduction Method. The appropriate design type curve is selected using the weighting procedure shown in Table 2.34.

The Area-Increment Method is based on the assumption that the area of sediment deposition remains constant throughout the reservoir depth. It is almost identical to the type II design curve (Figure 2.25) and is often used to estimate the new zero capacity elevation at the dam.

Strand and Pemberton (1982) give an example of a sediment distribution study for Theodore Roosevelt Dam, located on the Salt River in Arizona. Construction of the dam was completed in 1909, and a complete survey of the reservoir was made in 1981. The reservoir had an original total capacity of 1,530,500 acre-feet at elevation 2136 feet, the top of the active conservation pool. The purpose of this example is to: (1) compare the actual survey of 1981 with the distribution procedures; (2) show all of the steps involved in a distribution study; and (3) provide changes in capacity and projected sediment depths at the dam for 100, 200, and 300 years.

Table 2.35 gives the pertinent area-capacity data necessary to evaluate the actual 1981 survey and for use as a base in the distribution study. The total sediment accumulation in Theodore Roosevelt Lake, as determined from the 1981 survey, was 193,765 acre-feet. In the 72.4 years from closure of the dam in May 1909 until the survey in September 1981, the average annual sediment deposited was 2,676 acre-feet per year. The survey data from Table 2.35 were used to draw the sediment distribution design curve on Figure 2.26. To check the most appropriate design curve by the Empirical Area-Reduction Model, the volume of sediment accumulated in Theodore Roosevelt Lake from 1909 to 1981 was distributed by both a type II and III distribution, as shown in Figure 2.26. This comparison indicates that type II more closely resembles the actual survey. Figure 2.27 shows a plot of the area and capacity data from Table 2.35.

Table 2.35. Reservoir area and capacity data for Theodore Roosevelt Lake

	Original reservoir in 1909		1981 survey results	
Elevation (ft)	Area (acres)	Capacity (10^3 ac-ft)	Area (acres)	Capacity (10^3 ac-ft)
2136	17,785	1,530.5	17,337	1,336.7
2130	17,203	1,425.5	16,670	1,234.3
2120	16,177	1,258.5	15,617	1,072.4
2110	15,095	1,102.2	14,441	922.3
2100	14,104	956.5	13,555	782.6
2090	13,247	819.3	12,746	650.5
2080	11,939	693.3	11,331	530.0
2070	10,638	580.6	9,842	424.0
2060	9,482	479.9	8,230	333.8
2050	8,262	391.2	6,781	258.9
2040	7,106	314.6	5,569	197.6
2030	6,216	248.0	4,847	145.6
2020	5,286	190.3	4,212	100.3
2010	4,264	142.9	3,387	61.6
2000	3,544	103.8	2,036	35.0
1990	2,744	72.3	1,304	18.7
1980	1,985	48.9	903	7.6
1970	1,428	31.9	382	0.8
1960	1,020	19.7	[1]0	[1]0
1950	677	11.3		
1940	419	5.9		
1930	227	2.7		
1920	117	1.1		
1910	52	0.2		
1900	0	0		

[1] Sediment elevation at dam for 1981 survey is 1966 feet (599.2 m).

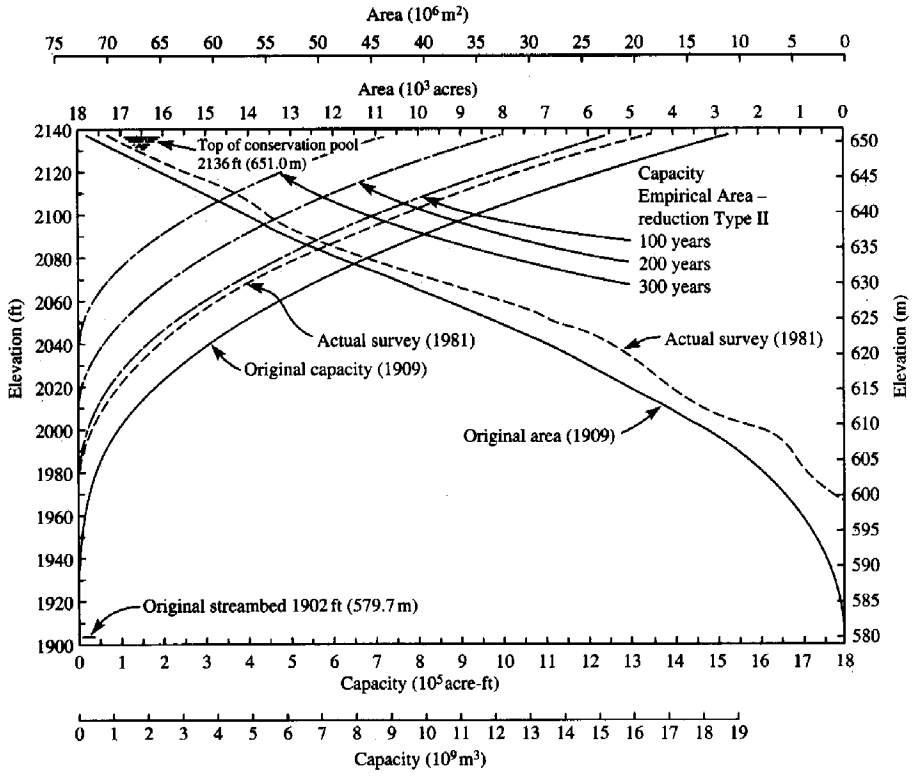

Figure 2.26. Area and capacity curves for Theodore Roosevelt Lake (Bureau of Reclamation, 1987).

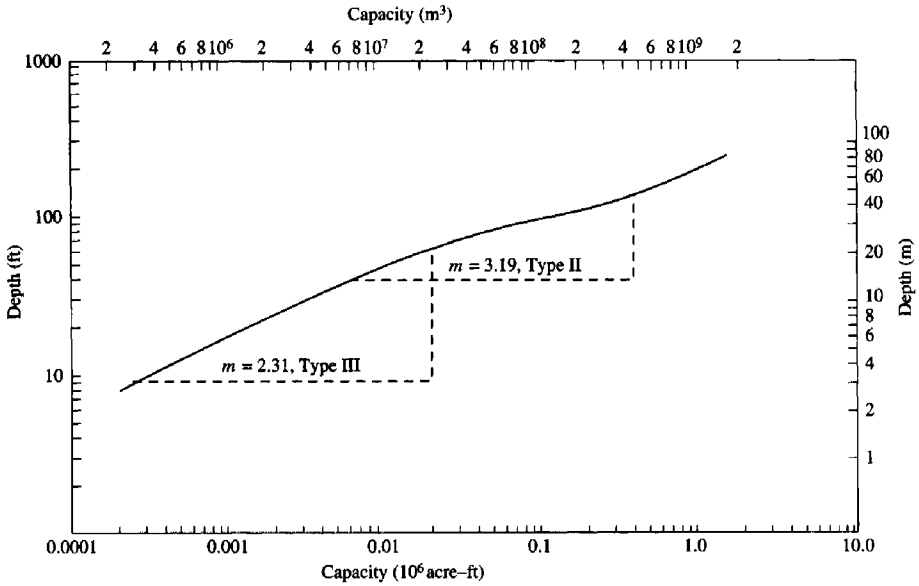

Figure 2.27. Depth versus capacity for Theodore Roosevelt Lake (Bureau of Reclamation, 1987).

The first step in the distribution study for the 100-, 200-, and 300-year period is a determination of the rate of sediment accumulation. In the case of Theodore Roosevelt Lake, the average annual rate determined from the 1981 survey and used for future projections, with the assumption that the compaction or unit weight of deposits will not change, is listed as follows:

Years	Sediment volume (acre-feet)
72.4 (1981)	193,765
100	267,600
200	535,200
300	802,800

No data existed on trap efficiency to apply to the above projections. The use of the rate from the 1981 survey results assumes that the trap efficiency for the first 72.4 years will remain the same through 300 years. In cases where sediment accumulation is determined from the total sediment load at a gauging station, then trap efficiency by use of Figure 2.19 and densities from Equations (2.39) and (2.40) are needed for computing the volume of sediment accumulation.

To complete this example, a logarithmic plot of the depth-capacity relationship for the original (1909) survey (Figure 2.27) for Theodore Roosevelt Lake, provided the shape factor for the reservoir type classification. Although the lower portion of the reservoir falls slightly in type III, the upper portion and overall slope indicate a type II classification. When assigning a type classification either for an existing reservoir or in distributing sediment on top of previous sediment deposits, it is important that the stage-capacity relationship only be plotted for the original survey. Studies have shown that a reservoir does not change type with continued sediment depositions. Once a reservoir has been assigned a type by shape, this classification will not change. However, it is possible that a change in reservoir operation could produce a new weighted type, as defined in Table 2.34.

The next step in the distribution study is computation of the elevation of sediment deposited at the dam. Table 2.36 shows a set of computations for determining the depth of sediment at the dam. The relative depth and a dimensionless function from the original area and capacity curves for Theodore Roosevelt Lake are computed as shown in Table 2.36 with the function:

$$F = \frac{S - V_h}{HA_h} \tag{2.42}$$

where F = dimensionless function of total sediment deposition, capacity, depth, and area,
S = total sediment deposition,
V_h = reservoir capacity at a given elevation h,
H = original depth of reservoir, and
A_h = reservoir area at a given elevation h.

Table 2.36. Determination of elevation of sediment at Theodore Roosevelt Dam (Bureau of Reclamation, 1987)

	Year	Total sediment deposition (ac-ft)	Original depth of reservoir (ft)
1981 survey	72.4	193,765	234
	100	267,600	
	200	535,200	
	300	802,800	

		Original survey (1909)			72.4 years		100 years		200 years		300 years	
Elevation (ft)	P relative depth	V_h capacity (ac-ft)	A_h area (ac)	HA_h 10^6 (ac-ft)	S-V_h *(ac-ft)*	F S-V_h HA_h	S-V_h *(ac-ft)*	F S-V_h HA_h	S-V_h *(ac-ft)*	F S-V_h HA_h	S-V_h *(ac-ft)*	F S-V_h HA_h
2080	0.761	693,315	11,939	2.79							109,485	0.0392
2070	0.718	580,590	10,638	2.49							222,210	0.0892
2060	0.675	479,928	9,482	2.22					55,272	0.0249	322,872	0.145
2050	0.632	391,207	8,262	1.93					143,993	0.0746	411,593	0.213
2040	0.590	314,623	7,106	1.66					220,577	0.133	488,177	0.294
2030	0.547	248,009	6,216	1.45			19,591	0.0135	287,191	0.198	554,791	0.383
2020	0.504	190,334	5,286	1.24			77,266	0.0623	344,866	0.278	612,466	0.494
2010	0.462	142,903	4,264	0.998	50,862	0.0510	124,697	0.125	392,297	0.393	659,897	0.661
2000	0.419	103,787	3,544	0.829	89,978	0.109	163,813	0.198	431,413	0.520	699,013	0.843
1990	0.376	72,347	2,744	0.642	121,418	0.189	195,253	0.304	462,853	0.721	730,453	1.138
1980	0.333	48,867	1,985	0.464	144,898	0.312	218,733	0.471	486,333	1.048	753,933	1.625
1970	0.291	31,935	1,428	0.334	161,830	0.485	235,665	0.706	503,265	1.507	770,865	2.308
1960	0.248	19,743	1,020	0.239	174,022	0.730	247,857	1.037	515,457	2.157	783,057	3.276
1950	0.205	11,328	677	0.158	182,437	1.155	256,272	1.622	523,872	3.316	791,472	5.009

A plot of the data points from Table 2.36 is superimposed on Figure 2.28 and the p value (relative depth) at which the line for any year crosses; the appropriate type curve will give the relative depth p_0 equal to the new zero elevation at the dam. Figure 2.28 contains plotted curves of the full range of F values for all four reservoir types and the Area-Increment Method, as developed from the capacity and area design curves. For Theodore Roosevelt Dam, the intersect points for type II, as well as for the Area-Increment Method curves, gave sediment depths shown in Table 2.37. The Area-Increment Method is often selected because it will always intersect the F curve and, in many cases, gives a good check on the new zero capacity elevation at the dam. In the case of Theodore Roosevelt Dam, the 1981 survey had an observed elevation at the dam of 1966 feet (599.2 m), which was in better agreement with the Area-Increment Method value than any of the type curves. Data from Table 2.37 can be used to predict useful life of a reservoir or projection beyond the 300 years.

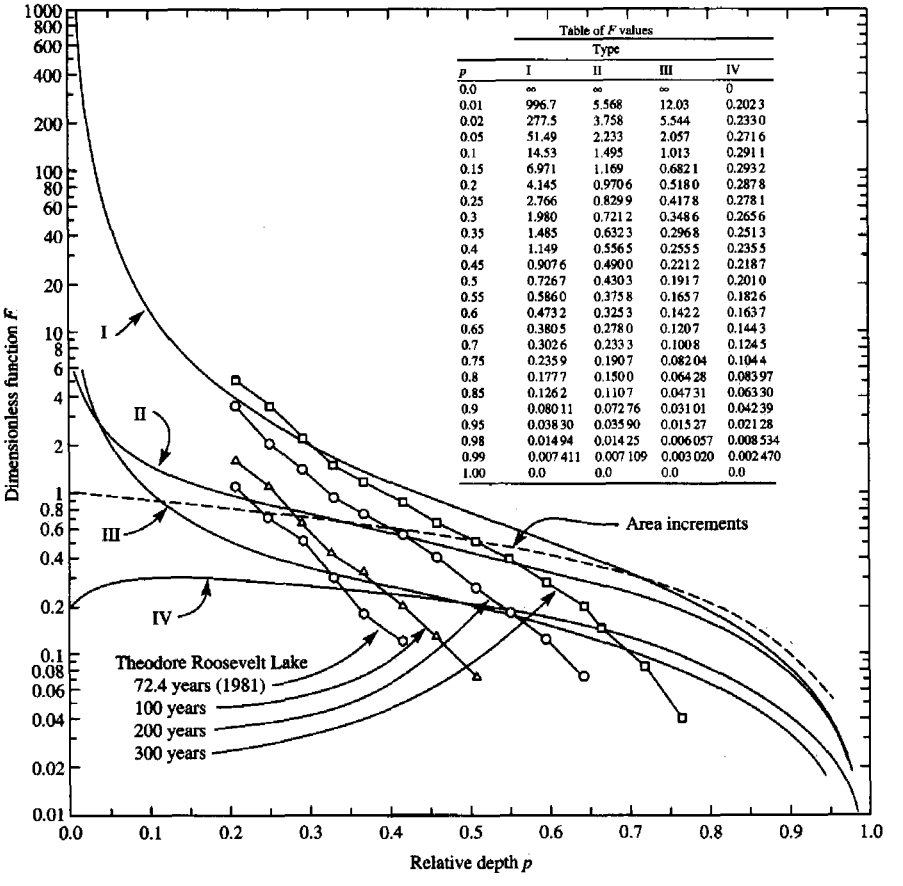

Figure 2.28. Curves to determine the depth of sediment at the dam (Bureau of Reclamation, 1987).

Table 2.37. Elevation of sediment at Theodore Roosevelt Dam
H = 234 ft

Years	Type II			Area increment		
	P_o	P_oH	Elevation (ft)	P_o	P_oH	Elevation (ft)
72.4 (1981)	0.23	54	1956	0.247	58	1960
100	0.284	66	1968	0.290	68	1970
200	0.418	98	2000	0.4	94	1996
300	0.553	129	2031	0.506	118	2020

The final step in the distribution study is to distribute a specified volume of sediment, which, for the example selected, involved the 72.4-, 100-, 200-, and 300-year volume in Theodore Roosevelt Lake by the type II design curve. Figure 2.26 shows the results of this distribution using procedures described by Lara (1962). Table 2.38 shows an example of the results for the 100-year distribution by use of the Empirical Area-Reduction Method and type II design curves. Although the example given is for type II, the equations for the relative sediment area a for each type are as follows (Bureau of Reclamation, 1987):

Type	Equation
I	$a = 5.074\, p^{1.85}\,(1 - p)^{0.35}$
II	$a = 2.487\, p^{0.57}\,(1 - p)^{0.41}$
III	$a = 16.967\, p^{1.15}\,(1 - p)^{2.32}$
IV	$a = 1.486\, p^{-0.25}\,(1 - p)^{1.34}$

where a = relative sediment area,
p = relative depth of reservoir measured from the bottom, and
p_o = relative depth at zero capacity.

2.6.4 Delta Deposits

Another phenomenon of reservoir sediment deposition is the distribution of sediment longitudinally as illustrated in Figure 2.22 for Lake Mead. The extreme upstream portion of the deposition profile is the formation of delta deposits. The major consequence of these delta deposits is the raising of the backwater elevations in the channel upstream from a reservoir. Therefore, the delta may cause a flood potential that would not be anticipated from pre-project channel conditions and proposed reservoir operating water surfaces. Predicting the delta development within a reservoir is a complex problem because of variables, such as operation of the reservoir, sizes of sediment, and hydraulics (in particular, the width of the upper reaches of the reservoir). Sediments deposited in the delta are continually being reworked into the downstream storage area at times of low reservoir stage and during extreme flood discharges.

Table 2.38. Theodore Roosevelt Lake; Type II reservoir sediment deposition study - empirical area reduction method. Sediment inflow = 267,600 acre-ft (Bureau of Reclamation, 1987)

	Original		Relative		Sediment		Revised	
Elevation	Area	Capacity	Depth	Area	Area	Volume	Area	Capacity
ft	acres	acre-ft			acres	acre-ft	acres	acre-ft
2136.0	17,785.0	1,530,499	1.000	0.000	0.0	267,600	17,785.0	1,262,899
2130.0	17,203.0	1,425,512	0.974	0.546	699.1	265,503	15,503.9	1,160,009
2120.0	16,177.0	1,258,547	0.932	0.795	1018.8	256,914	15,158.2	1,001,633
2110.0	15,095.0	1,102,215	0.889	0.945	1210.3	245,768	13,884.7	856,447
2100.0	14,104.0	956,455	0.846	1.050	1344.8	232,993	12,759.2	723,462
2090.0	13,247.0	819,272	0.803	1.127	1443.6	219,051	11,803.4	600,221
2080.0	11,939.0	693,315	0.761	1.184	1516.9	204,248	10,422.1	489,067
2070.0	10,638.0	580,590	0.718	1.225	1570.0	188,814	9,068.0	391,776
2060.0	9,422.0	479,928	0.675	1.254	1606.3	172,293	7,875.7	306,996
2050.0	8,262.0	391,207	0.632	1.271	1628.0	156,761	6,634.0	234,446
2040.0	7,106.0	314,623	0.590	1.277	1636.5	140,438	5,469.5	174,185
2030.0	6,216.0	248,009	0.547	1.274	1632.8	124,092	4,583.2	123,917
2020.0	5,286.0	190,334	0.504	1.263	1617.6	107,840	3,668.4	82,494
2010.0	4,264.0	142,903	0.462	1.242	1591.0	91,797	2,673.0	51,106
2000.0	3,544.0	103,787	0.419	1.212	1553.1	76,076	1,990.9	27,711
1990.0	2,744.0	72,347	0.376	1.174	1503.8	60,792	1,240.2	11,555
1980.0	1,985.0	48,867	0.333	1.126	1443.0	46,057	542.0	2,810
1970.0	1,428.0	31,935	0.291	1.068	1381.5	31,935	46.5	33
1968.6	1,369.7	29,983	0.284	1.059	1369.7	29,983	0.0	0
1960.0	1,020.0	19,743	0.248	0.999	1020.0	19,743	0.0	0
1950.0	677.0	11,328	0.205	0.918	677.0	11,328	0.0	0
1940.0	419.0	5,893	0.162	0.821	419.0	5,893	0.0	0
1930.0	227.0	2,735	0.120	0.704	227.0	2,735	0.0	0
1920.0	117.0	1,059	0.077	0.558	117.0	1,059	0.0	0
1910.0	52.0	211	0.034	0.358	52.0	211	0.0	0
1902.0	0.0	0	0.000	.000	0.0	0	0.0	0

A delta study is needed for situations involving the construction of railroads or highway bridges in the delta area, defining inundated property such as urban areas or farmland, and design of protective structures to control inundation of property. The 100-year flood peak discharge is often used for inundation comparison in the flood plain, with the delta size over the life of the project to represent average conditions for the 100-year event.

An empirical procedure exists for the prediction of delta formation that is based upon observed delta deposits in existing reservoirs (Strand and Pemberton, 1982). Figure 2.29 shows a typical delta profile. It is defined by a topset slope, foreset slope, and a pivot point between the two slopes at the median reservoir operating level. The quantity of material to be placed in the delta is assumed to be equal to the volume of sand-size material or coarser (> 0.062 mm) entering the reservoir over the project life. A trial and error method, utilizing topographic data and volume computations by average end-area method, is used to arrive at a final delta location.

The topset slope of the delta is computed by one or more of several methods: (1) a statistical analysis of existing delta slopes that support a value equal to one-half of the existing channel slope (Figure 2.30); (2) topset slope from a comparable existing reservoir; or (3) zero bedload transport slope from bedload equations, such as those by Meyer-Peter and Müller (1948), Sheppard (1960), or Schoklitsch (1934). An example of the topset slope computed by the Meyer-Peter and Müller beginning transport equation for zero bedload transport is given by:

$$S_T = K \frac{\frac{Q}{Q_B}\left[\frac{n_s}{(d_{90})^{1/6}}\right]^{3/2}}{D} d \qquad (2.43)$$

where S_T = topset slope,
K = coefficient equal to 0.19,
Q/Q_B = ratio of total flow in ft^3/s to flow over bed of stream in ft^3/s (Q/Q_B is normally equal to 1). Discharge is referred to as dominant discharge and is usually determined by either channel bank full flow or as the 1.5-year flood peak,
d = diameter of bed material on topset slope, usually determined as weighted mean diameter in millimeters,
d_{90} = diameter of bed material for 90% finer than in millimeters,
D = maximum channel depth at dominant discharge in feet, and
n_s = Mannings roughness coefficient for the bed of the channel.

The Meyer-Peter and Müller equation, or any other equation selected for zero transport, will yield slope at which the bed material will no longer be transported, which must necessarily be true for the delta to form.

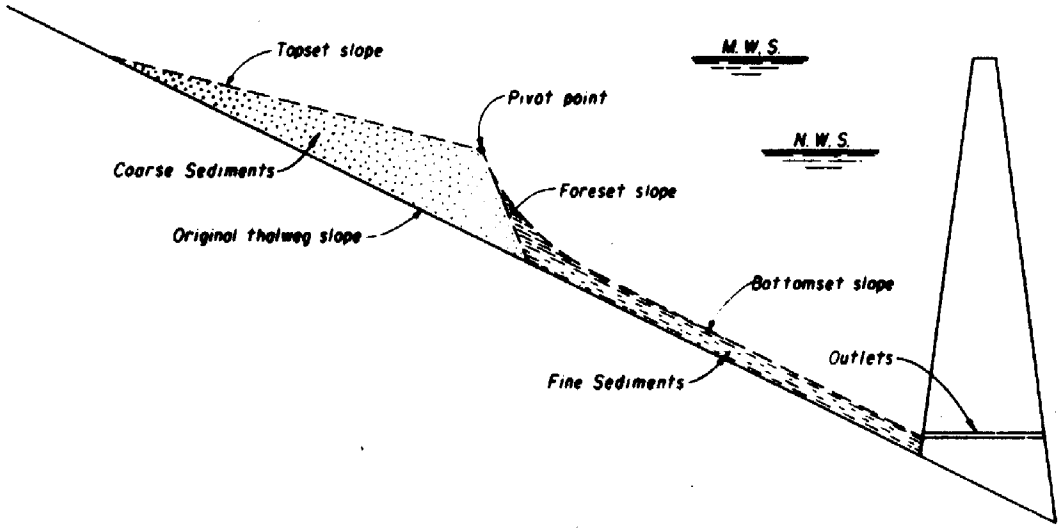

Figure 2.29. Typical sediment deposition profile (Bureau of Reclamation, 1987).

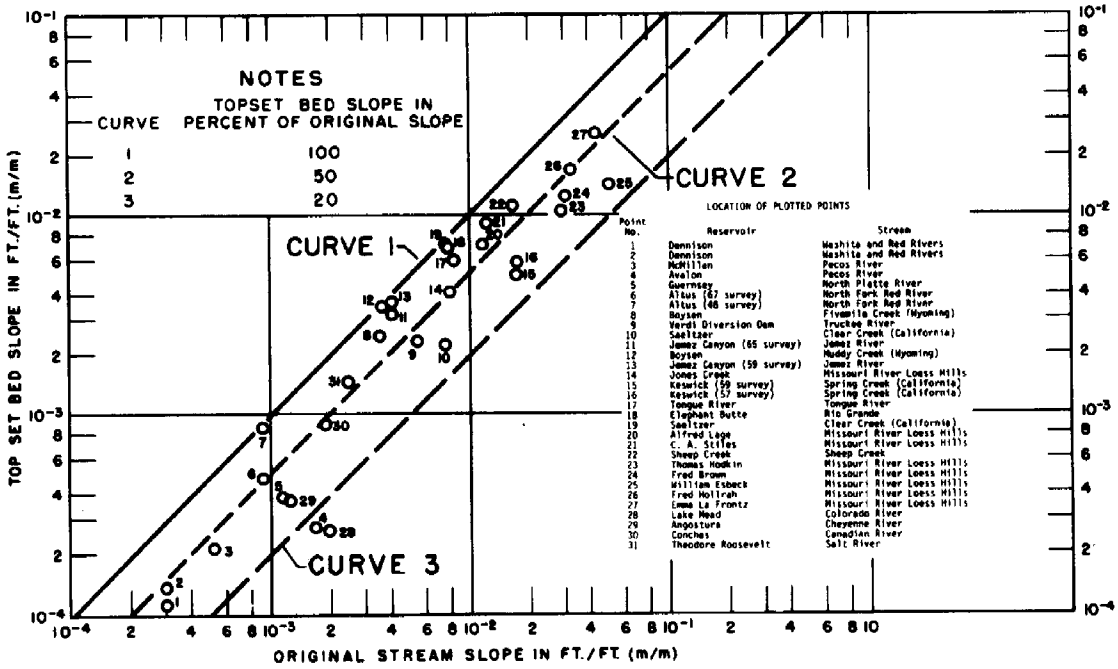

Figure 2.30. Topset slope versus original stream slope from existing reservoirs (Bureau of Reclamation, 1987).

The location of the pivot point between the topset and foreset slopes depends primarily on the operation of the reservoir and the existing channel slope in the delta area. If the reservoir is operated near the top of the conservation pool a large portion of the time, the elevation of the top of the conservation pool will be the pivot point elevation. Conversely, if the reservoir water surface has frequent fluctuations and a deeply entrenched inflow channel, a mean operating pool elevation should be used to establish the pivot point. In the extreme situation when a reservoir is emptied every year during the flood peak flows for sluicing sediment, the pivot point will be at the sluiceway.

As an initial guess, the upstream end of the delta is set at the intersection of the maximum water surface and the original streambed, and the topset slope is projected from that point to the anticipated pivot point elevation to begin the first trial computations of delta volume.

The average of foreset slopes observed in Reclamation reservoir resurveys is 6.5 times the topset slope. However, some reservoirs exhibit a foreset slope considerably greater than this; for example, Lake Mead's foreset slope is 100 times the topset. By adopting a foreset slope of 6.5 times the topset, the first trial delta fit can be completed.

The volume of sediment computed from the channel cross sections with the delta imposed on them should agree with the volume of sand size or larger material anticipated to come from the delta stream. The quantity of sediment in the delta above normal water surface elevation should also agree with that estimated to settle above the normal operating level, as shown in Figure 2.25. If the adjustment necessary to attain agreement is minor, it can usually be accomplished by a small change in the foreset slope. If a significant change in delta size is needed, the pivot point can be moved forward or backward in the reservoir, while maintaining the previously determined elevation of the point. The topset slope is then projected backward from the new pivot point location, and the delta volume is again computed. The intersection of the delta topset and the original streambed may fall above the maximum water surface elevation, a condition that has been observed in small reservoirs. The delta formation can also be determined from computer modeling (see Chapter 5, *Sedimentation Modeling for Rivers and Reservoirs*).

2.6.5 Minimum Unit Stream Power and Minimum Stream Power Method

Yang (1971) first derived the theory of minimum unit stream power for river morphology from thermodynamics. The theory states that for a closed and dissipative system under dynamic equilibrium:

$$\frac{dY}{dt} = \frac{dx}{dt}\frac{dY}{dx} = VS = \text{a minimum} \tag{2.44}$$

where Y = potential energy per unit weight of water,
x = distance,
V = average flow velocity,
S = slope,
VS = unit stream power, and
t = time.

The minimum value in Equation (2.44) depends on the constraints applied to the system. Yang (1976) later applied the theory to fluvial hydraulics computations. Yang (1976) and Yang and Song (1986, 1987) derived the theory of minimum energy dissipation rate from basic theories in fluid mechanics and mathematics. The theories of minimum stream power and minimum unit stream power are two of the special and simplified theories of the more general theory of minimum energy dissipation rate. These theories have been applied to solve a wide range of fluvial hydraulic problems.

Yang and Molinas (1982) showed that unit stream power can be obtained through the integration of the product of shear stress τ and velocity gradient du/dy, where u = time-averaged local velocity in an open channel flow. Consequently, minimization of VS is equivalent to minimization of τ (du/dy). Annandale (1987) called τ (du/dy) the applied unit stream power. It can be shown that minimization of applied unit stream power is equivalent to:

$$\sqrt{gDS} = \text{a minimum} = \text{a constant} \tag{2.45}$$

where g = gravitational acceleration, and
D = water depth.

Equation (2.45) can be used to determine the longitudinal bed profile of a reservoir in or near a stable condition. Annandale (1987) verified the validity of Equation (2.45) using data from Van Rhynereldpass Reservoir in South Africa, as shown in Figure 2.31. Figure 2.31 (b) indicates that a constant value of $\sqrt{gDS} = 6\times10^{-3}$ m/s can be used for the Van Rhynereldpass Reservoir. In order to apply Equation (2.45) to the determination of the longitudinal bed profile of a reservoir, it is assumed that the shear velocity of the river at the entrance of the reservoir remains constant through the reservoir. A modified backwater surface profile computation through the reservoir is then made by assuming two free surfaces; that is, water surface and bed surface. The bed surface is adjusted in the computation, such that Equation (2.45) is satisfied.

For most natural rivers and reservoirs, a more generalized theory of minimum stream power is applicable; that is:

$$QS = \text{a minimum} = \text{a constant} \tag{2.46}$$

where Q = water discharge, and
QS = stream power.

The minimum value in Equation (2.46) depends on the constraints applied to the system. Chang (1982) and Annandale (1984) found that when the stream power approaches a minimum value for relatively short reach:

$$\frac{dQ}{dx} \rightarrow 0 \tag{2.47}$$

The relationship between channel cross-sectional area A and wetted perimeter P becomes:

$$\frac{dA}{dx} = \frac{A}{Q}\frac{dQ}{dx} + \frac{A}{3P}\frac{dP}{dx} = \frac{A}{3P}\frac{dP}{dx} \tag{2.48}$$

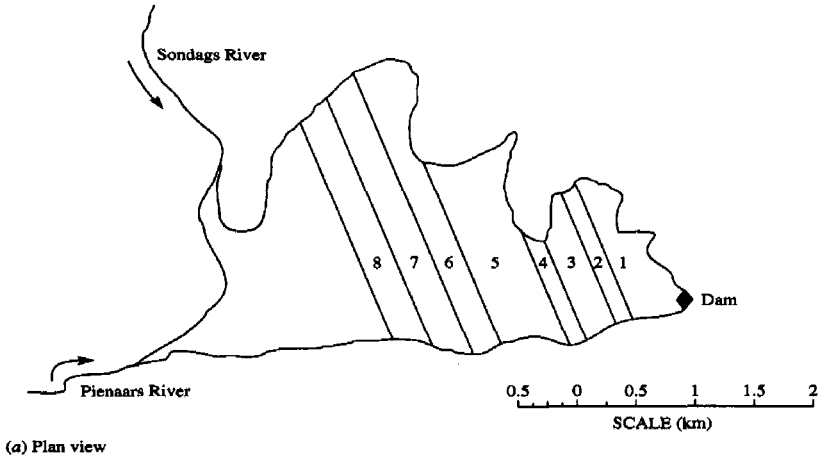

(*a*) Plan view

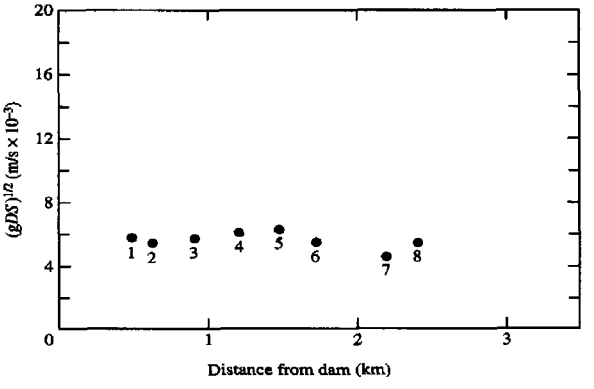

(*b*) Relationship between shear velocity and distance

Figure 2.31. Relationship between shear velocity and distance for the Van Rhyneveld Reservoir (Annandale, 1987).

Equation (2.48) can be used to develop dimensionless cumulative mass curves as a function of dP/dx. Figure 2.32 shows the curves developed by Annandale (1987) based on data from 11 reservoirs in South Africa, where sediments are deposited below full supply level or below the crest of the spillway of a reservoir. Figure 2.33 shows the result by Annandale for sediments deposited above the full supply level. To illustrate the computational procedures based on a minimum unit stream power and minimum stream power theory, Yang (1996) summarized examples used by Annandale (1987) in the following example problems.

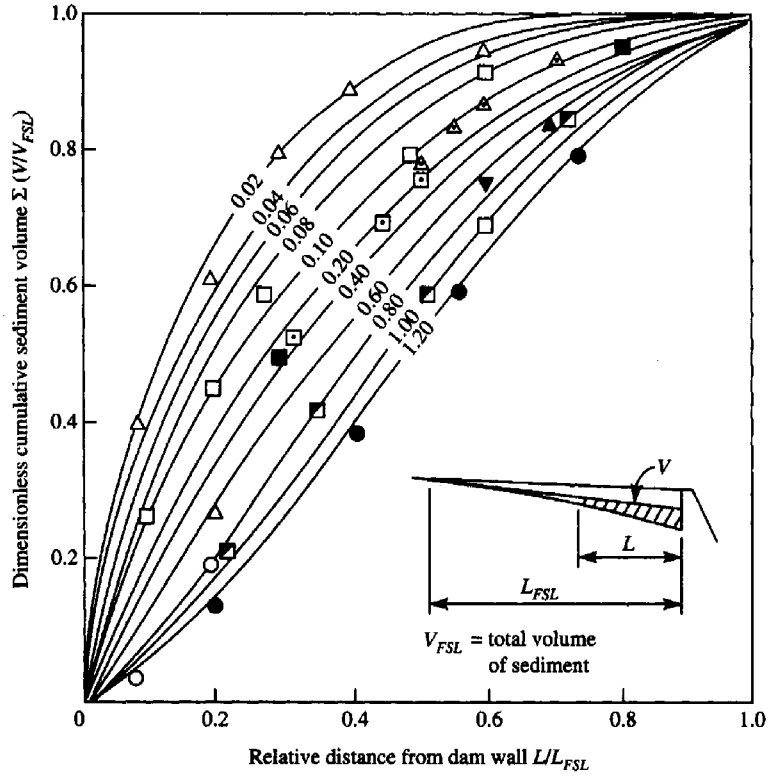

Figure 2.32. Dimensionless cumulative mass curves explaining sediment distribution below full supply level as a function of *dP/dx* for stable conditions (Annandale, 1987).

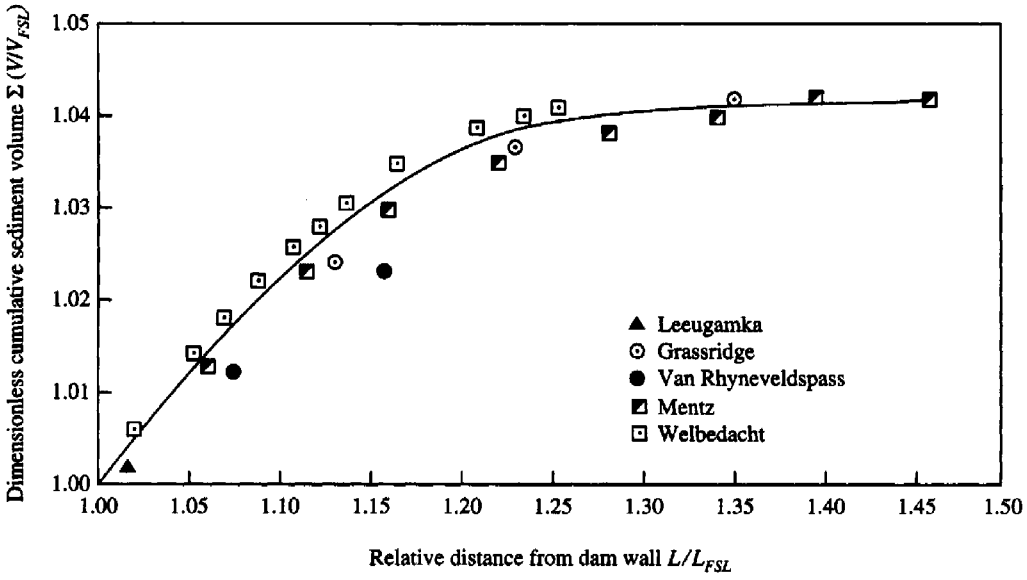

Figure 2.33. Sediment distribution above full supply level (Annandale, 1987).

Example 2.4 The river and reservoir schematic shown in Figure 2.34 below has the following properties: Width = B = 1 m; Flow depth in river = D = 1 m; Bed slope of river = S_0 = 0.002; Bed slope of reservoir = S_0' = 0.02; Manning's n = 0.03;

$$\text{Hydraulic radius of river reach} = R = \frac{B \times D}{2D + B} = 0.333 \text{ m};$$

$$\text{Flow velocity in river} = V = \frac{R^{2/3} S^{1/2}}{n} = 0.717 \text{ m/s};$$

Discharge = $Q = VA$ = 0.717 m^3/s; Shear velocity in river reach = $\sqrt{gDS_0}$ = 0.14 m/s.

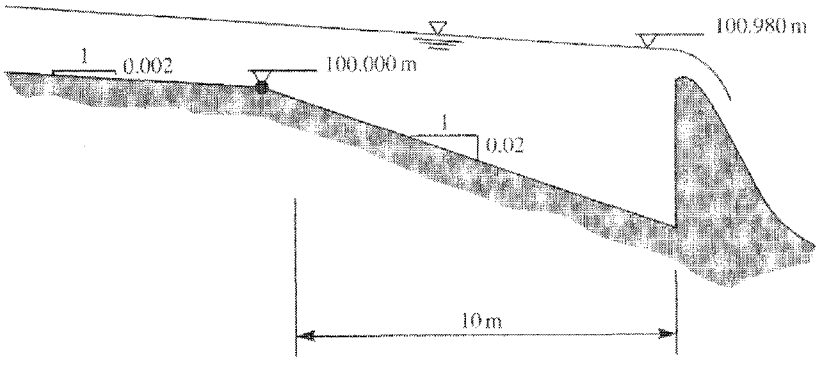

Figure 2.34. River and reservoir schematic for Example 2.4.

It is assumed that the river is in a dynamic, equilibrium condition. The constant value assumed for the shear velocity in the river is applicable for the reservoir and is therefore set at 0.14 m/s. Compute the reservoir bed surface profile based on minimum unit stream power theory.

Solution: Table 2.39 (Yang, 1996) summarizes the computation, based on Equation (2.45).

The final computed reservoir bed surface profile is:

Reach (m)	Bed level (m)
0	99.980
4	99.988
8	99.996
10	100.000

Table 2.39. Reservoir bed surface profile computation (Annandale, 1987; Yang, 1996)

Chainage (m) (1)	Stage (m) (2)	Assumed bed level (m) (3)	Flow depth (m) (4)	Area (m^2) (5)	$V^2/2g$ (m) (6)	Total head (m) (7)	P (m) (8)	R (m) (9)	$R^{4/3}$ ($m^{4/3}$) (10)	Friction slope S (m/m) (11)	Ave. S over reach (m/m) (12)	Reach length (m) (13)	h_f (m) (14)	Total head (m) (15)	$\sqrt{gDS}$ (m/s) (16)	Notes (17)
0	100.980	99.900	1.080	1.080	0.0225	101.002	3.160	0.341	0.239	0.0017					0.133	(i)
0	100.980	99.980	1.000	1.000	0.0262	101.006	3.000	0.333	0.231	0.0020					0.140	(ii)
4	101.000	99.990	1.010	1.010	0.0257	101.025	3.020	0.334	0.232	0.0020	0.0020	4	0.0078	101.014		(iii)
4	100.988	99.990	0.998	0.998	0.0263	101.014	2.996	0.333	0.230	0.0020	0.0020	4	0.0081	101.014	0.140	(iv)
4	100.988	99.988	1.000	1.000	0.0262	101.014	3.000	0.333	0.231	0.0020	0.0020	4	0.0080	101.014	0.140	(v)
8	101.100	99.990	1.110	1.110	0.0213	101.121	3.220	0.344	0.241	0.0016	0.0018	4	0.0071	101.021		(iii)
8	100.997	99.990	1.007	1.007	0.0259	101.022	3.014	0.334	0.231	0.0020	0.0020	4	0.0079	101.022	0.139	(iv)
8	100.996	99.996	1.000	1.000	0.0262	101.022	3.000	0.333	0.231	0.0020	0.0020	4	0.0080	101.022	0.140	(v)
10	101.000	100.00	1.000	1.000	0.0262	101.026	3.000	0.333	0.231	0.0020	0.0020	2	0.0040	101.026	0.1400	

Notes:

(i) Shear velocity $\neq 0.14$ m/s, repeat calculation with new assumed bed level

(ii) Shear velocity = 0.14 m/s, proceed to next reach

(iii) Total head in column (7) $\neq$ total head in column (15), adjust water stage and repeat calculation

(iv) Total heads balance but shear velocity $\neq 0.140$ m/s, adjust bed level and repeat calculation

Example 2.5 Figure 2.35(a) shows the plan view of Lake Mentz in South Africa. The estimated volume of sediment expected to be deposited in the reservoir is 129 x 10^6 m^3. Assume that the wetted perimeter can be replaced by reservoir width. Figure 2.35(b) shows the relationship between reservoir width and distance at full supply level. From Figure 2.35(b), $dP/dx = 0.8$. This value is used to select the curve from Figure 2.32 for sediment volume computation below full supply level. Sediment volume with L/L_{FSL} greater than 1.0, can be obtained from Figure 2.33. Table 2.40 summarizes the computations (Annandale, 1987; Yang, 1996).

Table 2.40. Lake Mentz reservoir sedimentation volume computation

Relative distance L/L_{FSL}	Actual distance (m)	Dimensionless cumulative sediment vol. $\Sigma(V/V_{FSL})$	Estimated cumulative sediment vol. (10^6 m^3)	Estimated sediment vol. sections (10^6 m^3)
0.0	0	0.00	0.00	0.00
0.1	1,200	0.08	0.92	9.92
0.2	2,400	0.20	24.81	14.89
0.3	3,600	0.36	44.65	19.84
0.4	4,800	0.50	62.02	17.37
0.5	6,000	0.60	74.42	12.40
0.6	7,200	0.70	86.83	12.41
0.7	8,400	0.82	101.71	14.88
0.8	9,600	0.90	111.63	9.92
0.9	10,800	0.95	117.84	6.21
1.0	12,000	1.00	124.04	6.20
1.1	13,200	1.02	126.52	2.48
1.2	14,400	1.03	127.76	1.24
1.3	15,600	1.04	129.00	1.24
1.4	16,800	1.04	129.00	0.00

The Sanmenxia Reservoir on the Yellow River in China has severe sedimentation problems. The project went through three phases of reconstruction to modify its operation since its completion. The modifications include reopening low level diversion tunnels and constructing side tunnels to sluice sediments. The operation rules also changed to releasing water with high sediment concentration during floods and storing water with lower sediment concentration after floods. Since these modifications, sediment inflow into and outflow from the reservoir is now in a state of dynamic equilibrium. During the long process of trial-and-error to determine the optimum reconstruction and modification of operation rules, the Yellow River Conservancy Commission (He et al., 1987) collected valuable data on scour and deposition in the reservoir. Yang (1996) used the Sanmenxia Reservoir data shown in Figure 2.36 to demonstrate the application of minimum stream power shown in Equation (2.46). Figure 2.36 shows that scour occurs when QS is greater than 0.3 m^3/s, while deposition occurs when QS is less than 0.3 m^3/s. The state of dynamic equilibrium can be maintained at $QS = 0.3$ m^3/s = a constant. These results indicate that the theory of minimum stream power, as stated in Equation (2.46), can be applied directly to the design and operation of a reservoir to maintain a dynamic equilibrium between sediment inflow and outflow. Figure 2.36 shows the actual measured values of QS x 10^{-4} m^3/s.

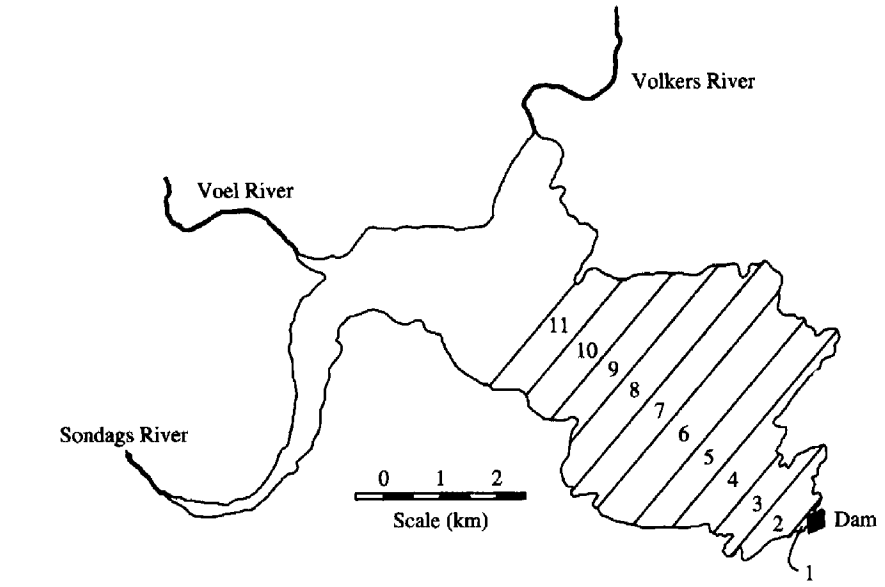

(*a*) Plan view

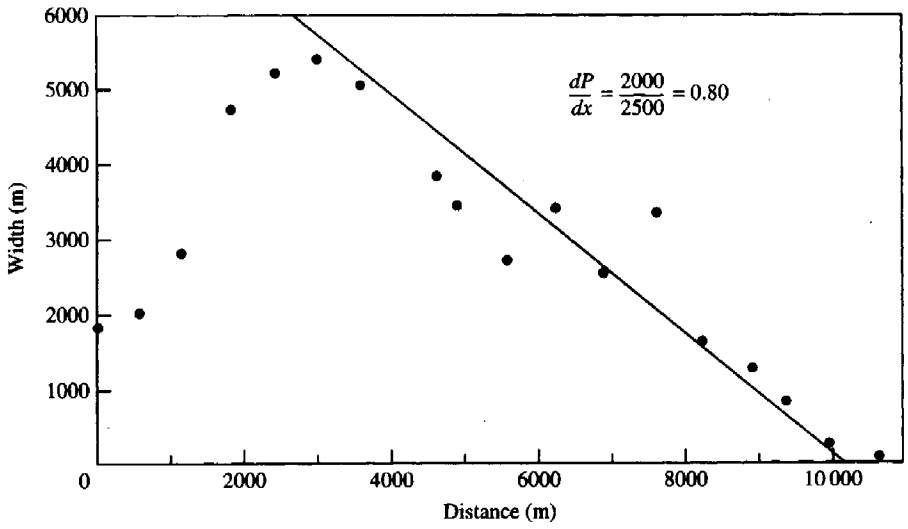

(*b*) Width–distance relationship

Figure 2.35. Plan view and width-distance relationship for Lake Metz in South Africa (Annandale, 1987).

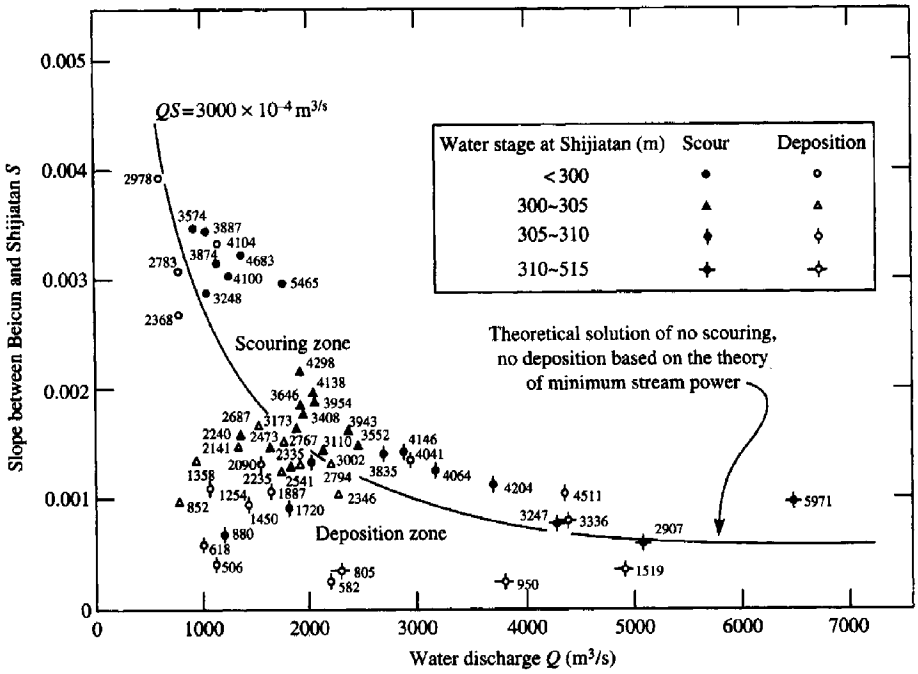

Figure 2.36. Determination of the Sanmenxia Reservoir scouring and deposition process based on the minimum stream power theory (Yang, 1996).

2.7 Summary

This chapter provides a detailed review and evaluation of empirical approaches used for the estimation of erosion rate or sediment yield. Empirical approaches include the use of the Universal Soil Loss Equation and its revised and modified versions, and direct measurement of sediment yield. Site-specific estimates of sediment yield from a watershed can also be computed from empirical equations based on drainage area or basin characteristics.

Theories of minimum energy dissipation rate and its simplified versions of minimum stream power or minimum unit stream power in conjunction with the unit stream power theory for sediment transport can be used as the basis for the computation of sheet, rill, and gully erosion rates. The GSTARS computer series can be used to systematically compute erosion rates and sediment transport, scour, and deposition in a watershed.

Reservoir sedimentation processes and computations based on empirical methods and analytical methods using minimum unit stream power and minimum stream power theories are included in this chapter. Example computations of erosion rates and reservoir sedimentation are used to illustrate the methods described in this chapter.

2.8 References

Annandale, G.W. (1984). "Predicting the Distribution of Deposited Sediment in Southern African Reservoirs," *IAHR Proceedings of the Symposium on Challenges in African Hydrology and Water Resources*, Harare, Zimbabwe.

Annandale, G. W. (1987). *Reservoir Sedimentation*, Elsevier Science Publishers, Amsterdam.

ASCE (1975). *Sedimentation Engineering*, American Society of Civil Engineering Manual No. 54, V.A. Vanoni, editor.

Basson, G. (2002). "Mathematical Modelling of Sediment Transport and Deposition in Reservoirs—Guidelines and Case Studies," *International Commission on Large Dams Sedimentation Committee Report.*

Beasley, D.B., L.F. Huggins, and E.J. Monke (1980). "ANSWERS: A model for watershed planning," *Transactions of the ASAE*, vol. 23, no. 4, pp. 938-944.

Bingner, R.L. (1996). "Runoff Simulated from Goodwin Creek Watershed Using SWAT," *Transactions of the ASAE*, vol 39, no. 1, pp. 85-89.

Bingner, R.L., C.E. Murphree, and C.K. Mutchler (1989). "Comparison of Sediment Yield Models on Watersheds in Mississippi," *Transactions of the ASAE*, vol. 32, no. 2, pp. 529-534.

Blanton, J.O., III (1982). "Procedures for Monitoring Reservoir Sedimentation," Bureau of Reclamation, Denver, Colorado.

Borland, W.M., and C.R. Miller (1960). "Distribution of Sediment in Large Reservoirs," *Transactions of the ASCE*, vol. 125, pp. 166-180.

Bouraoui, F.B., and T.A. Dillaha (1996). "ANSWERS-2000: Runoff and Sediment Transport Model," *Journal of Environmental Engineering*, vol. 122, no. 6, pp. 493-502.

Brown, L.C., and G.R. Foster (1987). "Storm Erosivity Using Idealized Intensity Distributions," *Transactions of the American Society of Agricultural Engineers*, vol. 30, no. 2, pp. 379-386.

Brune, G.M. (1953). "Trap Efficiency of Reservoirs," *Transactions of American Geophysical Union*, vol. 34, no. 3 pp. 407-418.

Bureau of Reclamation (1951). "Stable Channel Profiles," Hydraulic Laboratory Report no. Hyd. 325, Denver, Colorado.

Bureau of Reclamation (1987). *Design of Small Dams*, 3rd Edition, Denver, Colorado.

Chang, H.H. (1982). "Fluvial Hydraulics of Delta and Alluvial Fans," *Journal of the Hydraulics Division, ASCE*, vol. 108, no. HY11.

Churchill, M.A. (1948). Discussion of "Analysis and Use of Reservoir Sedimentation Data," by L.C. Gottschalk, *Proceedings, Federal Interagency Sedimentation Conference*, Denver, Colorado, pp. 139-140.

Daraio, J.A. (2002). "Assessing the Effects of Rainfall Kinetic Energy on Channel Suspended Sediment Concentrations for Physically-Based Distributed Modeling of Event-Scale Erosion," MS Thesis, Department of Civil and Environmental Engineering, University of Connecticut, Storrs, Connecticut.

Downer, C.W. (2002) "Identification and Modeling of Important Streamflow Producing Processes," Ph.D. Dissertation, Department of Civil and Environmental Engineering, University of Connecticut, Storrs, Connecticut.

Folly, A., J.N. Quinton, and R.E. Smith (1999). "Evaluation of the EUROSEM Model for the Catsop Watershed, The Netherlands," *Catena*, vol. 37, pp. 507-519.

Hong, S., and G.S. Govers (1985). "Selectivity and Transport Capacity of Thin Flows in Relation to Rill Generation," *Catena*, vol. 12, pp. 35-49.

Govers, G. (1985). "Selectivity and Transport of Thin Flows in Relation to Rill Erosion," *Catena*, vol. 12, pp. 35-49.

Govers, G., and G. Rauws (1986). "Transporting Capacity of Overland Flow on Plane and on Irregular Beds," *Earth Surface Processes and Landforms*, vol. 11, pp. 515-524.

Hairsine, P.B., and C.W. Rose (1992). "Modeling Water Erosion Due to Overland Flow Using Physical Principles 1, Sheet Flow," *Water Resources Research,* vol. 28, no. 1, pp. 237-243.

He, G., Z. Hua, and G. Wang (1987). "Regulation of Streamflow and Sediment Regimen by Sanmenxia Reservoir and Particularities of Scouring and Deposition," *Selected Papers of Researches on the Yellow River and Present Practice,* Yellow River Conservancy Commission, Zhengzou, China, pp. 166-175.

Hong, S., and S. Mostaghimi (1997). "Comparison of 1-D and 2-D Modeling of Overland Runoff and Sediment Transport," *Journal of the American Water Resources Association*, vol. 33, no. 5, pp. 1103-1116.

Horton, R.E., H.R. Leach, and R. Van Vlieit (1934). "Laminar Sheet-Flow," *Transactions of the American Geophysics Union*, vol. 2, pp. 393-404.

Johanson, R.C., J.C. Imhoff, J.L. Kittle, Jr., and A.S. Donigian (1984). *Hydrological Simulation Program CFORTRAN (HSPF): User Manual for Release 8.0*, EPA 600/3-84-066, Environmental Research Laboratory, U.S. EPA, Athens, Georgia.

Johnson, B.E., P.Y. Julien, D.K. Molnar, and C.C. Watson (2000). "The Two-Dimensional Upland Erosion Model CASC2D-SED," *Journal of the American Water Resources Association*, vol. 36, no. 1, pp. 31-42.

Jürgens, C., and M. Fander (1993). "Soil Erosion Assessment and Simulation by Means of SGEOS and Ancillary Digital Data," *International Journal of Remote Sensing*, vol. 14, no. 15, pp. 2847-2855.

Kilinc, M., and E.V. Richardson (1973). "Mechanics of Soil Erosion from Overland Flow Generated by Simulated Rainfall," Hydrology Paper no. 63, Colorado State University, Fort Collins, Colorado.

Kinsel, W.G. (1980). "CREAMS: A Field Scale Model for Chemicals, Runoff, and Erosion," in *Agricultural Management Systems*, U.S. Department of Agriculture, Conservation Report no. 26, 640 pp.

Kirnak, H. (2002). "Comparison of Erosion and Runoff Predicted by WEPP and AGNPS Models Using a Geographical Information System," *Turk J Agric For*, vol. 26, pp. 261-268.

Kothyari, U.C., and S.K. Jain (1997). "Sediment Yield Estimation Using GIS," *Hydrological Sciences Journal*, vol. 42, no. 6, pp. 833-843.

Kramer, L.A., and L.D. Meyer (1969). "Small Amount of Surface Runoff Reduces Soil Erosion and Runoff Velocity," *Transactions of the American Society of Agriculture Engineers*, vol. 12, pp. 638-648.

Lane, E.W. (1955). "The Importance of Fluvial Morphology in Hydraulic Engineering," *Journal of the Hydraulic Division, Proceedings, American Society of Civil Engineers*, vol. 81, paper 745, pp. 1-17.

Lane, E.W., and V.A. Koelzer (1943). "Density of Sediments Deposited in Reservoirs," in *A Study of Methods Used in Measurement and Analysis of Sediment Loads in Streams*, Report no. 9, Interagency Committee on Water Resources.

Lara, J.M. (1962). "Revision of the Procedure to Compute Sediment Distribution in Large Reservoirs," U.S. Bureau of Reclamation, Denver, Colorado.

Lara, J.M., and E.L. Pemberton (1965). "Initial Unit Weight of Deposited Sediments," *Proceedings, Federal Interagency Sedimentation Conference*, 1963, U.S. Agriculture Research Service Miscellaneous Publication, no. 970, pp. 818-845.

Lara, J.M., and H.I. Sanders (1970). "The 1963-64 Lake Mead Survey," U.S. Bureau of Reclamation, Denver, Colorado.

Leavesley, G.H., R.W. Lichty, B.M. Troutman, and L.G. Saindon (1983). *Precipitation-Runoff Modeling System—Users Manual*, USGS Water Resources Investigations Report 83-4238.

Linsley, R.K., and J.B. Franzini (1979). *Water-Resources Engineering*, McGraw-Hill Book Company, New York.

Linsley, R.K., Jr., M.A. Kohler, and J.L.H. Paulhus (1975). *Hydrology for Engineers*, McGraw-Hill Book Company, New York.

Meyer-Peter, E., and R. Müller (1948). "Formulas for Bed-load Transport," Meeting of the International Association for Hydraulic Structure Research, second meeting, Stockholm.

Miller, C.R. (1953). "Determination of the Unit Weight of Sediment for Use in Sediment Volume Computations," U.S. Bureau of Reclamation, Denver, Colorado.

Mitasova, H., L. Mitas, B. Brown, and D. Johnston (2002). "Distributed Hydrologic and Erosion Modeling for Watershed Management," online document http://skagit.meas.ncsu.edu/~helena/gmslab/courtcreek/wmb8.html.

Mitchell, J.K., B.A. Engel, R. Srinivasan, and S.S.Y. Wang (1993). "Validation of AGNPS for Small Watersheds using an Integrated AGNPS/GIS System," *Water Resources Bulletin*, vol. 29, no. 5, pp. 833-842.

Moore, I.D., and G.J. Burch (1986). "Sediment Transport Capacity of Sheet and Rill Flow: Application of Unit Stream Power Theory," *Water Resources Research*, vol. 22, no. 8, pp. 1350-1360.

Morgan, R.P.C., J.N. Quinton, R.E. Smith, G. Govers, J.W.A. Poesen, K. Auerswald, G. Chisci, D. Torri, and M.E. Styczen (1998). "The European Soil Erosion Model (EUROSEM): A Dynamic Approach for Predicting Sediment Transport from Fields and Small Catchments," *Earth Surface Process and Landforms*, vol. 23, pp. 527-544.

Morris, G.L., and J. Fan (1997). *Reservoir Sedimentation Handbook*, McGraw-Hill Book Company, New York, 758 pp.

Moss, A.J., P.H. Walker, and J. Hutka (1980). "Movement of Loose, Sandy Detritus by Shallow Water Flows: An Experimental Study," *Sedimentation Geology*, vol. 25, pp. 43-66.

Murthy, B.N. (1980). "Life of Reservoir," Technical Report No. 19, Central Board of Irrigation and Power, New Delhi.

Nash, J.E., and J.V. Sutcliffe (1970). "River Flow Forecasting through Conceptual Models Part ICA Discussion of Principles," *Journal of Hydrology*, vol. 10, pp. 282-290.

Nearing, M.A. 1998. "Why Soil Erosion Models Over-Predict Small Soil Losses and Under-Predict Large Soil Losses," *Catena*, vol. 32, pp. 15-22.

Nearing, M.A., L.J. Lane, and V.L. Lopes (1994). "Modeling Soil Erosion," in *Soil Erosion Research Methods*, Rattan Lal (ed.), St. Lucie Press, Delray Beach, Florida.

Nearing, M.A., G.R. Foster, L.J. Lane, and S.C. Finker (1989). "A Process-Based Soil Erosion Model for USDA-Water Erosion Prediction Project Technology," *Transactions of the American Society of Agricultural Engineers*, vol. 32, no. 5, pp. 1587-1593.

Nearing, M.A., L.D. Norton, D.A. Bulgakov, G.A. Larionov, L.T. West, and K.M. Dontsova (1997). "Hydraulics and Erosion in Eroding Rills," *Water Resources Research*, vol. 33, no. 4, pp. 865-876.

Ogden, F.L., and A. Heilig (2001). "Two-Dimensional Watershed Scale Erosion Modeling with CASC2D," Harmon, R.S., and Doe, W.W., III (eds.), in *Landscape Erosion and Evolution Modeling*, Kluwer Academic/Plenum Publishers, New York.

Ogden, F.L., and P.Y. Julien (2002). "CASC2D: A Two-Dimensional, Physically-Based, Hortonian, Hydrologic Model," in *Mathematical Models of Small Watershed Hydrology and Applications*, V.J. Singh, and D. Freverts, eds., Water Resources Publications, Littleton, Colorado.

Olmsted, F.H., O.J. Loeltz, and I. Burdge (1973). "Geohydrology of the Yuma Area, Arizona and California," *Water Resources of Lower Colorado River—Salton Sea Area*, Geological Survey Professional Paper 486-H, United States Government Printing Office, Washington DC.

Pacific Southwest Interagency Committee, Water Management Subcommittee (1968). "Factors Affecting Sediment Yield in the Pacific Southwest Area and Selection and Evaluation of Measures for Reduction of Erosion and Sediment Yield."

Pacific Southwest Interagency Committee (1968). "Factors Affecting Sediment Yield and Measures for the Reduction of Erosion and Sediment Yield."

Parsons, A.J., and A.M. Gadian (2000). "Uncertainty in Modelling the Detachment of Soil by Rainfall," *Earth Surface Processes and Landforms*, vol. 25, pp. 723-728.

Parsons, A.J., and J. Wainwright (2000). "A Process-Based Evaluation of a Process-Based Soil-Erosion Model," in *Soil Erosion: Application of Physically Based Models*, J. Schmidt, ed., Springer: Berlin, Germany.

Randle, T.J. (1996). "Lower Colorado River Regulatory Storage Study Sedimentation Volume After 100 Years for the Proposed Reservoirs Along the All American Canal and Gila Gravity Main Canal," U.S. Bureau of Reclamation, Technical Service Center, Denver, Colorado.

Randle, T.J. (1998). "Predicting Sediment Yield From Arid Drainage Areas" in *Proceedings of the First Federal Interagency Hydrologic Modeling Conference*, Interagency Advisory Committee on Water Data, Subcommittee on Hydrology, Las Vegas, Nevada, April 19-23, 1998.

Rauws, G. (1984). "De Transportcapaiteit van Afterfow Over Een Ruw Oppervla K: Laboratoriumexperimenten," Licentiaats thesis KUL, Fac. Wet., Leuven.

Renard, K.G., J.M. Laflen, G.R. Foster, and D.K. McCool (1994). "The Revised Universal Soil Loss Equation," in *Soil Erosion Research Methods,* Rattan Lal (ed.), St. Lucie Press, Delray Beach, Florida.

Renard, K.G., G.R. Foster, G.A. Weesies, D.K. McCool, and D.C. Yoder (1996). *Predicting Soil Erosion by Water: A Guide to Conservation Planning with the Revised Universal Soil Loss Equation*, U.S. Department of Agriculture, Agriculture Handbook 703, 384 pp.

Rubey, W.W. (1933). "Settling Velocities of Gravel, Sand, and Silt Particles," *American Journal of Science*, vol. 25, pp. 325-338.

Savat, J. (1980). "Resistance to Flow in Rough Supercritical Sheet Flow," *Earth Surface Processes and Landforms*, vol. 5, pp. 103-122.

Schoklitsch, A. (1934). "Der Gesuhiebetrieb und di Geschiebefracht," *Wasserkraft und Wasserwirtschaft*, vol. 29, no. 4, pp. 37-43.

Schröder, A. (2000). "WEPP, EUROSEM, E-2D: Results of Applications at the Plot Scale," in *Soil Erosion Application of Physically Based Models*, J. Schmidt (ed.), Springer, Berlin.

Senarath, S.U.S., F.L. Ogden, C.W. Downer, and H.O. Sharif (2000). On the Calibration and Verification of Two-Dimensional, Distributed, Hortonian, Continuous Watershed Models, *Water Resources Research*, vol. 36, no. 6, pp. 1495-1510.

Sharma, K.D., and S. Singh (1995). "Satellite Remote Sensing for Soil Erosion Modelling Using the ANSWERS Model," *Hydrological Sciences Journal*, vol. 40, no. 2, pp. 259-272.

Sheppard, J.R. (1960). "Investigation of Meyer-Peter, Müller Bed-load Formulas," U.S. Bureau of Reclamation, Denver, Colorado.

Singh, V.J. (1995). *Computer Models of Watershed Hydrology*, Water Resources Publication, Highlands Ranch, Colorado.

Smith, R.E., D.A. Goodrich, and J.N. Quinton (1995). "Dynamic Distributed Simulation of Watershed Erosion: KINEROS II and EUROSEM," *Journal of Soil and Water Conservation*, vol. 50, pp. 517-520.

Smith, S.J., J.R. Williams, R.G. Menzel, and G.A. Coleman (1984). "Prediction of Sediment Yield from Southern Plains Grasslands with the Modified Universal Soil Loss Equation," *Journal of Range Management*, vol. 37, no. 4, pp. 295-297.

Strand, R.I. (1975). "Bureau of Reclamation Procedures for Predicting Sediment Yield," in *Present and Prospective Technology for Predicting Sediment Yields and Sources*, Proceedings of the Sediment-Yield Workshop, USDA Sedimentation Laboratory, Oxford, Mississippi, November 28-30, 1972.

Strand, R.I., and E.L. Pemberton (1982). *Reservoir Sedimentation Technical Guidelines for Bureau of Reclamation*, U.S. Bureau of Reclamation, Denver, Colorado, 48 pp.

Swamee, P.K. (1974). "Analytic and Experimental Investigation of Streambed Variation Upstream of a Dam," Ph.D. Thesis, Department of Civil Engineering, University of Roorkee, India.

Tiwari, A.K., L.M. Risse, and M.A. Nearing (2000). "Evaluation of WEPP and its Comparison with USLE and RUSLE," *Transactions of the American Society of Agricultural Engineers*, vol. 43, no. 5, pp. 1129-1135.

U.S. Department of Agriculture (1978). "Sediment Deposition in U.S. Reservoirs, Summary of Data Reported Through 1975," Miscellaneous Publication No. 1362, Agriculture Research Service.

U.S. Environmental Protection Agency (2001). *A Watershed Decade*, EPA 840-R-00-002, Office of Wetlands, Oceans and Watersheds, Washington DC.

U.S. Interagency Committee on Water Resources (1957). Subcommittee on Sedimentation, "Some Fundamentals of Particle Size Analysis," Report no. 12.

U.S. Government Handbook (1978). "Chapter 3 - Sediment, National Handbook of Recommended Methods for Water-Data Acquisition."

U.S. Interagency Sedimentation Project, "A Study of Methods Used in Measurement and Analysis of Sediment Loads in Streams," Reports No. 1 through 14 and A through W, Subcommittee on Sedimentation, 1940 to 1981.

Vanoni, V.A. (1975). *Sedimentation Engineering*, ASCE Manual 54, ASCE, New York.

Wicks, J.M., and J.C. Bathurst (1996). "SHESED: A Physically Based, Distributed Erosion and Sediment Yield Component for the SHE Hydrological Modelling System," *Journal of Hydrology*, vol. 175, pp. 213-238.

Williams, J.R., A.D. Nicks, and J.G. Arnold (1985) "Simulator for Water Resources in Rural Basins," *Journal of Hydraulic Engineering, ASCE*, vol. 111, no. 6, pp. 970-986.

Williams, J.R., C.A. Jones, and P.T. Dyke (1984). "A modeling approach to determining the relationship between erosion and soil productivity," *Transaction of the American Society of Agricultural Engineers*, vol. 27, pp. 129-144.

Williams, J.R. (1975). "Sediment-Yield Prediction with Universal Equation Using Runoff Energy Factor," in *Present and Prospective Technology for Predicting Sediment Yields and Sources*, ARS-S-40, USDA-ARS.

Williams, J.R. (1981). "Testing the modified Universal Soil Loss Equation," in *Estimating Erosion and Sediment Yield on Rangelands*, USDA, ARM-W-26:157-164.

Wischmeier, W.H., and D.D. Smith (1962). "Soil-Loss Estimation as a Tool in Soil and Water Management Planning," Institute of Association of Scientific Hydrology, Publication No. 59, pp. 148-159.

Wischmeier, W.H., and D.D. Smith. (1965). *Predicting Rainfall—Erosion Losses from Cropland East of the Rocky Mountains*, U.S. Department of Agriculture, Agriculture Handbook No. 282, 48 p.

Wischmeier, W.H., and D.D. Smith (1978). *Predicting Rainfall Erosion Losses—Guide to Conservation Planning*, U.S. Department of Agriculture, Agriculture Handbook No. 537.

Woolhiser, D.A., R.E. Smith, and D.C. Goodrich (1990). *KINEROS, A Kinematic Runoff and Erosion Model: Documentation and User Manual*, U.S. Department of Agriculture, Agricultural Research Service, ARS-77, 130 p.

Wu, T.H., J.A. Hall, and J.V. Bonta (1993). "Evaluation of runoff and erosion models," *Journal of Irrigation and Drainage Engineering*, vol. 119, no. 2, pp. 364-382.

Yang, C.T. (1971). "Potential Energy and Stream Morphology," *Water Resources Research*, vol. 7, no. 2, pp. 311-322.

Yang, C.T. (1973). "Incipient Motion and Sediment Transport," *Journal of the Hydraulics Division, ASCE*, vol. 99, no. HY10, pp. 1679-1704.

Yang, C.T. (1976). "Minimum Unit Stream Power and Fluvial Hydraulics," *Journal of the Hydraulics Division, ASCE*, vol. 102, No. HY7, pp. 919-934.

Yang, C.T. (1979). "Unit Stream Power Equations for Total Load," *Journal of Hydrology*, vol. 40, pp. 123-138.

Yang, C.T. (1996). *Sediment Transport Theory and Practice*, The McGraw-Hill Companies, Inc., New York, 396 p. (reprint by Krieger Publishing Company, Malabar, Florida, 2003).

Yang, C.T. (2002). "Total Maximum Daily Load of Sediment," *Proceedings of the International Workshop on Ecological, Sociological, and Economic Implications of Sediment in Reservoirs*, April 8-10, Pestrum, Italy.

Yang, C.T., and A. Molinas (1982). "Sediment Transport and Unit Stream Power Function," *Journal of the Hydraulics Division, ASCE*, vol. 108, no. HY6, pp. 774-793.

Yang, C.T., and C.C.S. Song (1986). "Theory of Minimum Energy and Energy Dissipation Rate," *Encyclopedia of Fluid Mechanics*, Chapter 11, Gulf Publishing Company, Houston, Texas, pp. 353-399.

Yang, C.T., and C.C.S. Song (1987). "Theory of Minimum Rate of Energy Dissipation," *Journal of the Hydraulics Division*, ASCE, vol. 105, no. HY7, pp. 769-784.

Yang, C.T., and F.J.M. Simões (2000). *User's Manual for GSTARS 2.1 (Generalized Stream Tube model for Alluvial River Simulation Version 2.1)*, U.S. Bureau of Reclamation, Technical Service Center, Denver, Colorado.

Yang, C.T., and F.J.M. Simões (2002). *User's Manual for GSTARS3 (Generalized Sediment Transport model for Alluvial River Simulation Version 3)*, U.S. Bureau of Reclamation, Technical Service Center, Denver, Colorado.

Yang, C.T., C.C.S. Song, and M.J. Woldenberg (1981). "Hydraulic Geometry and Minimum Rate of Energy Dissipation," *Water Resources Research*, vol. 17, no. 4, pp. 1014-1018.

Yang, C.T., T.J. Randle, and S.K. Hsu (1998). "Surface Erosion, Sediment Transport, and Reservoir Sedimentation," *Proceedings of the Symposium on Modeling Soil Erosion, Sediment Transport, and Closely Related Hydrological Processes*, Vienna, International Association of Hydrologic Sciences Publication, no. 249, pp. 3-12.

Young, R.A., C.A. Onstad, D.D. Bosch, and W.P. Anderson (1989). "AGNPS: A Non-point-Source Pollution Model for Evaluating Agricultural Watersheds," *Journal of Soil and Water Conservation*, vol. 44, no. 2, pp. 168-172.

Zhang, X.C., M.A. Nearing, L.M. Risse, and K.C. McGregor (1996). "Evaluation of WEPP Runoff and Soil Loss Predictions Using Natural Runoff Plot Data," *Transactions of the American Society of Agricultural Engineers*, vol. 39, no. 3, pp. 855-863.

Ziegler, A.D., R.A. Sutherland, and T.W. Giambelluca (2000). "Partitioning Total Erosion on Unpaved Roads into Splash and Hydraulic Components: The Roles of Interstorm Surface Preparation and Dynamic Erodibility," *Water Resources Research.*, vol. 36, no. 9, pp. 2787-2791.